Development of Levelized Cost of Electricity, Life Cycle Greenhouse Gas Emissions and Net Energy Ratio of Solar-based Thermal Energy Storage Systems

By

Spandan Samirkumar Thaker

A thesis submitted in partial fulfillment of the requirements for the degree of

Master of Science

Department of Mechanical Engineering

University of Alberta

Abstract

In this study, a data-intensive model was developed to evaluate the levelized cost of electricity (LCOE), the life cycle greenhouse gas (GHG) emissions and the net energy ratio (NER) for thermal energy storage (TES) technologies, namely, sensible heat, latent heat, and thermochemical storage. To evaluate the LCOE, GHG emissions, and NER of storage systems, five scenarios were developed: two-tank indirect sensible heat storage (S1), two-tank direct sensible heat storage (S2), one-tank direct sensible heat storage (S3), latent heat storage (S4), and thermochemical storage (S5). A Monte Carlo simulation was performed for each scenario to examine the uncertainty in the LCOE, GHG emissions and NER.

The GHG emissions for individual scenarios were found to be 13.52 – 46.86 gCO_{2eq}/kWh (S1), 6.27 – 24.88 gCO_{2eq}/kWh (S2), 4.53 – 18.79 gCO_{2eq}/kWh (S3), 9.36 – 33.43 gCO_{2eq}/kWh (S4), and 9.69 – 28.99 gCO_{2eq}/kWh (S5). The results indicate that when uncertainty is considered, the GHG emissions can be greatly reduced in both S2 and S3. In S3, however, investment costs are also reduced (unlike in S2). The low investment costs are reflected in the LCOE. The LCOE ranges for individual scenarios are 0.08 – 0.59 $/kWh (S1), 0.03 – 0.22 $/kWh (S2), 0.02 – 0.16 $/kWh (S3), 0.06 – 0.43 $/kWh (S4), and 0.22 – 1.19 $/kWh (S5). The impact on LCOE was examined by varying the following key parameters; plant capacity, solar multiple, storage duration, capacity factor, and discount rate. Consequently, the impact on NER and GHG emission were examined by varying parameters such as, heat exchanger efficiency, material input requirement, pump efficiency, emission factors for electricity source, storage duration, solar multiple, capacity factor, emission factors for Canadian provinces, and plant

capacity. The NER ranges for individuals scenarios are 2.66 – 4.65 (S1), 13.34 – 18.59 (S2), 20.7 – 28.44 (S3), 0.21 – 2.03 (S4), and 5.63 – 8.57 (S5). In terms of NER, both S2 and S3 demonstrate a high potential to increase the energy output from TES systems. It can also be deduced from this study that S2 and S3 both have low investment costs and GHG emissions. For these reasons, S2 and S3 are more favourable scenarios to be implemented commercially. This study will provide key information for industry and policy makers in decision making and in determining which thermal storage technology is economically viable, energy efficient, and has the least environmental impact.

Preface

This thesis is an original work by Spandan Thaker completed under the guidance and supervision of Dr. Amit Kumar. Chapter 2 of this thesis has been published as Spandan Thaker, Abayomi Olufemi Oni, Amit Kumar, "Techno-economic evaluation of solar-based thermal energy storage systems," in Energy Conversion and Management. Chapter 3 of this thesis has been prepared for submission as Spandan Thaker, Abayomi Olufemi Oni, Eskinder D. Gemechu, Amit Kumar, "Development of life cycle greenhouse gas emissions and net energy ratio of solar-based thermal energy storage systems," in a peer-reviewed journal. I was responsible for the concept formulation, collection and analysis of data, model development, and manuscript composition. Dr. A.O. Oni contributed by assisting in model development using Aspen HYSYS and manuscript composition. Dr. E. Gemechu contributed by providing input in developing the life cycle assessment model and manuscript composition. Dr. A. Kumar was the supervisory author and was involved in concept formulation, assessment of results, and manuscript composition.

Acknowledgments

I would like to thank my supervisor, Dr. A. Kumar, for his professional input and guidance throughout my MSc journey. Thank you for giving me the opportunity to pursue research in thermal energy storage. Your mentorship and encouragement have inspired me to strive for academic excellence. Pursuing the MSc degree at the University of Alberta has helped me to develop the ability to think and analyze a complex problem critically.

I would like to acknowledge the NSERC Energy Storage Technology (NEST) Network (RYERU NSERC 468468 Kumar), the University of Alberta (UOFAB VPRGRF NEST KUMAR), and the NSERC/Cenovus/Alberta Innovates Associate Industrial Research Chair in Energy and Environmental Systems Engineering and the Cenovus Energy Endowed Chair in Environmental Engineering for their financial support provided to carry out this research.

I take great pleasure in thanking the examining committee members for their interest and time for my research. I feel privileged to be pursuing my research and learning from the scholars and experts who bring a wealth of knowledge in their respective fields. I would like to express my gratitude to the postdoctoral fellows, Dr. Abayomi Olufemi Oni and Dr. Eskinder Gemechu, for the technical guidance throughout my research. I am also thankful to Astrid Blodgett for providing the editorial assistance in this research. I would also like to express by gratitude to my friends and colleagues in the Sustainable Energy Research Group (SERG) for making it a memorable experience in graduate school.

It goes without saying, I am truly grateful for the unconditional love and support I have received from my family over the years. The wisdom imparted to me by my parents has helped me to persevere through all the challenges. Above all, I thank God for giving the limitless opportunities and the strength and intellect to pursue my dreams.

Table of Contents

Abstract ii

Preface iv

Acknowledgments v

Table of Contents vii

List of Tables x

List of Figures xi

Acronyms xiii

Nomenclature xiv

Chapter 1 1

1.1 Introduction 1

1.2 Literature Review and Knowledge Gap 3

1.3 Research Scope and Objectives 7

1.4 Limitations of the Thesis 8

1.5 Organization of the Thesis 9

References 11

Chapter 2 14

Techno-economic Evaluation of Solar-based Thermal Energy Storage Systems 14

2.1 Introduction 14

2.2 Methods 20

2.2.1 Indirect sensible heat storage using two tanks (S1) 20

2.2.2 Direct sensible heat storage using two tanks (S2) 22

2.2.3 Direct sensible heat storage using one tank (S3) 23

2.2.4 Latent heat storage using one tank (S4) 23

2.2.5 Thermochemical heat storage (S5) 25

2.2.6 Cost estimation 26
2.2.6.1 Mass flow rate requirement in condensing steam turbine 28
2.2.6.2 Heat exchanger energy balance 29
2.2.6.3 Heat exchanger area 29
2.2.6.4 Estimation of overall heat transfer coefficient 30
2.2.6.5 Assumptions to compute LCOE 31
2.2.7 Uncertainty Analysis 32
2.3 Results and discussion 32
2.3.1 Sensitivity analysis 39
2.3.2 Scenario optimization 42
2.3.3 Uncertainty analysis 45
2.4 Conclusion 48
References 50
Chapter 3 54
Development of Life Cycle Greenhouse Gas Emissions and Net Energy Ratio of Solar-based Thermal Energy Storage Systems 54
3.1 Introduction 54
3.2 Methods 58
3.2.1 Goal and scope definition 58
3.2.2 Process description 62
3.2.3 Material requirement calculation 63
3.2.4 Net energy ratio evaluation 66
3.3 Results and Discussion 68
3.3.1 The life cycle GHG emissions 68
3.3.2 Net energy ratio 73

3.4 Uncertainty Analysis 77

3.5 Conclusion 80

References.. 81

Chapter 4 84

4.1 Conclusions 84

4.2 Recommendations for future work 86

Bibliography 88

Appendix A: Derivation of LCOE 97

Appendix B: Supporting Information... 99

List of Tables

Table 1: Assumptions for cost estimation and LCOE calculation 27
Table 2: Parameters considered for bottom-up cost estimation 27
Table 3: Base case parameter values 33
Table 4: Base case values for condensing steam turbine 33
Table 5: Base case values for HTF (Dowtherm A©/Therminol VP©) heat exchanger... 34
Table 6: Base case values for evaporation heat exchanger 35
Table 7: LCOE and capital cost summary for the base case 38
Table 8: Optimized parameter values.. 44
Table 9: LCOE and cost summary for the optimized cases.. 45
Table 10: Monte Carlo input distributions 46
Table 11: Material requirement in metric tonnes (MT) for each material 65
Table 12: Base parameter values 73
Table 13: Heat values for the components in Figure 22 76
Table 14: Sampling error, standard deviation, and number of samples 102
Table 15: Monte Carlo input distributions 102

List of Figures

Figure 1: Schematic of two-tank indirect thermal storage (S1) 21
Figure 2: Schematic of two-tank direct sensible heat storage (S2) 22
Figure 3: Schematic of one-tank direct sensible heat storage (S3) 23
Figure 4: Schematic of one-tank latent heat storage (S4) 24
Figure 5: Thermochemical energy storage (S5) 26
Figure 6: LCOE sensitivity plot for two-tank indirect sensible heat storage (S1) 39
Figure 7: LCOE sensitivity plot for two-tank direct sensible heat storage (S2) 40
Figure 8: LCOE sensitivity plot for one-tank direct sensible heat storage (S3) 40
Figure 9: LCOE sensitivity plot for latent heat storage (S4) 41
Figure 10: LCOE sensitivity plot for thermochemical storage (S5) 41
Figure 11: Parabolic trough and solar tower cost comparison 43
Figure 12: Correlation between solar multiple and hours of storage 43
Figure 13: Correlation between solar multiple and capacity factor 44
Figure 14: LCOE uncertainty box plot for thermal energy storage systems 47
Figure 15: Common system boundary for thermal energy storage systems 61
Figure 16: Life cycle GHG emissions for thermal energy storage systems 69
Figure 17: GHG emissions associated with the production stage 70
Figure 18: Life cycle emissions sensitivity plot for 2-tank indirect sensible heat storage (S1) 72
Figure 19: Life cycle emissions sensitivity plot for thermochemical storage (S5) 72
Figure 20: NER for thermal energy storage technologies 74
Figure 21: NER sensitivity plot for 2-tank indirect sensible heat storage (S1) 75
Figure 22: NER block diagram for the thermal energy storage systems 76
Figure 23: NER uncertainty box plot for thermal energy storage systems 79
Figure 24: Life cycle GHG emissions uncertainty box plot for thermal energy storage systems 79
Figure 25: GHG emissions for 2-tank direct sensible heat storage (S2) 99
Figure 26: NER for 2-tank direct sensible heat storage (S2) 99
Figure 27: NER for 1-tank direct sensible heat storage (S3) 100

Figure 28: GHG emissions for 1-tank direct sensible heat storage (S3)...................... 100
Figure 29: NER for latent heat storage (S4).. 101
Figure 30: GHG emissions for latent heat storage (S4)... 101
Figure 31: NER for thermochemical storage (S5) 102

Acronyms

CSP → Concentrated solar power

CO_2 → Carbon dioxide

GHG → Greenhouse gas

GJ → Gigajoules

Gt → Gigatonnes

gCO_{2eq} → grams of carbon dioxide equivalent

HTF → Heat transfer fluid

IEA → International Energy Agency

kWh → Kilowatt-hours

LCOE → Levelized cost of electricity ($/kWh)

LCA → Life cycle assessment

NER → Net energy ratio

O&M → Operation and maintenance

PCM → Phase change material

R & D → Research and development

SM → Solar multiple

S1 → Indirect sensible heat storage using two tanks

S2 → Direct sensible heat storage using two tanks

S3 → Direct sensible heat storage using one tank

S4 → Latent heat storage using one tank

S5 → Thermochemical heat storage

TES → Thermal energy storage

TWh → Terrawatt-hours

U.S. DOE → United States Department of Energy

Nomenclature

A → Total heat exchanger area

C → Total investment cost ($)

c_{p} → Specific heat capacity

D → Discount rate (%)

Energy → Total energy produced (kWh)

G → Variable O&M escalation due to inflation (%)

h → Enthalpy

$\dot{m}$ → Mass flow rate

N → Total life (years)

$\dot{Q}$ → Rate of heat transfer

$\dot{Q}_{\mathrm{loss}}$ → Rate of heat loss

T → Temperature of heat transfer fluid

ΔT_{m} → Log mean temperature difference

U → Overall heat transfer coefficient

$\dot{W}$ → Rate of work

ΔE_{k} → Change in kinetic energy

ΔE_{p} → Change in potential energy

Chapter 1

1.1 Introduction

There is an ever-increasing concern about global warming and its adverse impacts on the Earth. The high demand for fossil energy, both due to increase in population and unsustainable economic growth, is one of the major contributors to the global greenhouse gas (GHG) emissions [1]. GHG emissions from electricity and heat production account for more than 12 $GtCO_2eq$ (Gigatonne of carbon dioxide equivalent), 25% of the total anthropogenic emissions in 2010 [2]. Reducing fossil fuel usage through promoting renewable and nuclear energy sources are considered as GHG mitigation options [2]. The share of global electricity generation from renewable energy sources including hydropower, has been increasing from 23% in 2005 to 30% in 2015 [3]. It is also projected to raise considerably in coming decades; 22,000 TWh (Terrawatt-hours) in 2012 to 40,000 TWh in 2050 [4].

Some examples of renewable energy systems are: biomass/biofuels, concentrated solar power (CSP), geothermal, hydroelectricity, solar photovoltaic, and wind energy. Even though renewable energy systems are regarded as GHG mitigation options, there are several challenges that could affect their wide deployment. For some sources such as hydroelectricity or bioenergy, the available technical potential is a constraint. For renewable energy sources such as wind and solar, location requirements and temporal variability are among the challenges. For example, in the case of wind, a site with strong wind velocity may be located far from where its energy is being used. Solar energy is more feasible in a region with high annual sunlight. Moreover, wind and solar plant produce energy only when there is high wind velocity and sunlight, respectively. They are intermittent and unable to supply power during peak demand. To address these issues, they need to be integrated with energy storage systems.

Energy storage systems can be broadly categorized into chemical, mechanical and thermal. Mechanical energy storage systems convert electrical energy into mechanical energy using technologies such as compressed air energy storage, liquid air energy storage, compressed carbon dioxide storage, flywheels, and pumped hydro storage [5]. Chemical energy storage systems use batteries to convert and store electricity from chemical energy. Thermal energy storage (TES) technologies can store energy in the form of heat. The global market for energy storage is expected to grow exponentially from 0.34 GW in 2012 to over 40 GW in 2022 [6]. Canada will contribute approximately 62 MW of capacity to the global energy storage market in 2018 [7].

This study focuses solely on evaluating the life cycle economic feasibility, environmental impact, and energy efficiency of TES systems. A TES system has the potential to store energy in the form of heat for long periods. TES can be broadly classified as sensible heat, latent heat, and thermochemical storage. Sensible heat storage can store heat for up to 15 hours using a heat transfer medium such as molten salt [8]. Molten salt is a commercially available heat transfer fluid that can retain heat with minimal heat loss due to a temperature loss of approximately 1°F per day [9]. Latent heat storage technology stores heat in phase change materials (PCMs). Heat is stored when the PCM changes from solid to liquid and released when the PCM changes from liquid to solid [10]. Latent heat storage is still in the research and development (R&D) phase because of the challenges faced in developing PCMs that are economical and energy efficient with low environmental impact. Thermochemical storage is also still in the R&D phase. For this reason, energy efficiency and economic and environmental impacts of TES technologies are not fully characterized. The economic feasibility of implementing TES systems can be evaluated by performing a techno-economic assessment (TEA). TEA is conducted for TES systems to evaluate their economic feasibility by assessing the costs (i.e., capital costs of individual equipment and maintenance costs) over a plant life. The environmental performance in terms of GHG emissions and energy efficiency of the TES systems is analyzed using a life cycle assessment (LCA). LCA is a stand-alone environmental management tool that quantifies the potential impacts associated with input and output requirements throughout a product's life cycle: from extraction to the final disposal. A life cycle inventory was compiled on the amount of material required in site preparation and construction of each TES system, fossil fuel required during the individual life cycle phases (i.e., production, construction, transportation, operation, dismantling, and disposal), and the associated GHG emissions. This study focuses on conducting both LCA and TEA to compare the environmental sustainability and economic feasibility of the TES systems.

1.2 Literature Review and Knowledge Gap

The economic feasibility, environmental impacts, and the energy efficiency of different TES technologies are examined in the literature. A widely used metric to evaluate the economic feasibility is the levelized cost of electricity (LCOE). LCOE is the price at which electricity would have to be sold to break-even of the costs (i.e. capital cost and maintenance cost) when amortized over the plant life. To assess the environmental impacts, the life cycle GHG emissions are evaluated using the 100-year global warming potential (GWP). The GWP is a measure of the amount of energy a gas (i.e., carbon dioxide, methane, and nitrous oxide) will absorb over a period of 100 years [11]. The other metric used in the environmental assessment is the net energy ratio (NER), a measure of heat output from a TES system for a unit of fossil fuel input. The first law efficiency, defined as the ratio of net work output to total heat input, could also be used to evaluate the system efficiency. However, the first law efficiency has limitations when comparing different TES systems [12]. One of the limitations is associated with the defined system boundary in this study. Since the system boundary in this study is focused solely on thermal storage, there is no work output from the TES systems. For this reason, to determine the useful heat delivered from the TES systems, a net energy ratio (NER) was evaluated instead of the first law efficiency. The NER is a unitless metric defined as the ratio of net heat (measured in gigajoules [GJ]) to the fossil fuel input [13].

Several studies have been conducted to assess the techno-economic [14-16] and environmental impacts [17-19] of sensible heat storage. For example, Hinkley et al. [14] performed a TEA of sensible heat storage using parameters such as unit capital cost ($/kW) and storage duration, while Turchi et al. [15] used Solar Advisor Model (SAM) software to evaluate the cost of thermal storage for parabolic troughs and central tower systems. Boudaoud et al. [20] used first principles to evaluate the investment costs of individual equipment. Burkhardt et al. [17] evaluated the life cycle GHG emissions for a parabolic trough concentrating solar power plant. Another study conducted by Burkhardt et al. [18] compared the life cycle GHG emissions for parabolic trough and central tower concentrated solar power (CSP) plants. Corona et al. [19] performed a comparative LCA to evaluate the environmental sustainability of a 50 MW hybrid parabolic trough plant with natural gas fuel input.

Several studies have examined the economic [21-23] and environmental [24-26] aspects of latent heat storage. Hubner et al. [21] and Seitz et al. [23] used a top-down approach to evaluate the levelized cost of electricity (LCOE) by calculating the unit capital cost of various phase change materials and individual equipment. Oro et al. [24] used hypothetical scenarios to compare the life cycle emissions of latent heat and sensible heat storage. Cabeza et al. [25] used phase change materials to conduct LCA for district heating of buildings.

Several studies address the economic impacts of thermochemical storage [27-29]. Hypothetical models were developed to estimate the LCOE for a 10 MW thermochemical storage plant [28] and a hybrid model combining battery storage with thermochemical storage [29]. However, the environmental impacts of thermochemical storage are not well covered in existing literature. Masruroh et al. [30] performed a “cradle-to-grave” LCA to estimate the total environmental impacts from a thermochemical storage system. The study shows that raw material acquisition and component manufacturing process are the most important stages and make up 99% of the environmental impacts (global warming potential, acidification potential, eutrophication, phosphate and photochemical oxidant).

The techno-economic and environmental impact results from different thermal storage systems are not comparable. This is mainly due to differences in goal and scope setting, system boundary and functional unit definitions, different assumptions and modelling parameters. Gaps in the literature include a holistic TEA and LCA of thermal storage systems. Moreover, few studies have been done on the uncertainty and sensitivity of the

LCOE and GHG emissions of thermal energy storage systems [14, 20]. Boudaoud et al. [20] performed uncertainty and sensitivity analyses to examine economic feasibility by varying parameters such as storage duration and solar multiple. Another study varied parameters such as capital cost and storage duration to assess their impact on the LCOE [14]. To address the research gaps and to compare the economic feasibility and environmental sustainability of each TES technology (i.e., sensible heat, latent heat, and thermochemical storage), this study uses a bottom-up approach that considers the full life cycle of each technology and examines the sensitivity and uncertainty in the LCOE, GHG emissions and the NER.

In addition to cost and GHG emissions, it is important to evaluate the NER of TES technologies. Some work has been done in this area. Koppelaar et al. [31] conducted an uncertainty analysis to evaluate the impact of NER for both monocrystalline and polycrystalline solar cells. Larrain and Escobar [32] performed a net energy analysis on a hybrid CSP plant with natural gas used as backup fuel. Colclough et al. [33] examined the NER for a seasonal thermal storage system used for district heating. In this study, the NERs of TES technologies are evaluated and the sensitivity and uncertainty of results are assessed by varying parameters such as heat exchanger efficiency, material input requirements, storage duration, solar multiple, capacity factor, pump efficiency, plant capacity, and electricity emission factors.

TES technologies can provide alternative forms of energy that are environmentally friendly. However, to ascertain their sustainability, it is important to perform techno-economic and environmental analyses. The economic feasibility can be examined through TEA and the environmental impact and energy efficiency through LCA. Sensitivity and uncertainty analyses are performed by examining the impacts on LCOE, GHG emissions, and the NER. Only a few published studies perform sensitivity and uncertainty analyses on the LCOE, GHG emissions, and NER for TES technologies. The key gap in the literature is to conduct a comprehensive comparative assessment of the TES technologies. This thesis is aimed as addressing this gap.

1.3 Research Scope and Objectives

This thesis aims to evaluate the sustainability of TES integrated into other energy systems by considering parameters that are consistent with each TES technology. Hence, the impact on LCOE is determined in this study by varying parameters such as plant capacity, storage duration, solar multiple, capacity factor, and discount rate. In addition to a TEA, the current literature on LCA examined the impact of GHG emissions and NER through sensitivity and uncertainty analyses using different assumptions and process conditions. In this study, the impact of GHG emissions and NER is examined by varying parameters such as heat exchanger efficiency, material input requirement, storage duration, solar multiple, capacity factor, pump efficiency, emission factors for electricity source, plant capacity, and electricity emission factors for Canadian provinces. The LCA, TEA, and NER of TES were investigated by developing process simulation models using assumptions and operating conditions based on data available in the literature. The level of risk in the assumed parameters was captured by conducting uncertainty analysis using Monte Carlo simulations. To the best of the author's knowledge, the proposed simulation model in this work is the first to holistically evaluate the LCOE, GHG emissions, and NER of TES technologies. This study will provide information pertinent to industry and policymakers in determining the economic feasibility, environmental impact, and energy efficiency of TES technologies.

The overall purpose of this study is to develop bottom-up data-intensive LCA and TEA models to determine, respectively, the life cycle GHG emissions and NER and the economic feasibility of TES technologies such as sensible heat, latent heat, and thermochemical storage. The specific objectives are:

- Developing the system boundary diagrams for sensible heat, latent heat and thermochemical storage.
- Collecting data and developing a life cycle inventory to perform techno-economic and environmental assessments to evaluate life cycle cost, GHG emissions, and NER
- Developing bottom-up spreadsheet-based LCA and techno-economic models
- Performing sensitivity and uncertainty analyses to assess the impact on the GHG emissions, LCOE, and NER for each storage technology

1.4 Limitations of the Thesis

The system boundary considered for the TES technologies includes the cost, energy, and material requirements for the storage components (i.e., heat exchangers, pumps, storage tanks, and piping). In other words, the LCOE calculated in this study does not include costs from the solar field or power plant components, and the NER does not consider fossil fuel input during the construction of solar field and power plant components. The LCA evaluates GHG emissions solely for the thermal energy storage systems (i.e., sensible heat, latent heat, and thermochemical storage). The life cycle phases considered in the evaluation of GHG emissions are the production, construction, transportation, operation, dismantling, and disposal phase. GHG emissions from the production, construction, transportation, operation, dismantling, and disposal of the solar field and power plant components were not considered. Thus, by focusing solely on thermal storage in the LCA, this study evaluated the NER to determine the unit heat output from thermal storage for a unit of fossil fuel input. The GHG emissions evaluated in this study only consider the global warming potential from carbon dioxide (CO_2), methane (CH_4), and nitrous oxide (N_2O). Chapters 2 and 3 discuss in further detail the scope and limitations of the study.

1.5 Organization of the Thesis

This is a paper-based thesis written such that each chapter can be read independently. As a result, the reader can expect repetition in the assumptions and results between chapters. There are four chapters in this thesis and basic details of each chapter are outlined as follows:

Chapter 2, Techno-economic evaluation of solar-based thermal energy storage systems: In this chapter, the author assesses the economic feasibility of sensible heat, latent heat, and thermochemical storage systems. Both sensitivity and uncertainty analyses are performed to examine the impact on LCOE by varying parameters such as plant capacity, solar multiple, storage duration, capacity factor, and discount rate. This version of the chapter is a published peer-reviewed journal paper.

Chapter 3, Development of the life cycle greenhouse gas emissions and net energy ratio of solar-based thermal energy storage systems: In this chapter, the author estimates the GHG emissions and determines the energy efficiency of sensible heat, latent heat, and thermochemical storage using LCA. Sensitivity and uncertainty analyses are performed to examine the impact on GHG emissions and NER by varying parameters such as heat exchanger efficiency, material input requirement, storage duration, solar multiple, capacity factor, pump efficiency, emission factors for electricity source, plant capacity, and emission factors for Canadian provinces.

Chapter 4, Conclusions and recommendations for future work: This chapter concludes the thesis and discusses the key findings from the research. The chapter also shares recommendations for future work.

References

[1] J.-C. Yeh and C.-H. Liao, "Impact of population and economic growth on carbon emissions in Taiwan using an analytic tool STIRPAT," Sustainable Environment Research, vol. 27, pp. 41-48, 2017.

[2] O. Edenhofer, R. Pichs-Madruga, Y. Sokona, E. Farahani, S. Kadner, K. Seyboth, et al., "Summary for policymakers climate change 2014, mitigation of climate change," IPCC 2014, Climate Change 2014: Contribution of Working Group III to the Fifth Assessment Report of the Intergovernmental Panel on Climate Change, 2014.

[3] P. Beiter and T. Tian, "2015 renewable energy data book," National Renewable Energy Laboratory, 2016.

[4] M. van der Hoeven and D. Houssin, "Energy technology perspectives 2015: mobilising innovation to accelerate climate action," International Energy Agency, 2015.

[5] R. Amirante, E. Cassone, E. Distaso, and P. Tamburrano, "Overview on recent developments in energy storage: Mechanical, electrochemical and hydrogen technologies," Energy Conversion and Management, vol. 132, pp. 372-387, 2017.

[6] Energy Storage Facts & Figures. Available: http://energystorage.org/energy-storage/facts-figures; accessed December 12, 2017.

[7] National Energy Board, Market Snapshot: Batteries Dominate Early Stage Testing for Energy Storage in Canada. Available: https://www.neb-one.gc.ca/nrg/ntgrtd/mrkt/snpsht/2016/07-03bttrsdmnttstng-eng.html; accessed January 15, 2018.

[8] M. Liu, N. S. Tay, S. Bell, M. Belusko, R. Jacob, G. Will, et al., "Review on concentrating solar power plants and new developments in high temperature thermal energy storage technologies," Renewable and Sustainable Energy Reviews, vol. 53, pp. 1411-1432, 2016.

[9] SolarReserve, Molten Salt Energy Storage. Available: http://www.solarreserve.com/en/technology/molten-salt-energy-storage; accessed November 3, 2017.

[10] D. Medveď, M. Kvakovský, and V. Sklenárová, "Latent heat storage systems," 2010. Available: http://home.zcu.cz/~tesarova/IP/Proceedings/Proc_2010/Files/001%20IP2010_Medved.pdf; accessed November 3, 2017.

[11] Environmental Protection Agency, Understanding Global Warming Potentials. Available: https://www.epa.gov/ghgemissions/understanding-global-warming-potentials; accessed January 20, 2018.

[12] A. G. McDonald and H. Magande, Introduction to thermo-fluids systems design: John Wiley & Sons, 2012.

[13] P. Denholm, Net energy balance and greenhouse gas emissions from renewable energy storage systems: Energy Center of Wisconsin, 2003. Available: http://www.seventhwave.org/sites/default/files/223-1.pdf; accessed December 20, 2017.

[14] J. T. Hinkley, J. A. Hayward, B. Curtin, A. Wonhas, R. Boyd, C. Grima, et al., "An analysis of the costs and opportunities for concentrating solar power in Australia," Renewable Energy, vol. 57, pp. 653-661, 2013.
[15] C. Turchi, M. Mehos, C. K. Ho, and G. J. Kolb, "Current and future costs for parabolic trough and power tower systems in the US market," in Proceedings of the 16th SolarPACES Conference, Perpignan, France, 2010.
[16] H. Lund, P. A. Østergaard, D. Connolly, I. Ridjan, B. V. Mathiesen, F. Hvelplund, et al., "Energy storage and smart energy systems," International Journal of Sustainable Energy Planning and Management, vol. 11, pp. 3-14, 2016.
[17] J. J. Burkhardt III, G. A. Heath, and C. S. Turchi, "Life cycle assessment of a parabolic trough concentrating solar power plant and the impacts of key design alternatives," Environmental science & technology, vol. 45, pp. 2457-2464, 2011.
[18] J. J. Burkhardt, G. Heath, and E. Cohen, "Life cycle greenhouse gas emissions of trough and tower concentrating solar power electricity generation," Journal of Industrial Ecology, vol. 16, 2012.
[19] B. Corona, G. San Miguel, and E. Cerrajero, "Life cycle assessment of concentrated solar power (CSP) and the influence of hybridising with natural gas," The International Journal of Life Cycle Assessment, vol. 19, pp. 1264-1275, 2014.
[20] S. Boudaoud, A. Khellaf, K. Mohammedi, and O. Behar, "Thermal performance prediction and sensitivity analysis for future deployment of molten salt cavity receiver solar power plants in Algeria," Energy Conversion and Management, vol. 89, pp. 655-664, 2015.
[21] S. Hübner, M. Eck, C. Stiller, and M. Seitz, "Techno-economic heat transfer optimization of large scale latent heat energy storage systems in solar thermal power plants," Applied Thermal Engineering, vol. 98, pp. 483-491, 2016.
[22] B. Xu, P. Li, and C. Chan, "Application of phase change materials for thermal energy storage in concentrated solar thermal power plants: a review to recent developments," Applied Energy, vol. 160, pp. 286-307, 2015.
[23] M. Seitz, M. Johnson, and S. Hübner, "Economic impact of latent heat thermal energy storage systems within direct steam generating solar thermal power plants with parabolic troughs," Energy Conversion and Management, vol. 143, pp. 286-294, 2017.
[24] E. Oró, A. Gil, A. De Gracia, D. Boer, and L. F. Cabeza, "Comparative life cycle assessment of thermal energy storage systems for solar power plants," Renewable Energy, vol. 44, pp. 166-173, 2012.
[25] L. EZA, A. Castell, and G. Pérez, "Life cycle assessment (LCA) of phase change materials (PCMs) used in buildings," Eco-efficient Construction and Building Materials: Life Cycle Assessment (LCA), Eco-Labelling and Case Studies, pp. 287, 2014.
[26] A. De Gracia, L. Rincón, A. Castell, M. Jiménez, D. Boer, M. Medrano, et al., "Life Cycle Assessment of the inclusion of phase change materials (PCM) in experimental buildings," Energy and Buildings, vol. 42, pp. 1517-1523, 2010.
[27] R. Dunn, K. Lovegrove, and G. Burgess, "A review of ammonia-based thermochemical energy storage for concentrating solar power," Proceedings of the IEEE, vol. 100, pp. 391-400, 2012.

[28] A. Luzzi, K. Lovegrove, E. Filippi, H. Fricker, M. Schmitz-goeb, M. Chandapillai, et al., "Techno-economic analysis of a 10 MW e solar thermal power plant using ammonia-based thermochemical energy storage," Solar Energy, vol. 66, pp. 91-101, 1999.
[29] E. Wenger, M. Epstein, and A. Kribus, "Thermo-electro-chemical storage (TECS) of solar energy," Applied Energy, vol. 190, pp. 788-799, 2017.
[30] N. A. Masruroh, B. Li, and J. Klemeš, "Life cycle analysis of a solar thermal system with thermochemical storage process," Renewable Energy, vol. 31, pp. 537-548, 2006.
[31] R. Koppelaar, "Solar-PV energy payback and net energy: Meta-assessment of study quality, reproducibility, and results harmonization," Renewable and Sustainable Energy Reviews, vol. 72, pp. 1241-1255, 2017.
[32] T. Larraín and R. Escobar, "Net energy analysis for concentrated solar power plants in northern Chile," Renewable Energy, vol. 41, pp. 123-133, 2012.
[33] S. Colclough and T. McGrath, "Net energy analysis of a solar combi system with Seasonal Thermal Energy Store," Applied Energy, vol. 147, pp. 611-616, 2015.

Chapter 2[1]

Techno-economic Evaluation of Solar-based Thermal Energy Storage Systems

2.1 Introduction

TES has the potential to store energy in the form of heat over a period for later use. It is a promising technology that can reduce reliance on fossil fuels and help avoid penalties related to environmental regulations. The use of TES to meet environmental standards and energy requirement is now receiving the attention it has always deserved. TES is expected to grow by 11% between 2017 and 2022 [1]. The growth rate of TES can be affected by the intermittency issues in solar radiation (i.e., cloudy days and night-time). For this reason, there is a need to integrate the storage of thermal energy (i.e., sensible heat, latent heat, and thermochemical) with electrical power generating systems. However, despite challenges around the integration of TES, it is not yet known if it is economically feasible. For this reason, the cost-effectiveness of integrating TES into existing technologies is a subject of discussion.

A recent development is to improve the cost-effectiveness of TES by reducing the levelized cost of electricity. For example, in March 2015, the U.S. Department of Energy (DOE) announced a plan to reduce the levelized cost of electricity from solar-based electrical power generation to below \$0.06/kWh by 2020 [2]. This plan prompted the search for cost-effective ways to store energy in the form of heat. In view of this, sensible heat, latent heat, and thermochemical storage are considered for storing thermal energy.

[1] A version of this chapter has been published in *Energy Conversion and Management*: Spandan Thaker, Abayomi Olufemi Oni, Amit Kumar, "Techno-economic evaluation of solar-based thermal energy storage systems," Energy Conversion and Management, vol. 153, pp. 423-434, 2017.

Sensible heat storage is a commercially available technology that can store thermal energy for up to 15 hours using a heat transfer medium such as molten salt [3]. Molten salts have high storage efficiencies that allow sensible heat storage to produce electricity during peak energy demand, thereby making electricity more economical [4]. Latent heat storage can store energy at relatively low investment costs [5]. Because of the high energy densities of the PCM used in latent heat storage, there is a potential to reduce storage tank costs compared to sensible heat storage [6]. However, latent heat storage is still in the R & D phase to optimize the trade-off between reducing the cost of the PCMs and improving its thermal conductivity. Thermochemical storage is also still in the R & D phase. Because there are insufficient data on it, its economic feasibility has been examined through hypothetical models [7]. A widely used economic indicator to assess the economic feasibility of TES is the LCOE.

The LCOE is often evaluated while performing techno-economic assessments. To accurately perform a techno-economic assessment, a system boundary needs to be defined. The system boundary determines which components are included. A solar-based TES system boundary has three parts: solar field, storage block, and power block [8]. A study by Sioshansi et al. [4] showed that the size of the equipment in all three affect the economic viability of solar-based power generation systems (i.e., concentrated solar power). The solar field equipment includes mirrors, piping, pumps, valves, and parabolic troughs. The storage block consists of heat exchangers, pumps, piping, valves and storage tanks to store the heat transfer fluid. The power block includes a turbine, condenser, pumps, piping, and valves. The sizing of this equipment affects the investment cost of CSP plants. Several researchers estimated the LCOE and investment costs for

TES technologies using different system boundaries. Flueckiger et al. [9] evaluated the LCOE of a thermocline storage system by considering solar field, storage block, and power block as a system boundary. In addition to the aforementioned system boundary, Montes et al. [10] included an auxiliary natural gas-fired boiler for steam generation. However, a study by Heller et al. [11] evaluated the LCOE without considering the power block in the system boundary.

Other than through a system boundary, the LCOE can be evaluated as a function of capacity factor, solar multiple, storage duration, and plant capacity. Storage duration is defined as the length of time heat can be stored in a system. The ability of TES to store energy for long periods suggests greater economic viability as stored heat can be used to generate power during peak load when solar energy is absent or insufficient. As storage time increases, it gives the freedom to dispatch electricity when electricity prices are at their peak and thereby increase profit [4].

Another important factor in evaluating the LCOE is the solar multiple. The solar multiple is the ratio of thermal energy collected in the solar field to the thermal energy input for the turbine [12]. A solar multiple of one, for instance, indicates that the energy produced in the solar field is equal to the energy consumed by the turbine, leaving no excess energy to be stored [4]. A solar multiple of two, on the other hand, indicates that the energy produced in the solar field is twice that consumed by the turbine, leaving excess energy to be stored as heat for later use, thus making the technology more economical. However, the solar multiple is not the sole indicator of economic feasibility. The capacity factor is also used to evaluate economic viability. It is the ratio of actual energy produced to the theoretical energy produced per annum [12]. The capacity factor of TES would affect the LCOE because the energy produced from thermal storage can be sold in the form of electricity. Plant capacity can also be used to evaluate the LCOE. Plant capacity is measured in megawatts (MW) and is defined as the electrical power output that can be provided by the thermal storage system. The LCOE associated with varying plant capacity would demonstrate economies of scale. Thus, storage duration, capacity factor, solar multiple, plant capacity, and system boundary are few of the key factors to be considered when evaluating the LCOE to determine the economic feasibility of TES.

A few studies developed techno-economic models to examine the economics of TES technologies. These models can be classified into three types. Type 1 models examined the economics of sensible heat storage [13]. The costs of thermal storage for parabolic troughs and central tower solar field systems were evaluated by Turchi et al. [14] using the Solar Advisor Model (SAM) software and found to be less than 11 cents/kWh. In a similar study by Hinkley et al. [15], the LCOE was evaluated for both technologies using SAM software. Hinkley et al. [15] showed that at a higher operating temperature, there is a significant potential to reduce LCOE. SAM software performed a techno-economic assessment of TES using input parameters such as unit capital cost ($/kW) and storage duration [15]. Boudaoud et al. [13] evaluated the investment costs of individual equipment using first principles. The estimated LCOE values were approximately 0.66 – 0.78 $/kWh and 0.6 – 1.3 $/kWh, respectively, when storage duration and solar multiples were varied [13]. Lund et al. [16] examined the economics of a hybrid system integrating thermal storage with battery storage and liquid fuel storage within the system boundary. The hypothetical storage system proposed in Lund et al. [16]

aims to take a holistic approach by integrating cross-sector energy conversion technologies to address the needs of district heating and power generation. The Type 1 techno-economic assessments had different system boundaries and assumptions, making it difficult to compare them. Type 2 models examined the economics of latent heat storage [17]. Hubner et al. [18] evaluated the unit capital cost of various phase change materials to examine its effect on the LCOE. Xu et al. [5] used first principles to evaluate investment costs of individual equipment. The investment costs were used to estimate the LCOE for latent heat storage. Xu et al. [5] estimated the LCOE for various phase change materials to be approximately 0.098 – 0.10 $/kWh. Seitz et al. [17] estimated the LCOE by evaluating unit costs of equipment in the solar field, power block, and storage block. It is difficult to assess the models developed in the previous studies because the system boundaries, process conditions, and economic parameters are different. Type 3 models examined the economics of thermochemical storage [19]. Wenger et al. [20] evaluated the economics of a hypothetical electrochemical plant that considered a hybrid of both thermochemical and battery systems. The proposed plant aimed to reduce investment costs by replacing turbine systems with a battery system to generate electricity. Luzzi et al. [7] assessed the economic viability of thermochemical storage by evaluating the LCOE for a hypothetical power plant. Luzzi et al. [7] estimated the LCOE to be approximately 0.25 AUD/kWh (Australian dollar per kilowatt-hour) for a 10 MW hypothetical plant capacity.

Few studies assess the economic feasibility of TES. The purpose of this study is to develop a techno-economic model that concurrently compares the economic feasibility of sensible heat, latent heat, and thermochemical storage. To make an “apples-to-apples” comparison between TES technologies, moreover, the LCOE must be evaluated using a well-defined system boundary. For these reasons, comprehensive cost models for sensible heat, latent heat and thermochemical storage were developed in this study. This study focuses solely on the storage block, which is the study's system boundary. In other words, the LCOE calculated in this study does not include costs from the solar field or the power block. In addition, a sensitivity analysis of the LCOE was done by varying parameters, i.e., plant capacity, solar multiple, storage duration, discount rate, and capacity factor. The impact of these parameters on the LCOE was determined through an uncertainty analysis. There is limited work done on uncertainty analyses in literature. Hanel and Escobar [21] have considered the uncertainty of the levelized cost of electricity by varying parameters such as solar radiation, plant configuration, and solar field area. However, other key parameters such as storage duration, solar multiple, capacity factor, discount rate, and plant capacity are not considered in the uncertainty analysis. Filling the gaps would provide key information to industry and policy makers in decision making and in determining the economic viability of TES systems.

The main objective of this study is to conduct a comprehensive techno-economic assessment of sensible heat, latent heat, and thermochemical storage using a data-intensive bottom-up methodology. The specific objectives of this study are to:

1. Develop a techno-economic model to estimate the LCOE for sensible heat, latent heat, and thermochemical storage.
2. Conduct a comprehensive sensitivity analysis to assess the impact on the LCOE for sensible heat, latent heat, and thermochemical storage.

3. Conduct an uncertainty analysis using a Monte Carlo simulation to determine the uncertainty in the LCOE.

2.2 Methods

A detailed description of the solar-based thermal energy storage systems is presented in this section. The assumptions and the techno-economical models developed to evaluate the economic feasibility of the storage systems are also discussed. The heat transfer fluids in each system were selected based on their commercial availability and potential applications in concentrated solar power (CSP) generation [9, 19, 22, 23]. In the commercially implemented CSP plants, natural gas auxiliary heat is used to produce superheated steam when demand for electricity cannot be met from thermal storage [24]. Since the focus of this study is to evaluate the useful heat that can be delivered solely from thermal storage, an auxiliary heating system is not considered in this study.

2.2.1 Indirect sensible heat storage using two tanks (S1)

In two-tank indirect sensible heat storage, heat transfer fluids (HTF) such as synthetic oils, Dowtherm A©, and Therminol VP© are heated through parabolic troughs. The HTF used in parabolic trough technology can be heated to approximately 608 – 752 °F (320 - 400 °C) [25]. The system boundary illustrated in Figure 1 shows heated HTF as input in a temperature range of 608 – 752°F (320 - 400 °C). During peak demand, the HTF flows through the 3-way valve allowing the fluid to flow through heat exchanger #2. Subsequently, heat is extracted from the HTF to convert water into superheated steam. The HTF is then re-circulated back to the system to be reheated. During low energy demand, the HTF flows through heat exchanger #1, where excess heat from the HTF (synthetic oil) is transferred to heat up molten salt. The chemical mixture of molten salt is taken to be 60% sodium nitrate ($NaNO_3$) and 40% potassium nitrate (KNO_3) [26]. The heated molten salt is stored in a hot tank and the cold molten salt in a cold tank. The cold molten salt would have to be stored at approximately 554°F (290°C) to prevent the salt from solidifying [25]. During night-time, heat is then extracted from the hot molten salt by circulating through heat exchanger #1 where HTF is reheated to approximately 725 °F (385 °C). Subsequently, the HTF is circulated in heat exchanger #2 to convert water into superheated steam. The superheated steam has two applications, power generation and process heating. A report published by Siemens© provides inlet steam operating temperature and pressure for steam turbines used in concentrated solar power (CSP) plants [27]. Siemens© developed steam turbines for CSP technology with turbine capacities from 1 to 250 MW [27]. The maximum attainable inlet steam temperature and pressure are 1050 °F (565 °C) and 165 bar (2393 psi), respectively [27].

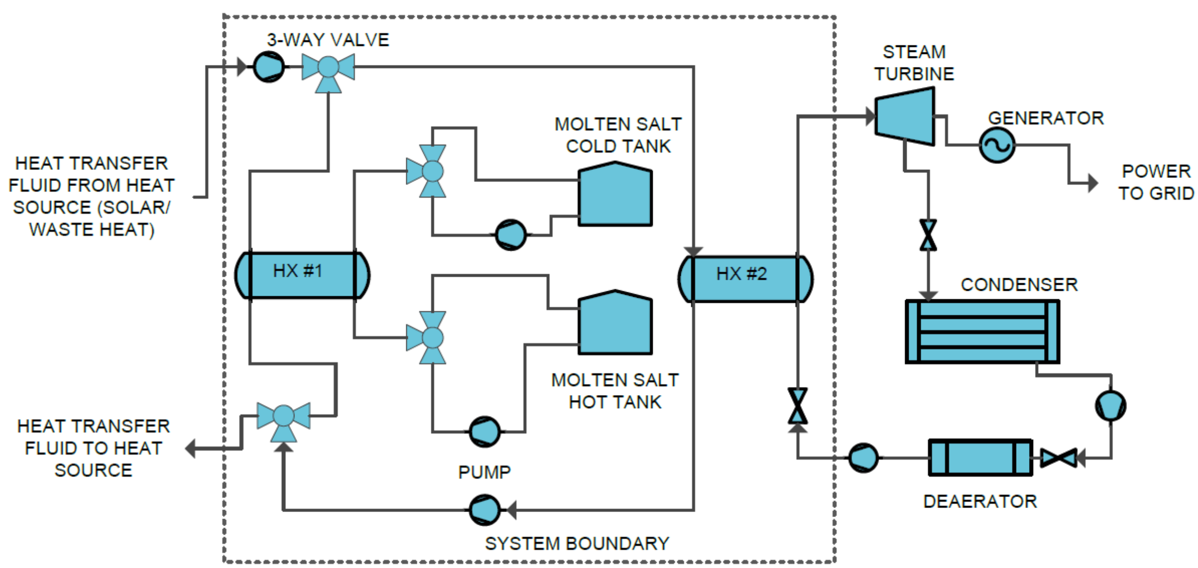

Figure 1: Schematic of two-tank indirect thermal storage (S1)

2.2.2 Direct sensible heat storage using two tanks (S2)

Two-tank direct sensible heat storage operates on the same principle as S1. However, one heat exchanger is used instead of two (see Figure 2). The elimination of a heat exchanger and pumps could reduce capital cost. Heat from the sun is directly concentrated onto a central tower, allowing direct heat transfer to heat molten salt. This direct heat transfer allows for a higher operating temperature of approximately 554 – 1050 °F (290°C – 565°C) [25]. In contrast, S1 requires an intermediate heat transfer medium such as synthetic oil that is heated to an operating temperature of approximately 608 – 752 °F (320 - 400 °C) [25].

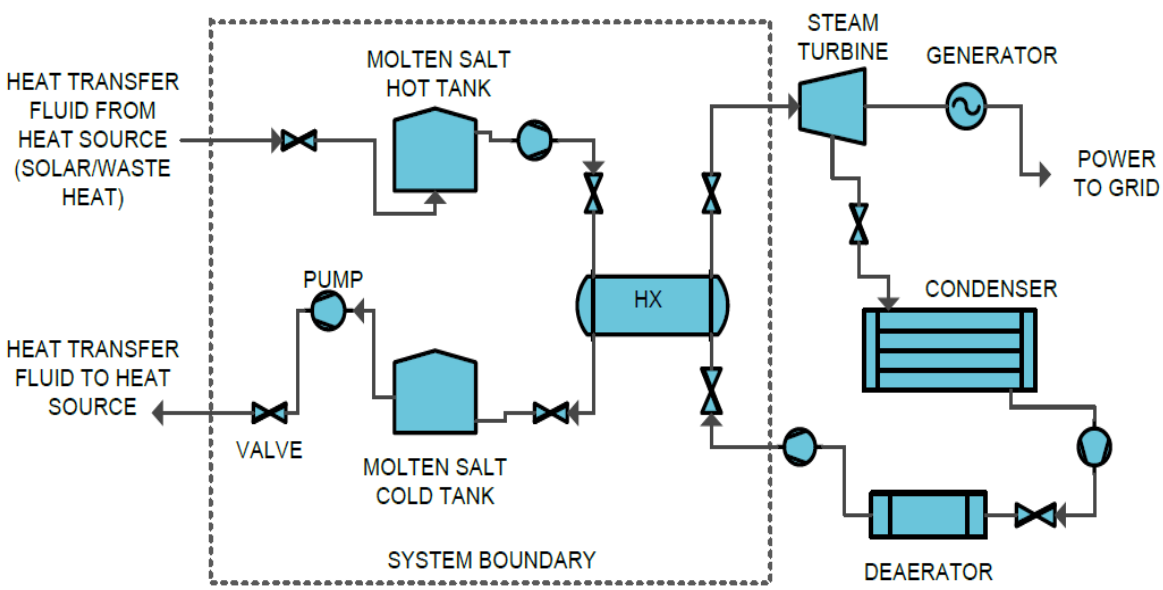

Figure 2: Schematic of two-tank direct sensible heat storage (S2)

2.2.3 Direct sensible heat storage using one tank (S3)

One-tank direct sensible heat storage, also known as thermocline storage, uses one tank to store both hot and cold molten salt. However, thermocline storage does not operate under steady state. In other words, as hot molten salt is pumped into the tank, cold molten salt is pump out and vice-versa. Figure 3 illustrates the single storage tank in which hot molten salt flows from the top while cold molten salt flows from the bottom. One of the advantages to thermocline storage is a reduced tank volume of approximately 66% from two-tank storage; this reduces the total amount of molten salt by 66% [28, 29].

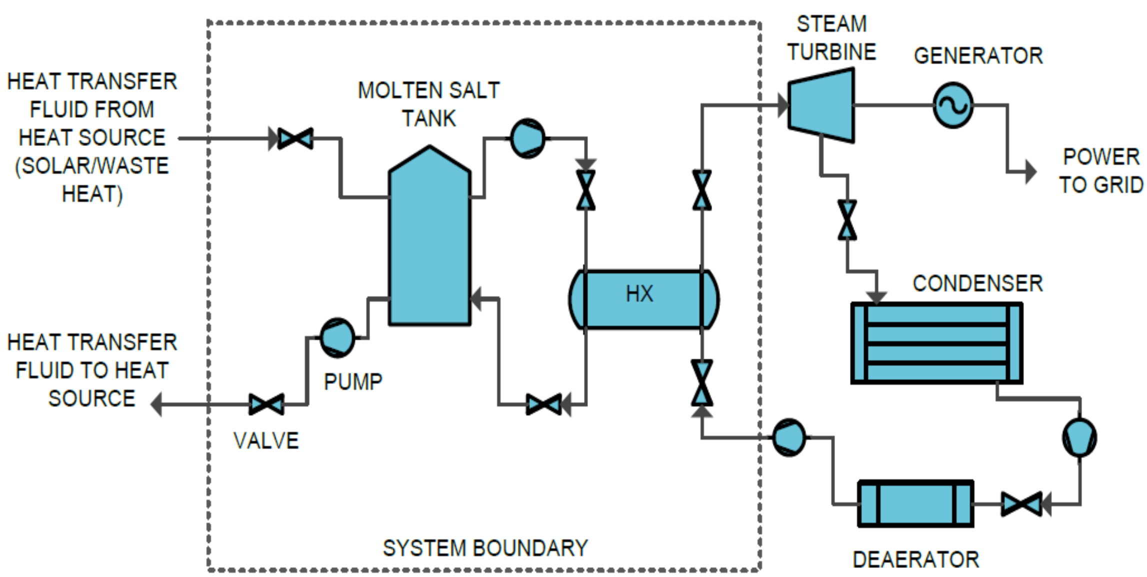

Figure 3: Schematic of one-tank direct sensible heat storage (S3)

2.2.4 Latent heat storage using one tank (S4)

In one-tank latent heat storage, phase change materials in the form of pellets are used as the heat transfer medium. The pellets change from solid to liquid when heat is absorbed from the sun. Subsequently, heat is released by reversing the phase change process from liquid to solid. This heat is used to convert water into superheated steam using a heat exchanger, as shown in Figure 4. Figure 4 outlines a schematic of one-tank latent heat storage where phase change materials in the form of pellets occupy the tank while the spaces between pellets are filled with molten salt. Kuravi et al. [29] reported that the phase change pellets occupy approximately 75% of the tank's volume, allowing the remaining volume to be filled with molten salt. Studies show that PCMs have higher energy densities than molten salt, resulting in an approximately 65% decrease in overall storage tank volume and a 30% decrease in storage material volume [30]. Smith et al. [30] reported a 40% reduction in cost for one-tank latent heat storage using PCMs as the storage medium compared to the widely used molten salt storage medium. The cost of thermal storage using PCM as the storage medium was calculated based on a 50% reduction in tank cost, a 30% reduction in storage material cost, a 50% reduction in cost for piping, and 40% cost reduction in construction materials [30].

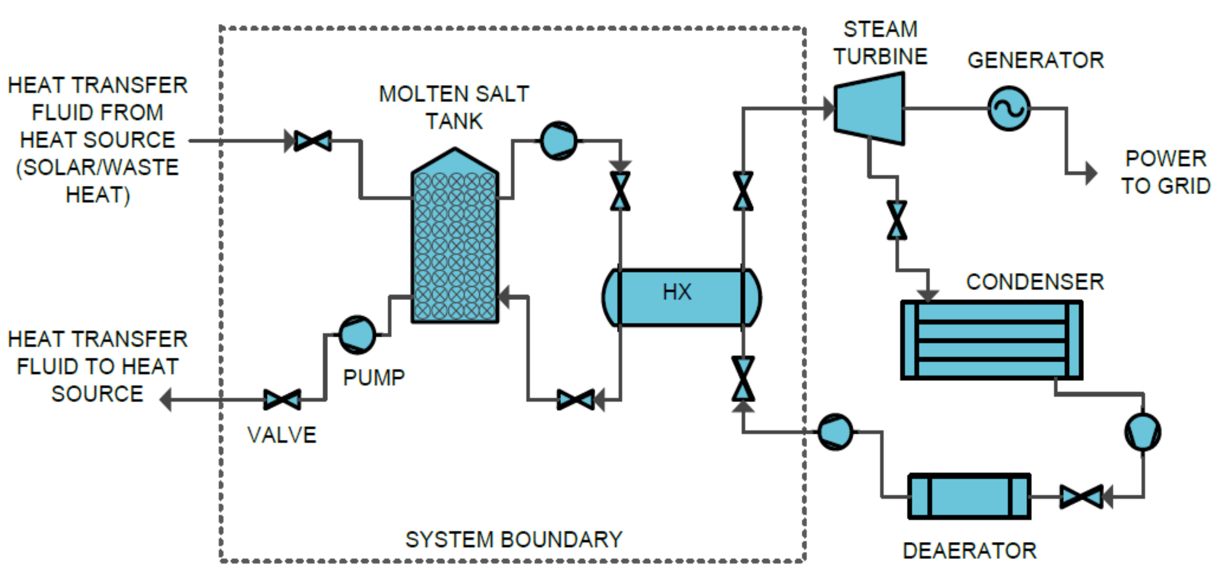

Figure 4: Schematic of one-tank latent heat storage (S4)

2.2.5 Thermochemical heat storage (S5)

Thermochemical energy storage was modelled in Aspen HYSYS [31], which simulated a reversible reaction through dissociation and synthesis of ammonia, as shown in the chemical formula below where ∆H represents reaction enthalpy:

$$\text{Endothermic dissociation reaction: } 2NH_3 + \Delta H \leftrightarrow N_2 + 3H_2$$

$$\text{Exothermic synthesis reaction: } N_2 + 3H_2 \leftrightarrow 2NH_3 + \Delta H$$

Figure 5 is a process flow schematic of thermochemical energy storage. In this scenario, a stream of pure ammonia in gaseous form is the input (labelled “1”). The input ammonia is assumed to be heated to approximately 1742 °F (950°C) and 2900 psi (20 MPa) using concentrated solar radiation. The mass flow of the input ammonia stream was calculated using mass and energy balance to be approximately 6.99×10^6 lb/hr (3.17×10^6 kg/h). The heated ammonia gas is diverted into a dissociation reactor labelled “GBR-100.” Studies show that the percentage of ammonia dissociation is directly proportional to high temperatures and high pressures [19]. The dissociated gas mixture of hydrogen and nitrogen is cooled to 77 °F (25 °C) by liquid ammonia in a heat exchanger below (labelled “E-100”) before being stored in a two-phase high-pressure tank (labelled “V-100”) [19]. The two-phase tank can store this gas mixture for long periods with minimal heat loss; this is a major advantage of thermochemical energy storage. To generate heat, the gas mixture is preheated in a heat exchanger (labelled “E-102”) to around 527 °F (275 °C). The resulting hot gas mixture is diverted into a synthesis reactor (“CRV-100”) where ammonia is produced in the presence of a catalyst. This synthesis reaction is highly exothermic and releases large amounts of heat that are used to convert water into high-pressure superheated steam at approximately 806 °F (430 °C) and 1500 psi (10MPa) [7]. The high-pressure steam can be used for power generation or process heating.

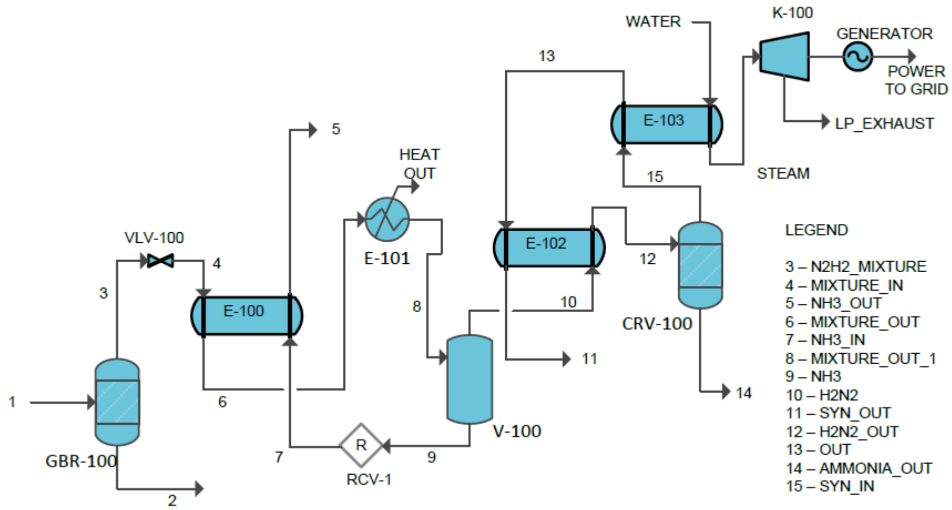

Figure 5: Thermochemical energy storage (S5)

2.2.6 Cost estimation

The methodology used in this study has three parts. First, technical parameters such as mass flow rate, heat transfer rate, and pressure drop across equipment were computed. Second, individual equipment costs were computed along with a sensitivity analysis and an uncertainty analysis (using a Monte Carlo simulation). Third, a comprehensive cost model was developed using the assumptions listed in Table 1. The total investment cost was estimated in a cost model by calculating individual equipment purchased and installed (P&I) cost as outlined in Table 2. All costs are evaluated in 2016 US dollars. The equipment P&I costs were calculated using equations reported by Gabbrielli et al. [32]. Their equations require parameters such as pump power, pump efficiency, heat exchanger area, and heat exchanger pressure drop. These parameters were calculated using the first principles of mass and energy balance to compute mass flow rates and pressure drop across equipment (heat exchangers, pumps, steam turbines). Furthermore, Excel-based spreadsheets were integrated with Aspen HYSYS to determine parameters such as heat transfer rate, mass flow rate, heat exchanger area, and pressure drop pertaining to unit operations.

Table 1: Assumptions for cost estimation and LCOE calculation

Assumptions	Parameter values	Refs.
N (yrs)	30	[33]
Inflation (2010 to 2016)	2.0%	[34, 35]
n (yrs) due to inflation from 2010[2]	6	
Variable O&M escalation per annum	2.5%	[36]
Variable O&M cost (% of investment cost)	2%	[33]
Fixed O&M cost (% of investment cost)	2%	[33]

[2] Number of years (*n*) due to inflation is taken as the difference between years 2016 and 2010

Table 2: Parameters considered for bottom-up cost estimation [32]

Components for bottom-up cost estimation	Cost estimation parameter values
Equipment purchase and installed (P&I) cost	Sum of individual equipment cost
Other miscellaneous equipment (i.e., piping, valves, deaerator)	10% of equipment of P&I cost
Process building cost ($)	Material cost (10% of P&I cost) Labour cost @$25.18/hr (5% of material cost)
Service building cost ($)	Material cost (7.5% of P&I cost) Labour cost @$25.18/hr (5% of material cost)
Service system cost ($)	Material cost (10% of P&I cost)

	Labour cost @$25.18/hr (2% of material cost)
Site development cost ($)	Material cost (1% of subtotal P&I cost) + land (2% of subtotal P&I cost) + freight cost (2% of subtotal P&I cost) + labour cost (2% of material cost)
Total indirect cost ($)	Contractor's cost (12% of direct cost) + owner's cost (5.6% of direct cost) + fees and insurance (8% of direct cost)
Contingency cost (3% of direct cost)	3% of direct cost
Total investment cost ($)	Summation of above costs

2.2.6.1 Mass flow rate requirement in condensing steam turbine

Mass flow rate of steam ($\dot{m}$) is calculated based on the capacity ($\dot{W}$) measured in MW, and the rate of heat loss ($\dot{Q_{\text{loss}}}$) in the steam turbine is assumed to be negligible [37]. The capacity can be computed by considering conservation of mass and energy within the turbine, and the equation for conservation of energy is shown in the equation below:

$$\dot{W} = \dot{m}(h_1 - h_2) + \dot{m}(\Delta E_{\text{k}}) + \dot{m}(\Delta E_{\text{p}}) + \dot{Q_{\text{loss}}}. \quad (1)$$

The isentropic efficiency is taken to be 70% and the expression for it is given in Equation 2 [37, 38]. The isentropic efficiency is the ratio of the actual rate of work done by the turbine (i.e., capacity) and the maximum possible rate of work done by the turbine. The maximum possible rate of work done is represented by the isentropic expansion of steam in the turbine ($h_1 - h_{2,\text{s}}$). The actual expansion of steam in the turbine ($h_1 - h_2$) corresponds to the actual rate of work done [37, 38]. The turbine losses are accounted for by computing the actual output enthalpy (h_2) using the isentropic efficiency ($\eta_{\text{isentropic}}$), whose expression is shown in Equation 2:

$$\eta_{\text{isentropic}} = \frac{h_1 - h_2}{h_1 - h_{2,\text{s}}}, \tag{2}$$

where h_1, h_2, $h_{2,\text{s}}$, ΔE_{k}, and ΔE_{p} represent the input enthalpy, actual output enthalpy, isentropic output enthalpy, change in kinetic energy, and change in potential energy, respectively for the steam turbine. The change in kinetic energy is assumed to be zero as the steam turbine operates at steady state conditions. The change in potential energy for the steam turbine is zero as the change in elevation is negligible.

2.2.6.2 Heat exchanger energy balance

The heat transfer rate ($\dot{Q}$) in the heat exchangers was calculated using the following energy balance equation, where T and t represent the temperatures of molten salt (also known as solar salt) and heat transfer fluid (HTF), respectively. Consequently, c_{p} and $\dot{m}$ represent the specific heat capacity and mass flow rate, respectively for molten salt and HTF as shown in Equation 3. The HTF can be either Dowtherm A or Therminol VP [37]:

$$\dot{Q} = \left[\dot{m}c_{\text{p}}(T_2 - T_1)\right]_{\text{molten salt}} = \left[\dot{m}c_p(t_2 - t_1)\right]_{\text{HTF}} \tag{3}$$

2.2.6.3 Heat exchanger area

Heat transfer area is calculated using the following equation [39]:

$$\dot{Q} = UA(\Delta T_{\text{LM}}) \tag{4}$$

where $\dot{Q}$, U, A, and ΔT_{LM} represent the heat transfer rate, overall heat transfer coefficient, total heat transfer area, and log mean temperature difference, respectively.

The log mean temperature difference can be computed using Equation 5 [40].

$$\Delta T_{\text{LM}} = \frac{(T_{1,\text{in}} - t_{2,\text{out}}) - (T_{2,\text{out}} - t_{1,\text{in}})}{ln\left(\frac{T_{1,\text{in}} - t_{2,\text{out}}}{T_{2,\text{out}} - t_{1,\text{in}}}\right)}, \tag{5}$$

where, T_1 and t_2 represent the fluids in the shell side and tube side, respectively. The subscripts "in" and "out" represent the inlet and outlet temperatures in the heat exchanger, respectively.

2.2.6.4 Estimation of overall heat transfer coefficient

The overall heat transfer coefficient was estimated by using the following equation [38]:

$$\frac{1}{U} = \frac{1}{h_{\mathrm{fluid},1}} + \left[\frac{1}{2\pi kL}\ln\left(\frac{r_{\mathrm{o}}}{r_{\mathrm{i}}}\right)\right] 2\pi r_{\mathrm{o}} L + \frac{1}{h_{\mathrm{fluid},1}}, \tag{6}$$

where U, k, L, $h_{\mathrm{fluid},1}$, r_{o}, and r_{i} represent the overall heat transfer coefficient (W/m^{2}·K), thermal conductivity (W/m·K), length of cylindrical wall (m), convective heat transfer coefficient (W/m^{2}·K), outer radius (m), and inner radius (m), respectively. The overall heat transfer coefficient for the heat exchange between molten salt and water to generate superheated steam can be computed by substituting the convective heat transfer coefficients of molten salt and boiling water into Equation 6. The convective heat transfer coefficients for molten salt at 575^{o}C and boiling water were taken to be 10000 W/m^{2}·K [41] and 50000 W/m^{2}·K [42], respectively. Similarly, the overall heat transfer coefficient for the heat exchange between molten salt and synthetic oil (i.e., Dowtherm A©/Therminol©) can be computed by substituting the convective heat transfer coefficients for synthetic oil and molten salt in Equation 6. Consequently, the convective heat transfer coefficient of synthetic oil (i.e., Dowthem A©/Therminol VP©) at 375^{o}C was taken to be 1400 W/m^{2}·K [43]. The thermal conductivity of stainless steel 304 at 400^{o}C and 575^{o}C were taken to be 20 and 23 W/m·K, respectively [44]. The above methodology was used to estimate the overall heat transfer coefficient in S1 – S4. The overall heat transfer coefficient in S5 was calculated within Aspen HYSYS.

Upon computing heat exchanger area, mass flow rate, heat transfer rate and pressure drop pertaining to unit operations, the total purchase and installed (P&I) cost of individual equipment were calculated. The LCOE was then evaluated for sensible heat, latent heat, and thermochemical storage. A comprehensive evaluation of the LCOE can be carried out using discounted cash flow analysis, which considers input parameters such as capacity factor, discount rate, plant capacity (MW), operation and maintenance (O&M) costs, total life (years), total investment cost ($ in USD), and total energy produced (kWh). Equation 7 outlines an expression, derived in Appendix A, for the LCOE using a discounted cash flow, which mathematically correlates the above parameters as follows:

$$LCOE = \frac{\left(C*(1+D)\right)+\left((C*0.02)*\left(\frac{1-\left(\frac{1+G}{1+D}\right)^{N}}{1-\left(\frac{1+G}{1+D}\right)}\right)\right)+\left((C*0.02)*\left(\frac{1-\left(\frac{1}{1+D}\right)^{N}}{1-\left(\frac{1}{1+D}\right)}\right)\right)}{\left(\frac{1-\left(\frac{1}{1+D}\right)^{N}}{1-\left(\frac{1}{1+D}\right)}\right)*(Energy)} \quad (7)$$

$$Energy\ = (MW)*(Storage\ duration)*(SM)*(capacity\ factor)*365*1000 \quad (8)$$

Where *LCOE, energy, MW,* and *SM* correspond to the levelized cost of electricity, total energy produced, plant capacity, and solar multiple, respectively. *C, D, G,* and *N* correspond to total purchase and installed (P&I) investment cost, discount rate, variable O&M escalation, and total asset life (years), respectively. The process of calculating the LCOE using a discounted cash flow analysis was performed with the following assumptions:

2.2.6.5 Assumptions to compute LCOE

1) The total energy produced is assumed to be constant over the life cycle
2) The total energy is assumed to be generated 365 days per annum

2.2.7 Uncertainty Analysis

The overall uncertainty in each of the systems was evaluated by considering the thermodynamic and economic parameters. A rigorous data-intensive model was developed in this study to evaluate the process conditions of each system by varying parameters such as plant capacity, storage duration, solar multiple, and capacity factor. Economic uncertainty, however, was evaluated by varying parameters such as discount rate and total plant life (*N*).

2.3 Results and discussion

Thermal energy storage (TES) systems can be sized using a few key parameters, namely, storage duration, capacity factor, solar multiple, and plant capacity. These parameters were given a base value, as shown in Table 3. The base case was selected from values commonly used in the industry. A base case of 50 MW was chosen for S1 based on an existing plant [45]. Subsequently, a base case of 100 MW was selected for S2 – S5 because the largest turbine capacity commercially operating is approximately 133 MW [46]. Furthermore, eight hours of storage time is commonly achieved commercially, along with a capacity factor of approximately 40%. Capacity factors of plants with thermal energy storage implemented commercially are typically 20% to 60% [47]. Solar multiple figures were also selected from values found in existing commercial plants, and they range from 1.5 to 2 [47].

Table 3: Base case parameter values

Base case parameters	S1[3]	S2 – S5	Refs.
Plant capacity (MW)	50	100	[45], [46]
Storage duration (hrs)	8	8	[47]
Solar multiple	1.75	1.75	[47]
Capacity factor (%)	40%	40%	[47]
Discount rate (%)	10	10%	[33]
Labour cost ($/hr)	$25.18	$25.18	[48]

[3]S1: two-tank indirect sensible heat storage; S2: two-tank direct sensible heat storage; S3: one-tank direct sensible heat storage; S4: latent heat storage; S5: thermochemical storage

The mass and energy balance was used to calculate the technical parameters of individual equipment (listed in Tables 4 - 6). As shown in Table 4, the inlet pressure and temperature in S1 are different from those in the other scenarios. Limitations to inlet steam pressure and temperature occur because of the maximum temperature to which molten salt can be heated in S1 is approximately 390 °C (734 °F). For this reason, the HTF (i.e., synthetic oil) in S1 can be heated to a temperature of approximately 385 °C (725 °F) using molten salt [25].

Table 4: Base case values for condensing steam turbine

Condensing steam turbine parameters	S1[4]	S2	S3	S4	S5	Refs.
Inlet pressure MPa (psia)	10 (1450)	16.5 (2393)	16.5 (2393)	16.5 (2393)	10 (1500)	[27]
Inlet temperature °C (°F)	377 (710.6)	552 (1025)	552 (1025)	552 (1025)	430 (806)	[27]
Outlet pressure kPa (psia)	103 (15)	103 (15)	103 (15)	103 (15)	0.137 (0.02)	[27]

Outlet temperature	100	100	100	100	-19	[27]
°C (°F)	(213)	(213)	(213)	(213)	(-3.68)	
Steam mass flow rate[4]	92	138	138	138	84	
kg/s (klb/hr)	(734)	(1094)	(1094)	(1094)	(665)	
Turbine losses	30%	30%	30%	30%	30%	[37]
Generator efficiency	95%	95%	95%	95%	95%	[38]

[4]S1: two-tank indirect sensible heat storage; S2: two-tank direct sensible heat storage; S3: one-tank direct sensible heat storage; S4: latent heat storage; S5: thermochemical storage; Steam mass flow rate is computed using Equation 1

Another key aspect to S1 is noted in Table 5 as no values are calculated for S2 - S4. The parabolic trough technology used in S1 requires an intermediate HTF (such as Dowtherm A©), which requires an additional heat exchanger where heat from the molten salt is transferred to the HTF. This heat can be used to convert water into superheated steam for expansion in the steam turbine. The absence of an additional heat exchanger means that no values need to be calculated for S2 – S4.

Table 5: Base case values for HTF (Dowtherm A©/Therminol VP©) heat exchanger

HTF heat exchanger parameters	**S1[5]**
Heat transfer coefficient (U) W/m2-K (btu/(hr ft^2 °F))	1201 (211)
T1 (for salt) °C (°F)	390 (734)
T2 (for salt) °C (°F)	293 (559.4)
t1 (for HTF) °C (°F)	290 (554)
t2 (for HTF) °C (°F)	385 (725)
Cp of HTF kJ/kg-K (btu/lb °F)	2.4 (0.58)
Pressure MPa (psia)	4 (580)
Salt mass flow rate kg/s (klb/hr)	1068 (8478)

[5]S1: two-tank indirect sensible heat storage

As noted in Table 6, the temperature of salt for S2 - S4 is 1050 °F (565 °C), well above the 734°F (390 °C) in S1. This is because S2 - S4 use solar power tower technology in which a centralized tower absorbs concentrated heat from surrounding mirrors. One of the key advantages of this technology is the ability to heat molten salt to a temperature of approximately 1050°F (565 °C) [25].

Table 6: Base case values for evaporation heat exchanger

Evaporation heat exchanger parameters	**S1[6]**	**Evaporation heat exchanger parameters**	**S2**	**S3**	**S4**
Overall heat transfer coefficient (U) W/m^2-K (btu/hr ft^2 °F)	1238 (218)	Overall heat transfer coefficient (U) W/m^2-K (btu/hr ft^2 °F)	4594 (809)	4594 (809)	4594 (809)
t1 (for HTF in shell) °C (°F)	385 (725)	t1 (for salt in shell) °C (°F)	565 (1050)	565 (1050)	565 (1050)
t2 (for HTF in shell) °C (°F)	290 (554)	t2 (for salt in shell) °C (°F)	290 (554)	290 (554)	290 (554)
T1 (for water in tube) °C (°F)	30 (86)	T1 (for water in tube) °C (°F)	30 (86)	30 (86)	30 (86)
T2 (for water in tube) °C (°F)	377 (710.6)	T2 (for water in tube) °C (°F)	552 (1025)	552 (1025)	552 (1025)
Cp of HTF kJ/kg-K (btu/lb °F)	2.4 (0.58)	Cp of salt (btu/lb °F)	1.5 (0.358)	1.5 (0.358)	1.5 (0.358)
Pressure MPa (psia)	10 (1450)	Pressure MPa (psia)	16.5 (2393)	16.5 (2393)	16.5 (2393)
Water mass flow rate kg/s (klb/hr)	92 (734)	Water mass flow rate kg/s(klb/hr)	138 (1094)	138 (1094)	138 (1094)
HTF mass flow rate kg/s (klb/hr)	1227 (9739)	Salt mass flow rate kg/s (klb/hr)	1147 (9103)	1147 (9103)	1147 (9103)

[6]S1: two-tank indirect sensible heat storage; S2: two-tank direct sensible heat storage; S3: one-tank direct sensible heat storage; S4: latent heat storage; S5: thermochemical storage

The LCOE is an important factor that is often used for comparing the economic viability of technologies. To compare the LCOE for the scenarios in Table 7, it is important to understand the definition of LCOE. The LCOE is the price at which electricity would have to be sold to offset the total investment over the total plant life cycle. Often mature fossil fuel technologies have a low LCOE in the range of approximately 6 to 8 cents/kWh [49]. To compete with fossil fuels, the US Department of Energy devised a goal to reduce the LCOE for thermal storage to around 2 cents/kWh by 2020 [2]. A disadvantage to using solar as a renewable energy source is its intermittency, which results in a higher LCOE to produce electricity. The inability to supply energy during peak demand using solar energy increases the LCOE. Thus, thermal energy storage technologies such as sensible heat, latent heat, and thermochemical storage can bridge the gap between energy demand and energy supplied during peak loads and lower the LCOE.

Furthermore, the LCOE is affected by the total investment cost of individual thermal storage scenarios, as shown in Table 7. S1 uses parabolic troughs, which is the most mature technology and thus the most widespread commercially. However, the LCOE of 61 cents/kWh (as shown in Table 7) demonstrates the need to implement other forms of thermal storage technologies. It is imperative to note that the LCOE for S1 includes the cost of an extra heat exchanger, which includes extra pumps, piping, and valves. Synthetic oils are another cost incurred in S1 that contribute to a higher total investment cost. The component costs of an extra heat exchanger, heat transfer fluid pumps, along with the cost of synthetic oils, amount to approximately $93 million, as calculated through an Excel-based model. The cost of synthetic oils makes up nearly

83%, which is $78 million. This is because of the high cost of synthetic oil, which is approximately $2.2/kg [50].

The LCOE for S2 was calculated to be approximately 10 cents/kWh. S2 uses centralized tower technology with concentrated solar power (CSP). The overall component cost in S2 was calculated to be approximately $46 million. This cost is significantly lower than the component cost of S1 since no additional heat exchanger or pumps are required. The major portion of the component cost incurred in S2 is the cost of molten salt, which is approximately $36 million. The raw material per unit cost of molten salt used in the calculation is $1.08/kg [26].

The lower LCOE of approximately 7 cents/kWh for S3 is because of the lower total investment cost. As shown in Figure 3, the configuration requires only one tank for storing both hot and cold molten salts. Advantages of this configuration are lower storage tank and molten salt costs. Studies show that a configuration with one storage tank results in a savings of approximately 33% in required molten salt [9]. Additionally, the cost of the storage tank falls by approximately 66% [29].

Figure 4 illustrates a configuration for S4 where phase change materials (PCM) in the form of pellets fill a single storage tank and gaps are filled with molten salt. One of the key advantages to using PCMs is their high energy density compared to molten salt. This high energy density means less molten salt is required, as pellets would occupy approximately 75% of the tank volume [29], leaving only 25% molten salt. The cost of the PCM used to calculate material cost is approximately $3.21/kg [5]. The cost of the storage tank is reduced by approximately 66% along with an increase in PCM cost per unit cost

[29]. This results in a relatively high LCOE, which was calculated to be approximately 19 cents/kWh.

The LCOE for S5 was calculated to be approximately 44 cents/kWh, as shown in Table 7. This high cost is likely due to the high investment cost of approximately $600 million. The cost of ammonia used as the working fluid is approximately $100 to $920 per tonne [51]. The high cost of ammonia used increased both the investment cost and the LCOE for thermochemical storage. Another component that contributes to high investment cost is the ammonia pump. A mass flow of input ammonia stream was taken to be approximately 6.99×10^6 lb/hr (3.17×10^6 kg/h), which requires a high capacity pump.

As noted at the start of the chapter, that the LCOE was calculated for thermal energy storage; it does not include the cost of the solar field or power generation components. A report published by the International Renewable Energy Agency (IRENA) suggests that capital costs for solar field and power generation components add nearly 53% to the total investment cost [52]. Thus, the LCOE shown in Table 7 would increase proportionately if the capital cost of solar field components and power generation components are included.

Table 7: LCOE and capital cost summary for the base case

Costs	S1[7]	S2	S3	S4	S5
Total investment cost ($ millions)	410	135	89	255	600
LCOE (cents/kWh)	61	10	7	19	44

[7]S1: two-tank indirect sensible heat storage; S2: two-tank direct sensible heat storage; S3: one-tank direct sensible heat storage; S4: latent heat storage; S5: thermochemical storage

2.3.1 Sensitivity analysis

To analyze the effect of individual parameters on a given output parameter, a sensitivity analysis was performed. The sensitivity plot for S1 (Figure 6) shows that the most sensitive parameters are solar multiple and capacity factor while the second most sensitive parameter is material cost variation, thus implying solar multiple, capacity factor, and material cost would have a significant impact on the LCOE given in equations 4 and 5. In contrast, the sensitivity plots for S2 - S4 (shown in Figures 7 through 9) correspond to a solar tower configuration where solar multiple, storage duration, capacity factor, and material cost variation are highly sensitive to LCOE. One of the primary reasons is that the solar tower configuration entails direct heat transfer from solar heat to the molten salt. Subsequently, it can be noted from the plots that parameters such as discount rate, plant capacity, and labour cost have relatively little impact on the LCOE. The most sensitive factors in thermochemical storage (S5), as illustrated in Figure 10, are solar multiple and capacity factor. Storage duration, however, was found to be the second most sensitive parameter.

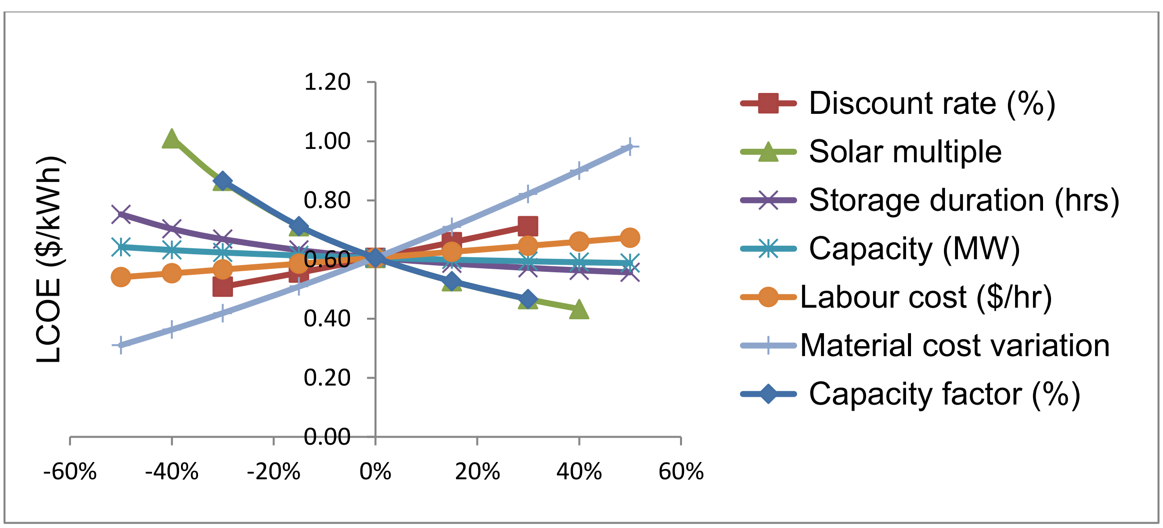

Figure 6: LCOE sensitivity plot for two-tank indirect sensible heat storage (S1)

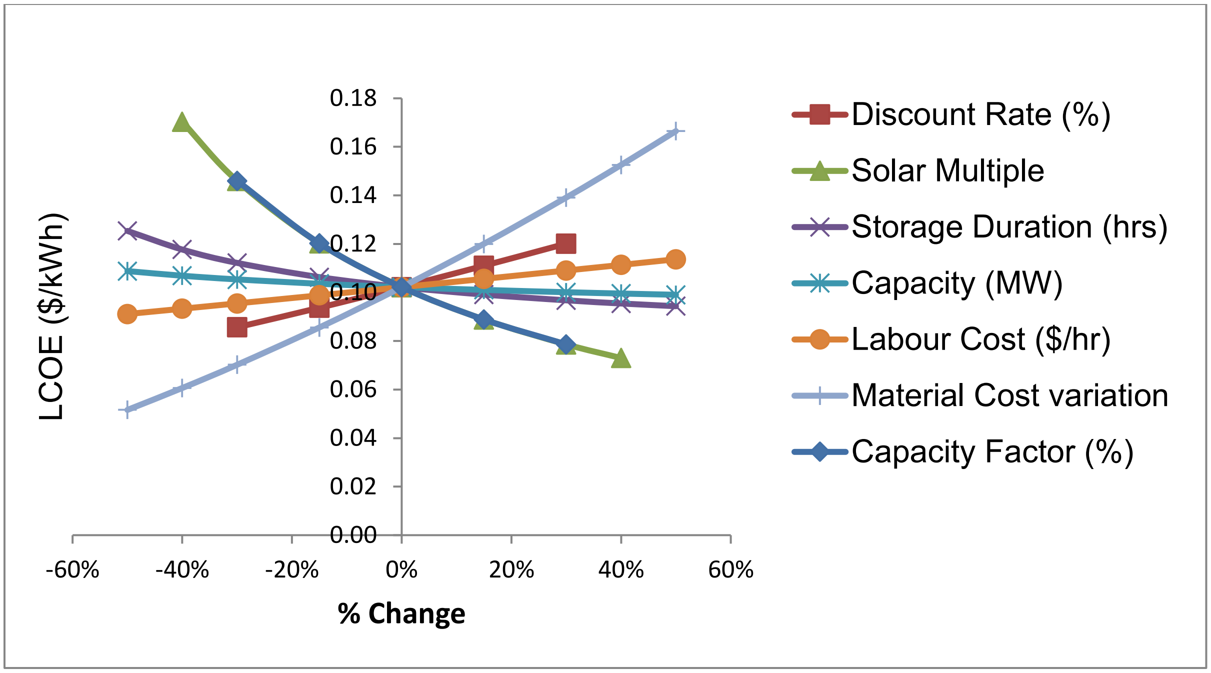

Figure 7: LCOE sensitivity plot for two-tank direct sensible heat storage (S2)

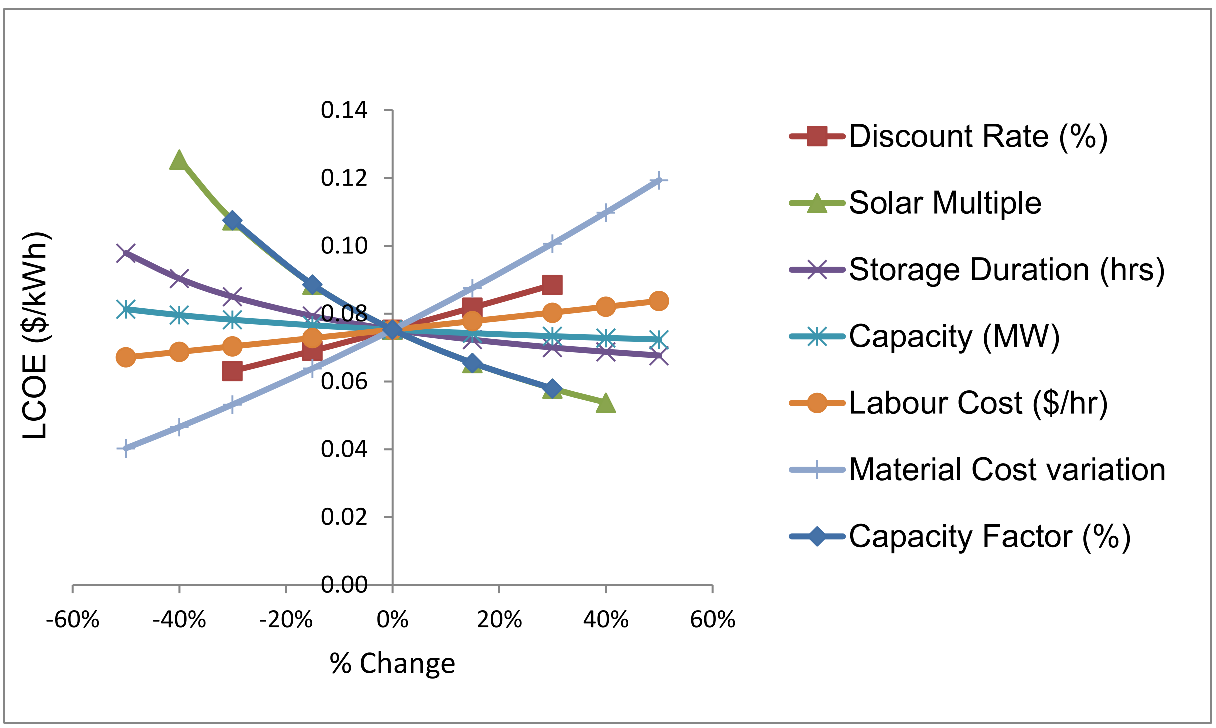

Figure 8: LCOE sensitivity plot for one-tank direct sensible heat storage (S3)

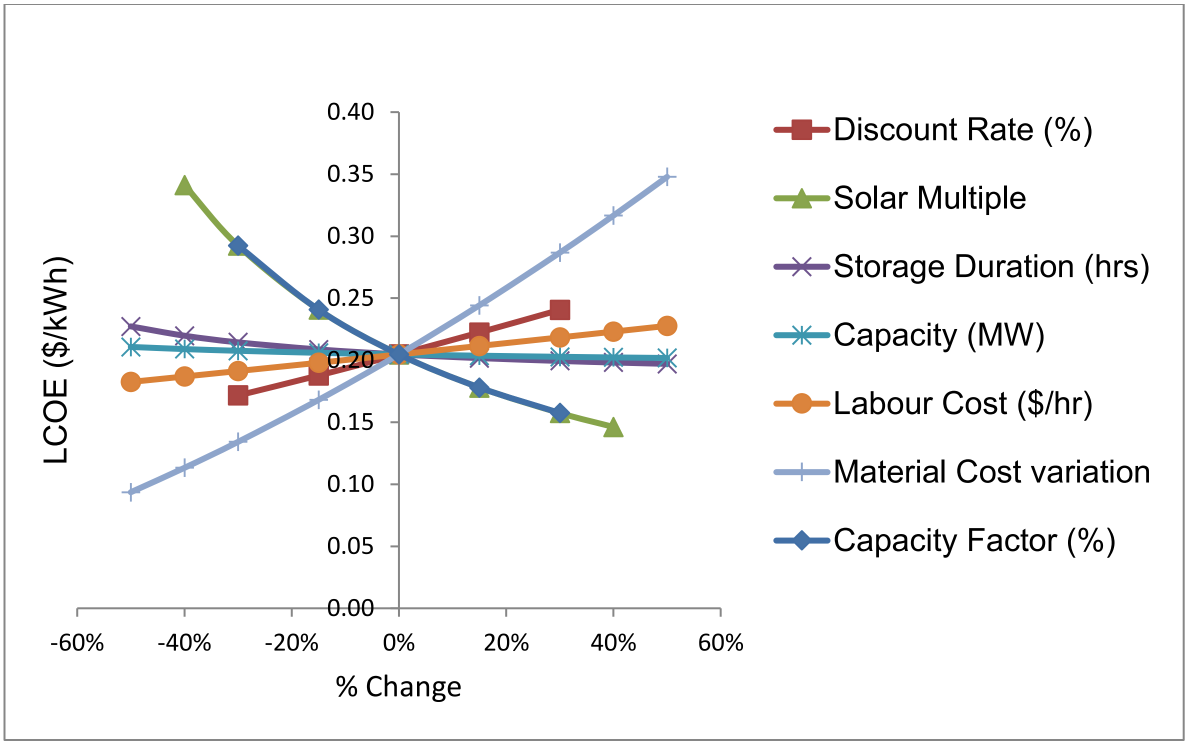

Figure 9: LCOE sensitivity plot for latent heat storage (S4)

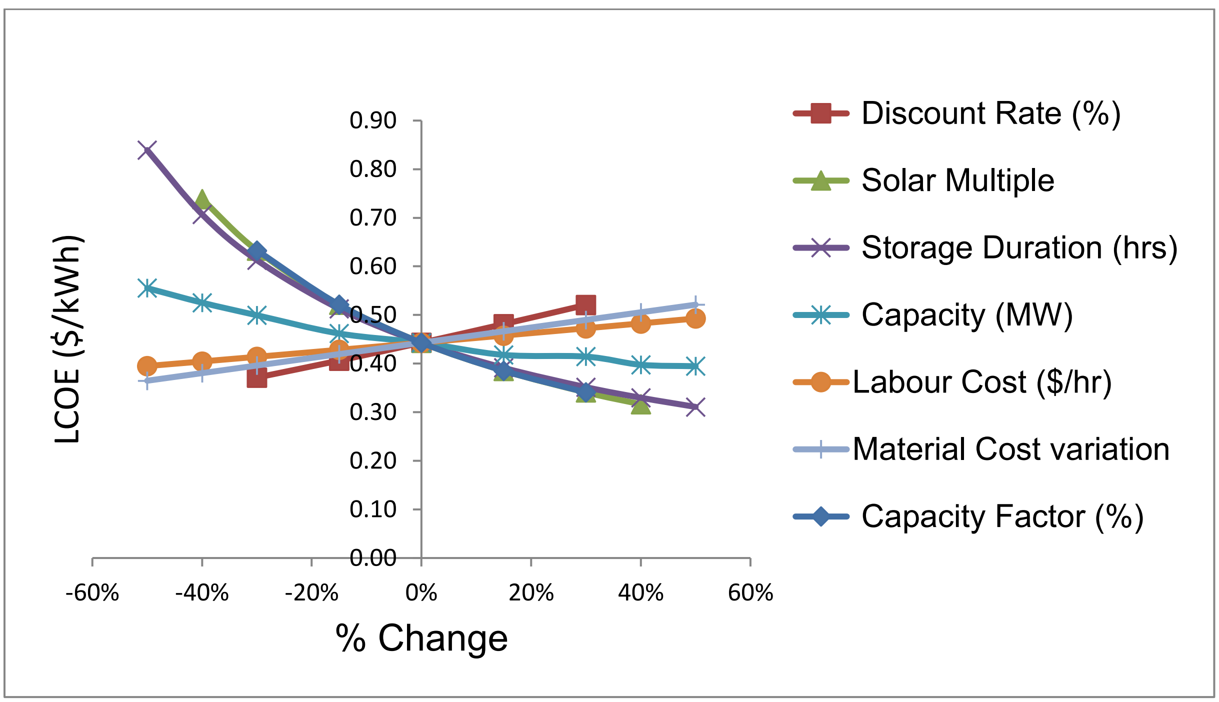

Figure 10: LCOE sensitivity plot for thermochemical storage (S5)

2.3.2 Scenario optimization

The optimization of thermal energy storage is a key aspect to competing with mature fossil fuel technologies with low LCOEs. The optimization process adopted in this study uses correlations reported by the International Renewable Energy Agency (IRENA) [47]. The sensitive parameters identified in the prior discussion (plant capacity, storage duration, solar multiple, and capacity factor) are considered in the optimization process. For S1, the parabolic trough configuration, the lowest cost is reached at nine hours of storage (see Figure 11). Figure 12 shows that nine hours of storage reach its lowest value when the solar multiple is 2.5. A capacity factor of approximately 45% corresponds to nine hours of storage and 2.5 solar multiple (shown in Figure 13). Lastly, the change in LCOE for plant capacity higher than 180 MW is not significant. Thus, 180 MW is the optimized capacity for S1.

In contrast, S2 - S5 corresponds to a solar tower configuration. Figure 11 suggests 13.4 hours of storage duration to minimize cost. The optimal solar multiple and capacity factor were determined to be 3 and 55%, respectively and the optimal capacities for S2 - S5 were deduced to be 130 MW, 135 MW, 120 MW and 190 MW, respectively. Table 8 gives the optimized parameters for all scenarios.

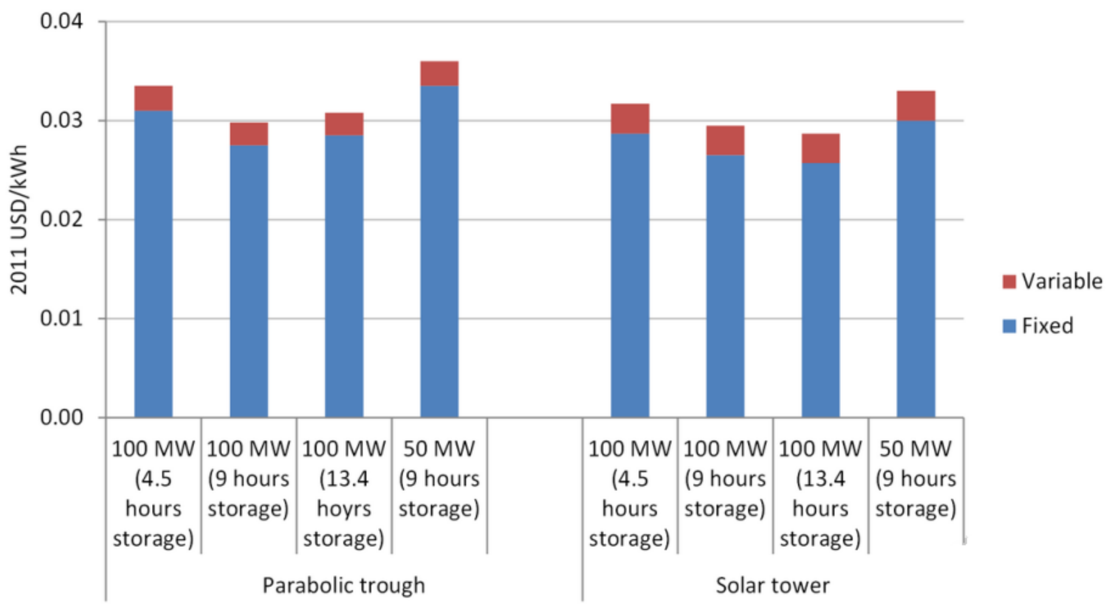

Figure 11: Parabolic trough and solar tower cost comparison [53]

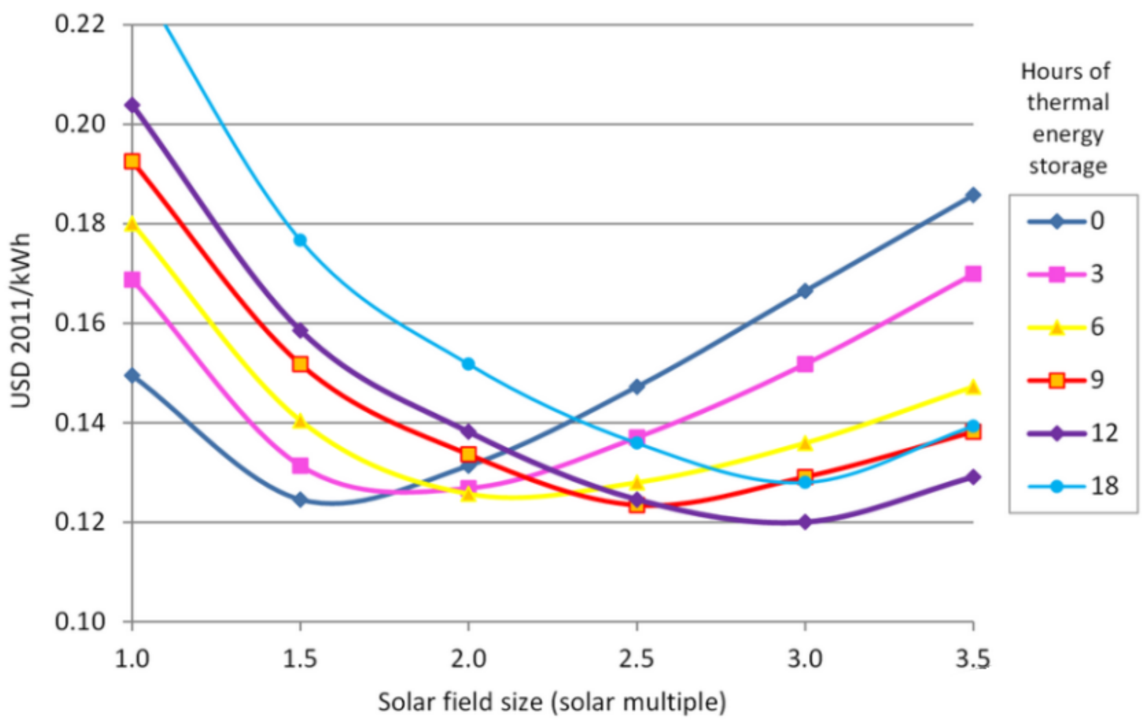

Figure 12: Correlation between solar multiple and hours of storage [54]

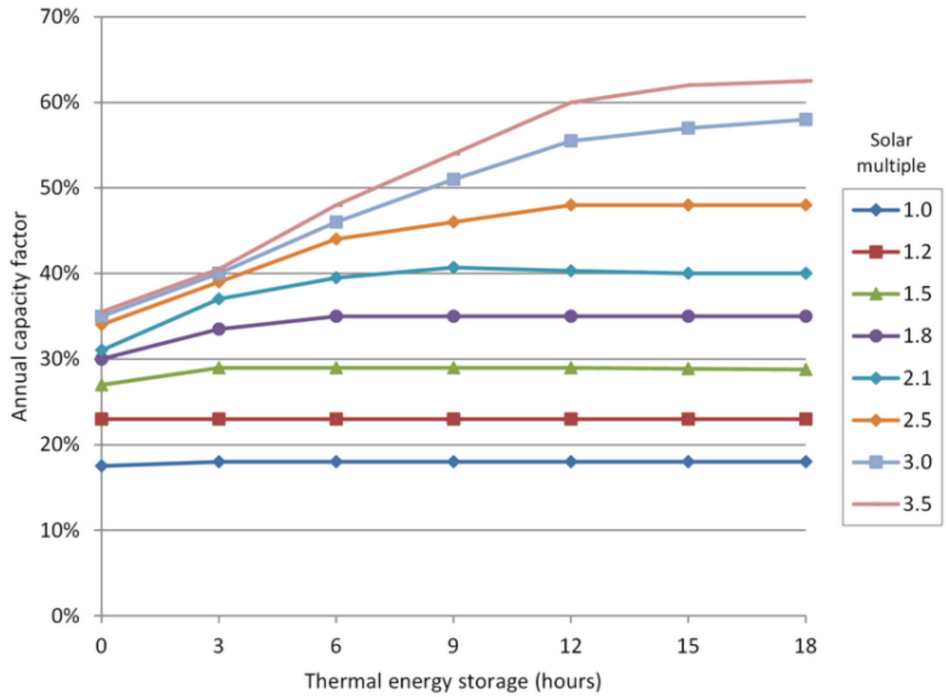

Figure 13: Correlation between solar multiple and capacity factor [55]

Table 8: Optimized parameter values

Optimized parameters	**S1[8]**	**S2**	**S3**	**S4**	**S5**
Capacity (MW)	180	130	135	120	190
Storage duration (hrs)	9	13.4	13.4	13.4	13.4
Solar multiple	2.5	3	3	3	3
Capacity factor (%)	45%	55%	55%	55%	55%
Discount rate (%)	10%	10%	10%	10%	10%
Labour cost ($/hr)	$25.18	$25.18	$25.18	$25.18	$25.18

[8]S1: two-tank indirect sensible heat storage; S2: two-tank direct sensible heat storage; S3: one-tank direct sensible heat storage; S4: latent heat storage; S5: thermochemical storage

Table 9 lists the calculated LCOE for each scenario taking into consideration the optimized parameters listed in Table 8. It can be noted in Table 9 that the optimized LCOEs for individual scenarios are significantly lower than the base case LCOE in Table

7. It is imperative to note that the LCOEs in Table 9 include the cost of storing thermal energy but not the cost of the solar field or power generation components. As suggested in a report published by IRENA, the cost of solar field and power generation components adds up to approximately 53% of the total investment cost [52]. Therefore, the LCOEs listed in Table 9 would increase accordingly if the costs of solar field and power generation components were to be considered.

Table 9: LCOE and cost summary for the optimized cases

Costs	S1[9]	S2	S3	S4	S5
Total investment cost ($ millions)	1495	265	179	503	642
LCOE (cents/kwh)	34	4	2	8	6

[9]S1: two-tank indirect sensible heat storage; S2: two-tank direct sensible heat storage; S3: one-tank direct sensible heat storage; S4: latent heat storage; S5: thermochemical storage

2.3.3 Uncertainty analysis

An uncertainty analysis can give a pictorial representation of the LCOEs falling within a given quartile. The sampling error, standard deviation, and number of samples considered in calculating uncertainties were approximately 0.001, 0.18, and 200000, respectively. Figure 14 depicts a box plot representation of uncertainty in each scenario. Note that the LCOE for storage in S1 ranges from approximately 13 – 30 cents/kWh while uncertainty ranges from 8 – 59 cents/kWh. Output values for the LCOE in S1 have a relatively wider range of possible values, which is due to the uncertainty in the cost of the heat transfer fluid. As discussed earlier, S1 is the configuration in which total investment costs vary greatly with the cost of the synthetic oils used as the heat transfer fluid. S2 and

S3 have less uncertainty as investment costs are lower than in S1. The LCOE uncertainty values for S2 are from 3 – 22 cents/kWh and 2 – 16 cents/kWh for S3. However, S4 has a wider range of uncertainty, around 6 – 43 cents/kWh, which can be attributed to the commodity pricing of industry grade PCM materials ($0.05/kg to $5.71/kg) [5]. Figure 14 shows quartile ranges of 25% and 75% for S5 do not overlap with the other scenarios, indicating that S5 has highest LCOE (as it does, at 32 – 64 cents/kWh). Figure 14 shows a significantly higher uncertainty in S5. This is because thermochemical storage is still in the R&D phase. For this reason, the modelling parameters for S5 were considered for a 100 MW capacity using the available data from literature which developed a hypothetical scenario for a 10 MW thermochemical storage [7].

Table 10 gives the Monte Carlo input distributions used for each parameter. The input values for a triangle distribution are the minimum value, most likely value, and maximum value. The most likely value is the base case value while minimum and maximum values are taken from the literature.

Table 10: Monte Carlo input distributions

Costs	**Monte Carlo input distributions**	**Refs.**
Capacity (MW)	Vosetriangle (50,100,250)	[27]
Storage duration (hrs)	Vosetriangle (1.05,8,15)	[47]
Solar multiple	Vosetriangle (1,1.75,3.5)	[47]
Capacity factor (%)	Vosetriangle (0.3,0.4,0.55)	[47]
Discount rate (%)	Vosetriangle (0.07,0.1,0.14)	[33]
N (yrs) =	Vosetriangle (25,30, 40)	[33]

The uncertainty of LCOE illustrated in Figure 14 has two components, system uncertainty and economic uncertainty. The system uncertainty can be observed when equipment such as pumps and heat exchangers are sized according to the required plant capacity. Thus, the data-intensive model developed in this study calculates the mass flow rate requirement in individual equipment by varying parameters such as plant capacity, storage duration, solar multiple, and capacity factor. Economic uncertainty, however, is evaluated by varying parameters such as discount rate and total plant life (N). Therefore, the overall uncertainty illustrated in Figure 14 encompasses both system uncertainty and economic uncertainty.

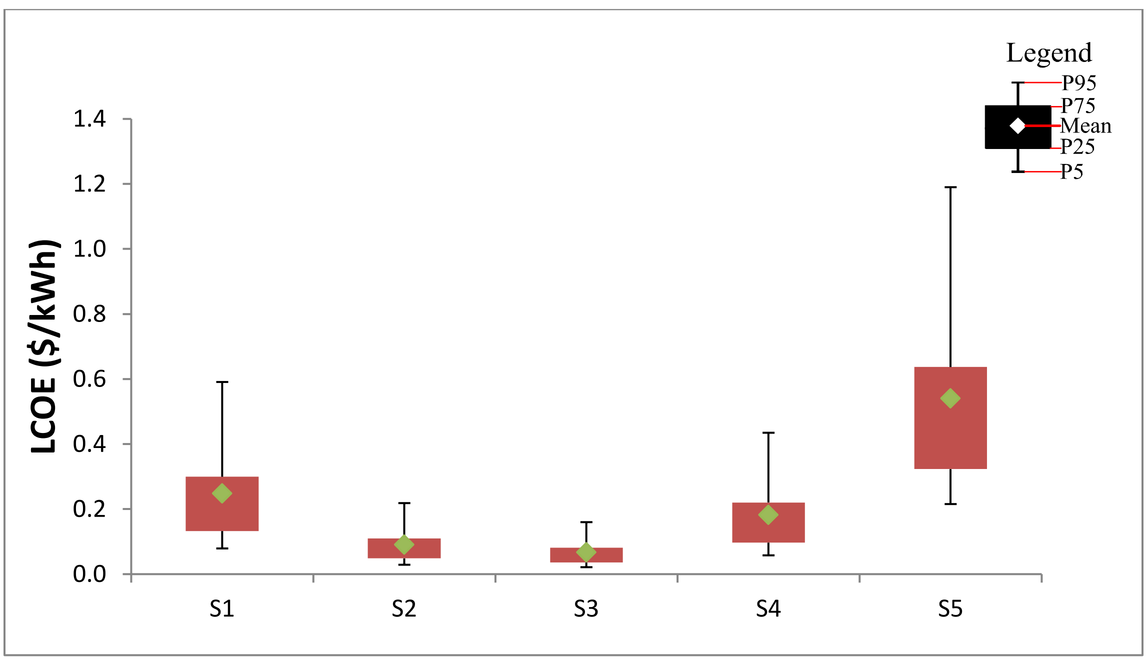

Figure 14: LCOE uncertainty box plot for thermal energy storage systems

(S1: two-tank indirect sensible heat storage; S2: two-tank direct sensible heat storage; S3: one-tank direct sensible heat storage; S4: latent heat storage; S5: thermochemical storage)

2.4 Conclusion

In conclusion, the focus of this study was to develop a data-intensive techno-economic model to evaluate the economic feasibility of various thermal energy storage scenarios. Economic feasibility was determined by evaluating the LCOE for five systems (i.e., two-tank indirect sensible heat storage, two-tank direct sensible heat storage, one-tank direct sensible heat storage, latent heat storage, and thermochemical storage). Two-tank indirect sensible heat storage is the most mature technology in concentrated solar power and showed relatively higher LCOE for storage due to the increased raw material cost for heat transfer fluids. Two-tank indirect sensible heat storage has higher capital investment than two-tank direct sensible heat storage because of the additional component costs of the added heat exchanger, extra pumps, and greater amount of heat transfer fluids. Two-tank direct sensible heat storage, on the other hand, has a lower investment cost because it does not need an additional heat exchanger or extra pumps. Because of the higher operating temperatures of 554 – 1050 ^oF (290 – 565 ^oC) in two-tank direct sensible heat storage, the heat transfer rate from molten salt to water is greater and generating higher quality superheated steam. Two-tank indirect sensible heat storage and two-tank direct sensible heat storage are widely implemented for commercial applications. In contrast, one-tank direct sensible heat storage, latent heat storage, and thermochemical storage are still in the research and development phase and thus there is greater scope for improving their economic viability. Although the cost of a thermocline system (i.e., one-tank direct sensible heat storage) is relatively lower than the other systems, there is significant opportunity to reduce investment cost and the LCOE. Latent heat storage is another system in which PCMs greatly affect the cost of latent heat storage. PCMs have higher energy density than materials used in sensible heat storage. Thus, optimizing the system would be the first step to achieve a lower LCOE. The optimized LCOEs of storage for the individual systems were estimated to be approximately 34 cents/kWh (two-tank indirect sensible heat storage), 4 cents/kWh (two-tank direct sensible heat storage), 2 cents/kWh (one-tank direct sensible heat storage), 8 cents/kWh (latent heat storage) and 6 cents/kWh (thermochemical storage), respectively. The US Department of Energy recommended the goal of LCOE of 2 cents/kWh for thermal storage by 2020. The optimized scenarios in this study demonstrate a potential to achieve that goal.

References

[1] Thermal Energy Storage Market by Technology, Storage Material, Application, End-User, and Region - Global Forecast to 2022. 2016. Available: http://www.crossroadstoday.com/story/34975289/thermal-energy-storage-market-by-technology-storage-material-application-end-user-and-region-global-forecast-to-2022; accessed January 12, 2016.

[2] U.S. Department of Energy, Solar energy technologies office FY2016 budget at-a-glance. 2015, Available: https://energy.gov/sites/prod/files/2015/03/f20/fy16_seto_at-a-glance.pdf; accessed January 20, 2016.

[3] M. Liu, N. S. Tay, S. Bell, M. Belusko, R. Jacob, G. Will, et al., "Review on concentrating solar power plants and new developments in high temperature thermal energy storage technologies," Renewable and Sustainable Energy Reviews, vol. 53, pp. 1411-1432, 2016.

[4] R. Sioshansi and P. Denholm, "The value of concentrating solar power and thermal energy storage," IEEE Transactions on Sustainable Energy, vol. 1, pp. 173-183, 2010.

[5] B. Xu, P. Li, and C. Chan, "Application of phase change materials for thermal energy storage in concentrated solar thermal power plants: A review to recent developments," Applied Energy, vol. 160, pp. 286-307, 2015.

[6] B. Xu, P. Li, C. Chan, and E. Tumilowicz, "General volume sizing strategy for thermal storage system using phase change material for concentrated solar thermal power plant," Applied Energy, vol. 140, pp. 256-268, 2015.

[7] A. Luzzi, K. Lovegrove, E. Filippi, H. Fricker, M. Schmitz-goeb, M. Chandapillai, et al., "Techno-Economic analysis of a 10 MW e solar thermal power plant using ammonia-based thermochemical energy storage," Solar energy, vol. 66, pp. 91-101, 1999.

[8] M. Mehos, J. Jorgenson, P. Denholm, and C. Turchi, "An assessment of the net value of CSP systems integrated with thermal energy storage," Energy Procedia, vol. 69, pp. 2060-2071, 2015.

[9] S. M. Flueckiger, B. D. Iverson, and S. V. Garimella, "Simulation of a Concentrating Solar Power Plant With Molten-Salt Thermocline Storage for Optimized Annual Performance," in ASME 2013 7th International Conference on Energy Sustainability collocated with the ASME 2013 Heat Transfer Summer Conference and the ASME 2013 11th International Conference on Fuel Cell Science, Engineering and Technology, 2013.

[10] M. Montes, A. Abánades, and J. Martínez-Val, "Performance of a direct steam generation solar thermal power plant for electricity production as a function of the solar multiple," Solar Energy, vol. 83, pp. 679-689, 2009.

[11] L. Heller and P. Gauché, "Modeling of the rock bed thermal energy storage system of a combined cycle solar thermal power plant in South Africa," Solar Energy, vol. 93, pp. 345-356, 2013.

[12] S. Izquierdo, C. Montañés, C. Dopazo, and N. Fueyo, "Analysis of CSP plants for the definition of energy policies: the influence on electricity cost of solar multiples,

capacity factors and energy storage," Energy Policy, vol. 38, pp. 6215-6221, 2010.

[13] S. Boudaoud, A. Khellaf, K. Mohammedi, and O. Behar, "Thermal performance prediction and sensitivity analysis for future deployment of molten salt cavity receiver solar power plants in Algeria," Energy Conversion and Management, vol. 89, pp. 655-664, 2015.

[14] C. Turchi, M. Mehos, C. K. Ho, and G. J. Kolb, "Current and future costs for parabolic trough and power tower systems in the US market," in Proceedings of the 16th SolarPACES Conference, Perpignan, France, 2010.

[15] J. T. Hinkley, J. A. Hayward, B. Curtin, A. Wonhas, R. Boyd, C. Grima, et al., "An analysis of the costs and opportunities for concentrating solar power in Australia," Renewable Energy, vol. 57, pp. 653-661, 2013.

[16] H. Lund, P. A. Østergaard, D. Connolly, I. Ridjan, B. V. Mathiesen, F. Hvelplund, et al., "Energy storage and smart energy systems," International Journal of Sustainable Energy Planning and Management, vol. 11, pp. 3-14, 2016.

[17] M. Seitz, M. Johnson, and S. Hübner, "Economic impact of latent heat thermal energy storage systems within direct steam generating solar thermal power plants with parabolic troughs," Energy Conversion and Management, vol. 143, pp. 286-294, 2017.

[18] S. Hübner, M. Eck, C. Stiller, and M. Seitz, "Techno-economic heat transfer optimization of large scale latent heat energy storage systems in solar thermal power plants," Applied Thermal Engineering, vol. 98, pp. 483-491, 2016.

[19] R. Dunn, K. Lovegrove, and G. Burgess, "A review of ammonia-based thermochemical energy storage for concentrating solar power," Proceedings of the IEEE, vol. 100, pp. 391-400, 2012.

[20] E. Wenger, M. Epstein, and A. Kribus, "Thermo-electro-chemical storage (TECS) of solar energy," Applied Energy, vol. 190, pp. 788-799, 2017.

[21] M. Hanel and R. Escobar, "Influence of solar energy resource assessment uncertainty in the levelized electricity cost of concentrated solar power plants in Chile," Renewable energy, vol. 49, pp. 96-100, 2013.

[22] Dowtherm used in concentrated solar power. Available: https://www.dow.com/en-us/heat-transfer/applications/solar-power; accessed April 15, 2018.

[23] National Renewable Energy Laboratory, Gemasolar Thermosolar Plant, 2011. Available: https://www.nrel.gov/csp/solarpaces/project_detail.cfm/projectID=40; accessed April 5, 2018.

[24] National Renewable Energy Laboratory, System Advisor Model (SAM) Case Study: Andasol-1. Available: https://sam.nrel.gov/sites/default/files/content/case_studies/sam_case_csp_physical_trough_andasol-1_2013-1-15.pdf; accessed March 19, 2017.

[25] R. I. Dunn, P. J. Hearps, and M. N. Wright, "Molten-salt power towers: newly commercial concentrating solar storage," Proceedings of the IEEE, vol. 100, pp. 504-515, 2012.

[26] H. Zhang, J. Baeyens, G. Cáceres, J. Degrève, and Y. Lv, "Thermal energy storage: Recent developments and practical aspects," Progress in Energy and Combustion Science, vol. 53, pp. 1-40, 2016.

[27] Efficiency: More value to your facility Siemens Turbine Model SST-600. Available: https://www.siemens.com/content/dam/webassetpool/mam/tag-siemens-com/smdb/power-and-gas/steamturbines/steam-turbine-product-overview-01-2018.pdf; accessed January 25, 2018.
[28] A. Modi and C. D. Pérez-Segarra, "Thermocline thermal storage systems for concentrated solar power plants: One-dimensional numerical model and comparative analysis," Solar Energy, vol. 100, pp. 84-93, 2014.
[29] S. Kuravi, Y. Goswami, E. K. Stefanakos, M. Ram, C. Jotshi, S. Pendyala, et al., "Thermal energy storage for concentrating solar power plants," Technology & Innovation, vol. 14, pp. 81-91, 2012.
[30] C. Smith, Y. Sunb, B. Webby, A. Beath, and F. Bruno, "Cost analysis of high temperature thermal energy storage for solar power plant," in Proceedings of the 52nd Annual Conference, Australian Solar Energy Society (Australian Solar Council) Melbourne, 2014.
[31] Aspen HYSYS. 2017. Available: http://www.aspentech.com/products/aspen-hysys/; accessed June 24, 2016
[32] R. Gabbrielli and R. Singh, "Economic and scenario analyses of new gas turbine combined cycles with no emissions of carbon dioxide," in ASME Turbo Expo 2004: Power for Land, Sea, and Air, 2004, pp. 665-673.
[33] C. Parrado, A. Marzo, E. Fuentealba, and A. Fernández, "2050 LCOE improvement using new molten salts for thermal energy storage in CSP plants," Renewable and Sustainable Energy Reviews, vol. 57, pp. 505-514, 2016.
[34] M. I. Hussain, A. Ali, and G. H. Lee, "Performance and economic analyses of linear and spot Fresnel lens solar collectors used for greenhouse heating in South Korea," Energy, vol. 90, pp. 1522-1531, 2015.
[35] Current US Inflation Rates: 2006-2017. Available: http://www.usinflationcalculator.com/inflation/current-inflation-rates/; accessed March 7, 2016
[36] M. Mehos, C. Turchi, J. Jorgensen, P. Denholm, C. Ho, and K. Armijo, "Advancing concentrating solar power technology, performance, and dispatchability," ed: Golden, CO: National Renewable Energy Laboratory. NREL/TP-5500-65688, 2016.
[37] M. J. Moran, H. N. Shapiro, D. D. Boettner, and M. B. Bailey, Fundamentals of engineering thermodynamics: John Wiley & Sons, 2010.
[38] A. G. McDonald and H. Magande, Introduction to thermo-fluids systems design: John Wiley & Sons, 2012.
[39] M. Nitsche and R. O. Gbadamosi, "Chapter 1 - Heat Exchanger Design," in Heat Exchanger Design Guide, ed Boston: Butterworth-Heinemann, pp. 1-19, 2016.
[40] M. Nitsche and R. O. Gbadamosi, "Chapter 2 - Calculations of the Temperature Differences LMTD and CMTD," in Heat Exchanger Design Guide, ed Boston: Butterworth-Heinemann, pp. 21-35, 2016.
[41] L. Heller, B. Mesnil, and J. Hoffmann, "Initial investigation of liquid glass as a thermal medium in CSP plants," in 3rd Southern African Solar Energy Conference, South Africa, 2015.
[42] J. H. Whitelaw, "Convective heat transfer," Thermopedia: Guide to Thermodynamics, Heat & Mass Transfer and Fluids Engineering, p. 237, 1997.

[43] H. Grirate, N. Zari, A. Elmchaouri, S. Molina, and R. Couturier, "Life time analysis of thermal oil used as heat transfer fluid in CSP power plant," in AIP Conference Proceedings, pp. 040005, 2016.
[44] J. Sweet, E. Roth, and M. Moss, "Thermal conductivity of Inconel 718 and 304 stainless steel," International journal of thermophysics, vol. 8, pp. 593-606, 1987.
[45] National Renewable Energy Laboratory, Andasol-1. Available: https://www.nrel.gov/csp/solarpaces/project_detail.cfm/projectID=3; accessed September 15, 2016.
[46] National Renewable Energy Laboratory, Ivanpah Solar Electric Generating System. Available: https://www.nrel.gov/csp/solarpaces/project_detail.cfm/projectID=62; accessed September 30, 2016.
[47] International Renewable Energy Agency, Concentrating Solar Power. 2012. Available: http://www.irena.org/documentdownloads/publications/re_technologies_cost_analysis-csp.pdf; accessed November 3, 2016.
[48] Organization for Economic Co-operation and Development, Average annual wages. Available: https://stats.oecd.org/Index.aspx?DataSetCode=AV_AN_WAGE; accessed February 16, 2016.
[49] World Energy Council, World Energy Perspective Cost of Energy Technologies, 2013. Available: https://www.worldenergy.org/wp-content/uploads/2013/09/WEC_J1143_CostofTECHNOLOGIES_021013_WEB_Final.pdf; accessed April 12, 2017.
[50] R. Chacartegui, L. Vigna, J. Becerra, and V. Verda, "Analysis of two heat storage integrations for an Organic Rankine Cycle Parabolic trough solar power plant," Energy Conversion and Management, vol. 125, pp. 353-367, 2016.
[51] Ammonia Prices Fell Slightly from the Previous Week. 2016. Available: http://marketrealist.com/2016/03/weekly-ammonia-price-update-week-ending-march-4-2016/; accessed November 28, 2016
[52] International Renewable Energy Agency, Concentrating Solar Power Technology Brief. 2013, Available: http://www.irena.org/DocumentDownloads/Publications/IRENA-ETSAP%20Tech%20Brief%20E10%20Concentrating%20Solar%20Power.pdf; accessed December 3, 2016.
[53] International Renewable Energy Agency, Operations and maintenance costs for parabolic trough and solar tower CSP plants. 2014. Available: http://costing.irena.org/media/3553/fig-73.png; accessed December 10, 2016
[54] International Renewable Energy Agency, The LCOE of CSP plants as a function of the solar multiple and hours of thermal energy storage. 2014. Available: http://costing.irena.org/media/3550/fig-77.png; accessed December 12, 2016
[55] International Renewable Energy Agency, Annual capacity factor for a 100MW parabolic trough plant as a function of solar field size and size of thermal energy storage. 2014. Available: http://costing.irena.org/media/3585/75.png; accessed December 12, 2016

Chapter 3[1]

Development of Life Cycle Greenhouse Gas Emissions and Net Energy Ratio of Solar-based Thermal Energy Storage Systems

3.1 Introduction

Due to growing concerns around climate change, there is increased focus on reducing its adverse effects while GHG emissions continue to rise. It is estimated that global GHG emissions could increase from 49 $GtCO_{2eq}$ (gigatonnes of carbon dioxide equivalent) in 2010 to approximately 700 $GtCO_{2eq}$ by 2030 [1]. The electricity production sector is a major contributor and is responsible for nearly 25% of global emissions [1]. Clean energy technologies are the way forward to reduce GHG emissions from the power generation sector. CSP is a widely known clean energy technology used to enhance GHG emission mitigation targets in the power sector. The International Energy Agency (IEA) announced a plan in 2014 to reduce about 2.1 gigatonnes (Gt) of carbon dioxide (CO_2) annually through the installation of CSP plants by 2050 [2]. This plan prompted the search for energy efficient ways to store heat in CSP plants. One of the factors in CSP technologies that affects their energy performance is the intermittency of solar energy (i.e., night-time and cloudy days). TES systems provide a solution to the intermittent nature of solar energy. TES systems have the potential to store energy in the form of heat for long durations, allowing the CSP plant to operate even when solar energy is intermittent.

[1] This chapter has been prepared for submission as Spandan Thaker, Abayomi Olufemi Oni, Eskinder D. Gemechu, Amit Kumar, "Development of life cycle greenhouse gas emissions and net energy ratio of solar-based thermal energy storage systems," in a peer-reviewed journal.

TES systems are categorized into sensible heat, latent heat, and thermochemical storage. Sensible heat storage uses a heat transfer medium such as molten salt. Molten salt is a commercially available heat transfer fluid that can retain heat with minimal heat loss due to a temperature loss of approximately 1 ^{o}F per day [3]. Latent heat storage technology can store heat in PCM. As the PCM changes phase from solid to liquid, heat is stored in the process [4]. Heat is released when the PCM changes phase from liquid to solid. Latent heat storage and thermochemical storage are still in the research and development phase since obtaining energy-efficient and low GHG emission profile heat transfer fluid is very challenging.

Progress in TES system development is expected to change the way heat is stored in the power generation industry and provide an opportunity to reduce fossil fuel use. However, the decision to use TES technologies depends on several factors such as plant energy performance and environmental friendliness. These factors are crucial to the sustainability of different TES systems in the future energy market. A cradle-to-grave LCA is an appropriate tool to evaluate the energy and environmental performances of TES systems. The life cycle GHG emissions and NER are the metrics used to examine and compare the environmental and energy profiles of the TES systems. Such evaluations provide useful insights into life cycle stages of TES systems. Their application in TES systems can enhance sustainable decision-making in power generation. LCA has been applied for a comparative evaluation of various systems [5, 6]. A critical part of a successful comparative LCA is the definition of system boundaries. Inappropriate definition of boundaries between systems leads to unreasonable comparative studies and decision-making. Therefore, for a good selection of system boundaries, it is essential to examine the system from both the functional and technical perspectives.

There are some LCA studies that provide insights into the life cycle stages of TES systems. Some studies focus on the life cycle environmental impacts of selected TES systems independent of the system energy performance and vice versa. Decisions are hard to make in many of these studies because of differences in goal and scope definition, system boundary selection, the choices of modelling parameters, and the level of uncertainty associated with those variations. Uncertainty is one of the key elements in the LCA and it needs to be performed to better understand the results and interpret their implications. Earlier studies on the LCA of TES systems focus to understand the environmental performance of individual storage systems in terms of GHG emissions and NER. The GHG emissions characterization of individual TES systems, with different system boundaries, has been a subject of discussion in several papers [7, 8], while other papers examine the energy performance of TES systems [9, 10]. Other studies address hybrid systems. Good et al. [11] examined the performance of a hybrid solar PV/T (photovoltaic and thermal) system used for a district heating application. Larrain and Escobar [12] focused on the energy performance of a CSP plant with a hybrid direct steam generation plant using natural gas as the backup fuel. A study by Burkhardt et al. performed a LCA for a parabolic trough CSP plant with a two-tank TES system and also considered other design alternatives for TES that could minimize GHG emissions and water consumption in a parabolic trough CSP plant [5]. One of the main purposes of LCA is to compare the environmental performances of different products with the same functionality. To the best of the author’s knowledge, there is no comprehensive comparative life cycle GHG emissions assessment of sensible heat, latent heat, and thermochemical storage. Some performed LCA to compare environmental performance of two systems. For example, Oro et al. [8] examined the GHG emissions for sensible and latent heat storage systems while not considering thermochemical storage. Other limitations identified from the study by Oro et al. [8], are the differences in the assumptions and modelling parameters. For example, the study did not consider the heat transfer fluid circulating within the TES system and assumed the total plant life to be 20 years. The results from prior studies cannot be directly compared because of differences in life cycle boundaries and the lack of information on the reliability of model uncertainties. Further research is required to address the limitations associated with decision-making in TES systems. In addition to the limitations in decision-making due to differences in the system boundaries, examining model uncertainties for TES technologies is another gap in the literature. With the aim of filling the literature gap, this study, therefore, focuses on performing a comparative assessment of the life cycle GHG emissions and NER for sensible heat, latent heat and thermochemical storages. It is the first comprehensive LCA study that considers all types of TES technologies.

The main purpose of this study is to develop a bottom-up data-intensive LCA model to determine the life cycle GHG emissions and NER of TES technologies (sensible heat, latent heat, and thermochemical storage). The general objective is accomplished through the following specific objectives:

1. Setting the main goal of the study and determining the system boundaries for sensible heat, latent heat and thermochemical storage technologies.

2. Developing life cycle inventory data to assess the GHG emissions and NERs for the TES technologies.
3. Performing sensitivity and uncertainty analyses to assess the impact on the GHG emissions and NERs for each storage technology for better decision making.

3.2 Methods

The LCA methodology presented in this research is in accordance with the International Organization for Standardization (ISO) 14040 and 14044 [13, 14]. The ISO provides a guideline principle and framework on how to conduct an LCA. LCA has four major phases: goal and scope definition, inventory analysis, life cycle impact assessment, and interpretation [15]. This section discusses each aspect of the LCA stages in the context of the study.

3.2.1 Goal and scope definition

The goal of the research is to perform a comparative LCA of three TES systems including sensible heat, latent heat, and thermochemical storage systems with the aim of identifying the most environmentally sustainable alternative system. GHG emissions and NER are the environmental metrics used to form the basis of comparison. The NER is defined as the ratio of output energy to the fossil fuel input energy in a system. This study highlights the main contributing processes in each TES system. The life cycle GHG emissions and NER characterization of alternative TES systems could be an important source of environmental data for the scientific community in this field and could be helpful for policy development and decision making.

As stated earlier in this chapter, there are LCA studies on different TES systems, however each study uses different system boundary definitions, input and output requirements, operational conditions, parameters, and so on. Any comparative assessment using only the existing literature is subject to high level of uncertainty. To address this problem, this study attempts to provide comprehensive LCAs of TES systems by using the same boundaries and input parameters for each. The following life cycle stages were included for each system: production, construction, transportation, operation, dismantling, and disposal. Material and energy requirements at each stage were computed for the individual components used in the TES systems (i.e., material used in the construction of the heat exchangers, piping, storage tanks, and pumps). Subsequently, GHG emission factors (gCO_{2eq}/kWh) and energy consumed in producing these materials were determined using the literature [16]. Electricity consumption emissions in the production phase were also considered. For the NER evaluation, the energy consumption in each unit operation during individual life cycle phases was calculated. The NER for each scenario was evaluated using mass and energy balances for individual equipment including the storage tanks, heat exchangers, and pumps. The mass and energy balances were used to compute the heat lost from storage tanks and heat exchangers. The heat gained in the pumps was also computed. The net heat delivered in each scenario was evaluated to compare the energy yield of individual TES technologies.

The functional unit is one of the key elements in an LCA study, especially when comparing the environmental performance of several products. This unit provides a reference through which the input and output requirements from different systems are normalized. Here the functional unit is defined as one kWh of energy produced from stored heat. The life cycle GHG emissions are calculated using the 100-year global warming potential normalized by the functional unit (kWh). The NER is a unit-less metric evaluated as the ratio of the heat output from thermal storage to the fossil fuel input from individual life cycle phases (i.e., production, construction, transportation, operation, dismantling, and disposal).

Figure 15 shows the common system boundary that was established to accurately assess and compare the GHG emissions and NERs of different TES systems. Upstream material and energy requirements along with associated GHG emissions from resource extraction, material production, and transportation efforts, are included in the boundary. The material requirement for TES components such as the storage tank, piping, pumps, heat exchangers, molten salt, and synthetic oils (Dowtherm A©/Therminol VP©) were computed using mass and energy balances. Values from literature were used to compute the emissions and energy input requirement for the materials production phase [16]. Key input resources such as molten salt (sodium nitrate and potassium nitrate [17]), Dowtherm A©/Therminol VP© [18], and phase change materials (lithium carbonate [19] and potassium carbonate [17]) are assumed to be manufactured separately in different locations. Since a case study for Alberta is the focus of this work, the emission factors and energy requirement to transport material from their respective manufacturing sites to the plant (Medicine Hat, Alberta) are 202 $\mathrm{gCO_{2eq}/tonne-km}$ and 1148 $\mathrm{kJ/tonne-km}$, respectively [20]. However, the methodology and the parameters considered in this study would be valid for other locations with minor adjustments in the model. Emissions from site preparation in the construction of the plant and downstream emissions at the end of life stages (dismantiling and disposal) were also considered. The emission factors corresponding to the electricity consumed during the production phase were obtained from the literature. The emissions from the operations phase were due to electricity consumption in pumps. The life cycle GHG emission factor for using solar photovoltaic energy as the source of electricity in the operational phase was considered to be 41 $\mathrm{gCO_{2eq}/kWh}$, [21]. For the end of life cycle stage, only the transportation effort to dispose Dowtherm A©/Therminol VP© at the incineration facility in Whitecourt, Alberta was considered [22]. Other end of life cycle treatments such as recycling, landfilling, and incineration are beyond the scope of the study.

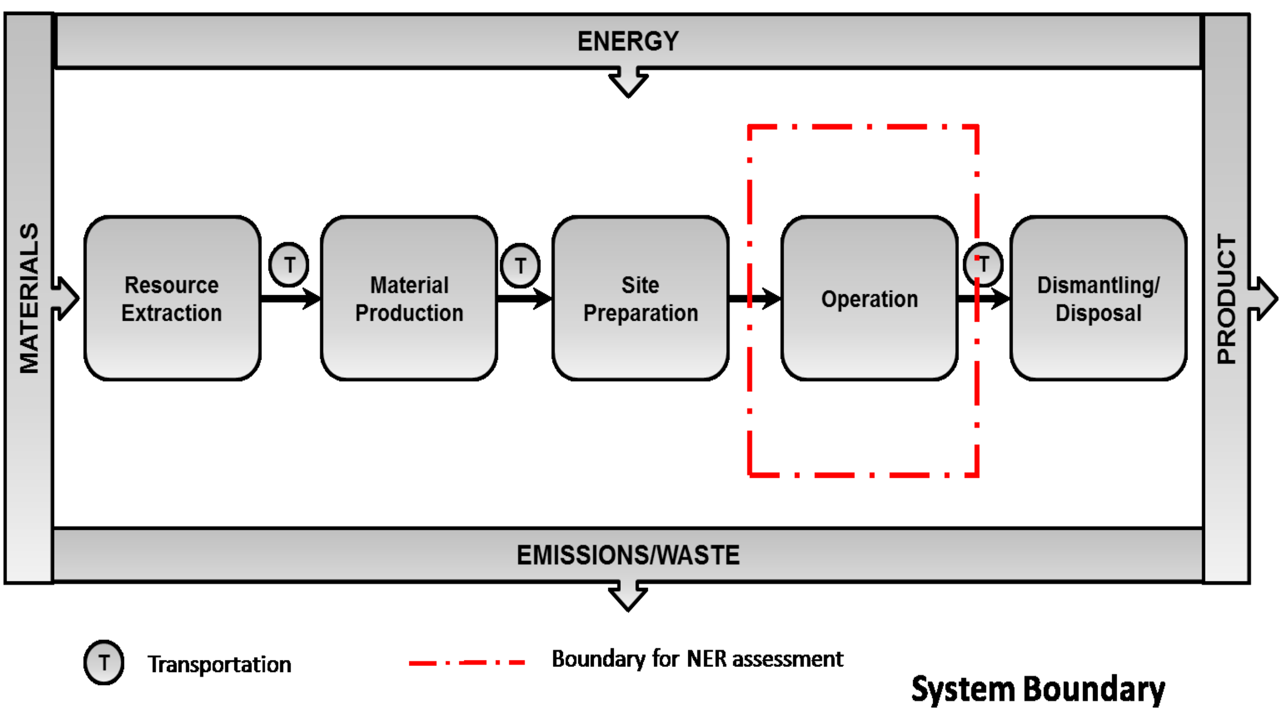

Figure 15: Common system boundary for thermal energy storage systems

3.2.2 Process description

A comparative environmental LCA based on GHG emissions and NERs was performed for the following alternative thermal energy storage systems: two-tank indirect sensible heat storage (S1), two-tank direct sensible heat storage (S2), one-tank direct sensible heat storage (S3), latent heat storage (S4), and thermochemical storage (S5). This section briefly describes the main process for each system. Detailed description of each process and flow diagram can be found in (Chapter 2) Thaker et al. [23].

Two-tank indirect sensible heat storage (S1): As shown in Figure 1, Dowtherm A©/Therminol VP© fluid is used to transfer heat to water and produce superheated steam in a heat exchanger (HX #2). This operation takes place during the daytime when ample sunlight is available and during peak demand. During low energy demand, excess heat from the sun is stored in molten salt and can be extracted during the night in the heat exchanger (HX #1). The operating temperature in S1 ranges from 608-752 ^{o}F [24].

Two-tank direct sensible heat storage (S2): This scenario (shown in Figure 2) uses molten salt as the heat transfer medium to convert water into superheated steam in the heat exchanger. Thus, it does not require an additional heat exchanger and pump. Instead, the system uses a central tower CSP plant configuration to reflect sunlight, which heats molten salt to operating temperatures of approximately 554-1050 ^{o}F [24]. S2 has a higher operating temperature range and potentially higher energy yield than S1.

One-tank direct sensible heat storage (S3): This scenario, shown in Figure 3, operates on the same principle as S2. The key difference is the reduced tank volume and molten salt requirement, which could reduce the material requirement for plant construction.

Latent heat storage (S4): This scenario, shown in Figure 4, uses PCM as the heat transfer medium. The PCM in the top of the tank melt when part of the heat from hot molten salt is absorbed by the PCM. The melted PCM settle at the bottom of the tank while the pellets at the bottom float to the top. The heat retained from melted PCM is released into the cold molten salt that enters the tank bottom. Then the PCM pre-heats the cold molten salt leaving the tank before being further heated in the solar field.

Thermochemical heat storage (S5): The input ammonia stream (stream 1) is heated in the solar field by concentrating heat onto a central tower using mirrors (Figure 5). The heated ammonia enters at around 1742 ^{o}F and 2900 psi. Ammonia is dissociated to a hydrogen and nitrogen gas mixture in the presence of a catalyst inside the dissociation reactor (GBR-100). The mixture is then cooled to ambient temperature in a heat exchanger (E-100) before being stored in a two-phase high-pressure storage tank (V-100) with minimal heat loss [25]. To recover stored heat, the hydrogen and nitrogen gas mixture is preheated in a heat exchanger (E-102) to approximately 527 ^{o}F. The gas mixture is then diverted to a synthesis reactor (CRV-100) to produce ammonia. The synthesis reaction releases large amounts of heat that is used in another heat exchanger (E-103) to convert water to superheated steam at approximately 806 ^{o}F and 1500 psi [26]. The high-pressure superheated steam can be used in applications such as power generation and process heating.

3.2.3 Material requirement calculation

Pressure vessels: The thickness of a pressure vessel determines how much material is required to construct the vessel. Pressure vessels are designed based on the internal pressure and maximum allowable stress of the material. According to the ASME Boiler and Pressure Vessel Section VIII standard, the minimum wall thickness of a pressure vessel with known variables such as design pressure (*P*), vessel outer radius (*R*), maximum allowable stress (*S*), and joint efficiency (*E*) can be calculated with the Equation 9 [27]. If the thickness is less than one half of the inner radius, then the minimum thickness shall be the greater thickness of the values corresponding to circumferential stress and longitudinal stress. The minimum thickness computed in Equation 9 corresponds to the greater thickness.

$$t = \frac{P*R}{(S*E)+(0.4*P)} \tag{9}$$

The allowable stress in Equation 9 is a function of the operating temperature. The allowable stress for carbon steel is assumed to be 103 MPa for operating temperatures up to 300 °C [28]. The allowable stress for stainless steel is taken to be 65.4 MPa and 103 MPa for operating temperatures up to 600°C and 450°C, respectively. The operating pressure in the ammonia reactors and storage tank is considered to be around 20 MPa [25], and the vessel outer diameter and vessel height are assumed to be 4.9 meters and 7.2 meters, respectively.

Storage tank: The wall thickness of a molten salt storage tank is computed using the American Petroleum Institute (API) 650 standard for storage tanks [29] (Equation 10):

$$t = \frac{2.6*D*(H-1)*G}{S} + CA \tag{10}$$

where, *t, D, H, G, S,* and *CA* are tank wall thickness (in), nominal tank diameter (ft), tank height (ft), specific gravity of fluid in the tank, maximum allowable stress (psi), and corrosion allowance (in), respectively [29]. The mass of the tank is evaluated by multiplying the tank volume (computed by multiplying wall thickness and tank surface area) with its material density.

Process piping and heat exchanger tubes: The wall thickness was computed using both pipeline rules of thumb [30] and the ASME B31.3 standard for process piping [31], and was calculated using Equation 11. In order for Equation 11 to apply, the pipe wall thickness must be less than one sixth of the pipe outer diameter [31]. The minimum wall thickness computed in Equation 11 satisfies this condition for a straight pipe under internal pressure:

$$t = \frac{P*D_i}{(2*S*E)+(2*P*(Y-1))} \tag{11}$$

where t, P, D_i, S, E, Y correspond to the pipe wall thickness (m), internal pressure (Pa), inner pipe diameter (m), maximum allowable stress (Pa), joint efficiency, and temperature coefficient, respectively. The mass of the pipes is computed using the same procedure as for the storage tank. Table 11 summarizes the main material requirement results for different unit operations. The values correspond to 50 MW for S1 and 100 MW for S2 – S5.

Table 11: Material requirement in metric tonnes (MT) for each material [5, 32-34]

	S1[2]	S2	S3	S4	S5
Aluminum	0.3	23	23	23	23
Concrete	4903	55880	55880	55880	55880
Copper	1	52	52	52	52
Iron	0.4	0.8	0.8	0.8	0.8
Polyethylene	4	2	2	2	2
Polypropylene	39	0.03	0.03	0.03	0.03
Heat transfer medium					
Molten salt	34089	34771	23181	8693	N/A

Dowtherm A©/Therminol VP© HTF	37199	N/A	N/A	N/A	N/A
PCM	N/A	N/A	N/A	26078	N/A
Ammonia	N/A	N/A	N/A	N/A	25360
Storage tanks/pressure vessel					
Carbon steel	2041	2041	N/A	N/A	N/A
Stainless steel	2107	2107	1405	738	1373
Mineral wool	284	337	169	169	24
Fiberglass	2.7	3.2	1.6	1.6	0.21
Foam glass	23	34	34	34	N/A
Firebrick	66	95	95	95	N/A
Heat exchangers					
Stainless steel	233	20	20	20	4
Piping					
Carbon steel	71	42	42	42	273
Stainless steel	197	627	627	627	658
Calcium silicate	319	158	158	158	164
Pumps					
Stainless steel	13	13	13	13	13
Total stainless steel (tonnes)	2549	2767	2064	1397	2047
Total carbon steel (tonnes)	2112	2083	42	42	273

[2]S1: two-tank indirect sensible heat storage; S2: two-tank direct sensible heat storage; S3: one-tank direct sensible heat storage; S4: latent heat storage; S5: thermochemical storage

3.2.4 Net energy ratio evaluation

NER is defined as the ratio of net heat delivered by the thermal storage system, measured in gigajoules (GJ), to the fossil fuel input to the thermal storage system (GJ), as shown in Equation 12:

$$\mathrm{NER} = \frac{\mathrm{Q_{delivered}}}{\sum \mathrm{Energy\ use\ in\ life\ cycle\ phases}} \qquad (12)$$

The NER examined in this study focuses solely on the thermal storage components. The heat losses incurred in the solar field and power plant components are not considered. The net heat delivered by the thermal storage system ($Q_{delivered}$) is computed using Equation 13.

$$Q_{\text{delivered}} = \sum Q_{\text{gain in pumps}} - \sum Q_{\text{loss in heat exchanger and tanks}} \tag{13}$$

The heat gain in pumps is computed using the flowing equations [35]:

$$T_{rise} = \frac{P_{\text{s}} * (1 - \eta)}{c_{\text{p}} * V * \rho} \tag{14}$$

$$Q_{\text{gain in pumps}}\ (\text{kJ}) = m * c_{\text{p}} * T_{\text{rise}} \tag{15}$$

where $P_{\text{s}},\ \eta, c_{\text{p}},\ V,\ \rho,\ m$, represent brake power (kW), pump efficiency, specific heat capacity ($\text{kJ/kg}\ ^\circ\text{C}$), volume flow rate ($m^3/s$), density ($kg/m^3$), and mass of fluid (kg), respectively.

The heat loss (GJ) from a heat exchanger depends on the efficiency (η) of the heat exchanger. The efficiency of the heat exchanger is considered to be 95% [36]. The rate of energy balance for the heat exchanger is expressed in Equation 16.

$$\dot{Q} = \eta * \left[\dot{m}_1 c_{\text{p1}} (T_2 - T_1)\right]_{\text{Fluid,1}} = \left[\dot{m}_2 c_{\text{p2}} (t_2 - t_1)\right]_{\text{Fluid,2}}. \tag{16}$$

A wide range of heat exchanger efficiencies were considered to capture the uncertainty associated with it. The input ranges for each parameter used in the uncertainty analysis are shown in Appendix B (Table 15). It should be noted from Table 15 that the heat exchanger efficiency was varied from 70 to 95% to ascertain the uncertainty associated with varying heat exchanger efficiencies.

The heat loss from the molten salt storage tank can be computed using Equation 17:

$$Q_{tank} = m_{\text{molten salt}} * c_{\text{p}} * (\Delta T) \tag{17}$$

where $m_{\text{molten salt}}$, c_{p}, and ΔT represent the molten salt mass, specific heat capacity of molten salt, and change in temperature loss over a period of one day, respectively. The change in temperature loss for molten salt is considered to be around 1 °F per day [37].

3.3 Results and Discussion

3.3.1 The life cycle GHG emissions

The global GHG emissions of all the TES systems considered here are shown in Figure 16. With 11 gCO_{2eq}/kWh, S3 appears to have lower GHG emissions, followed by S2. S1 shows higher GHG emissions when compared with the others. As the diagram shows, the largest share of GHG emissions in all TES systems is from production. This GHG emissions share can influence overall results. The high GHG emissions share is mainly due to fossil fuel and electricity consumption by the production facilities. Transportation and construction GHG emissions in S1 are considerably higher than in the other systems. The transportation GHG emissions are from delivering large quantities of Dowtherm A©/Therminol VP© from the manufacturing facilities to the plant site and the disposal site. Dowtherm A©/Therminol VP© HTF used in S1 degrades over its life cycle and must be disposed off at the end of the plant life. Since S2 – S5 do not use Dowtherm A©/Therminol VP© as the heat transfer medium, the GHG emissions contribution from the transportation effort for these scenarios is very low.

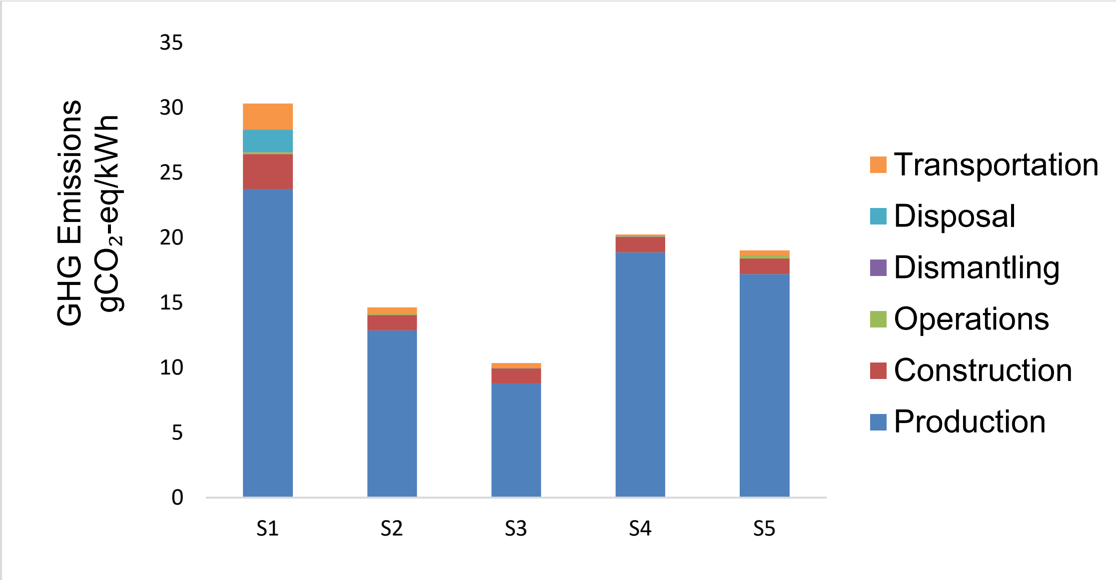

Figure 16: Life cycle GHG emissions for thermal energy storage systems

(S1: two-tank indirect sensible heat storage; S2: two-tank direct sensible heat storage; S3: one-tank direct sensible heat storage; S4: latent heat storage; S5: thermochemical storage)

The GHG emissions variations in the different TES technologies can be attributed to their energy requirements at the production phase. Figure 17 provides a detailed breakdown of GHG emissions during the production stage for each scenario. For example, the production of molten salt and Dowtherm A©/Therminol VP© in S1 shows the highest GHG emissions contribution compared to the other systems, around 80%. This is because S1 has a parabolic trough CSP plant configuration, which needs both Dowtherm A©/Therminol VP© and molten salt as the heat transfer medium. Though not so high, the significance of molten salt is reflected in the process GHG emissions of S2 and S3. S3 has the lowest production GHG emissions of all the scenarios because its tank volume requirement is approximately 66% that of a two-tank system [38, 39]. S3 uses only one tank to store the molten salt and S2 uses two. Production GHG emissions in S4 come primarily from PCMs, as 75% of the tank's volume is PCMs and 25% is molten salt [38]. PCMs have high energy density, which effectively store heat, thereby lowering the storage tank volume requirement by 65% [38]. In S5, the high production GHG emissions are a result of the operating conditions of ammonia. One of the factors affecting the operating conditions is the mass flow rate of ammonia, which requires high temperature and pressure and thus, energy requirement and associated GHG emissions are high. Ammonia makes up nearly 70% of production GHG emissions. Concrete is another material that has important GHG emissions contributions in S2 – S5. This is because, these systems have central towers in which heat from the sun is concentrated to heat the transfer medium (i.e., molten salt and ammonia). The central tower can be as high as 450 ft, so a large amount of concrete is required to support the structure [40].

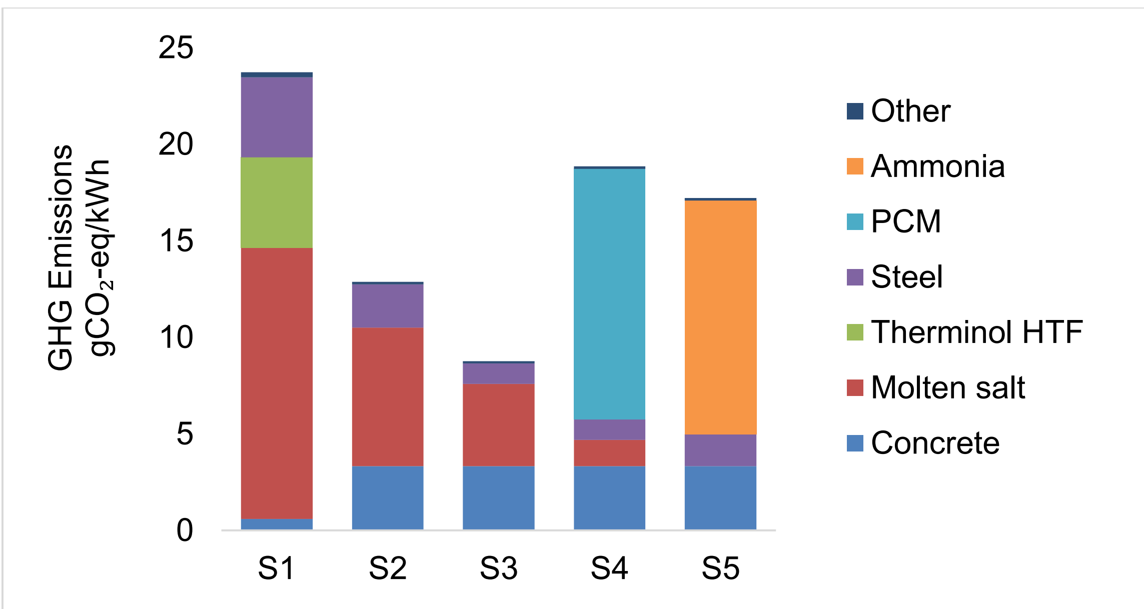

Figure 17: GHG emissions associated with the production stage

(S1: two-tank indirect sensible heat storage; S2: two-tank direct sensible heat storage; S3: one-tank direct sensible heat storage; S4: latent heat storage; S5: thermochemical storage)

A sensitivity analysis was performed to determine which parameters are sensitive to the overall results. Figures 18 and 19 show the trends for S1 and S5. The other scenarios (S2 – S4) follow the same trend as shown in Appendix B (Figures 25, 28, and 30), that is, the capacity factor and the solar multiple are the most sensitive parameters. The capacity factor and the solar multiple are used to determine the amount of energy that can be generated from the CSP plant. The amount of energy stored in the system is the main function from which the functional unit is derived (kWh). All input and output requirements are normalized to the functional unit. A system with more storage capacity results in fewer GHG emissions per functional unit. Therefore, it would be ideal to increase energy production by increasing the solar multiple and the capacity factor, as they directly affect the energy produced from the system. For example, a solar multiple of one means the energy produced in the solar field equals the energy consumed by the turbine to generate electricity. A solar multiple of two, however, indicates that the solar field produces twice as much energy as what is required to generate electricity. The excess energy can be stored for later use during off-peak hours (i.e., night-time). In addition to the solar multiple, the capacity factor influences the energy produced. The capacity factor is the ratio of the actual energy produced per year to the theoretical energy produced per year [41]. In addition to the capacity factor and the solar multiple, the material requirement in S1 – S4 and the storage duration in S5 are sensitive parameters, as shown in Figures 18 and 19. In S5, heat is stored in a two-phase tank during an endothermic chemical reaction. This allows heat to be stored for long durations with minimal heat loss, thereby reducing associated GHG emissions [25].

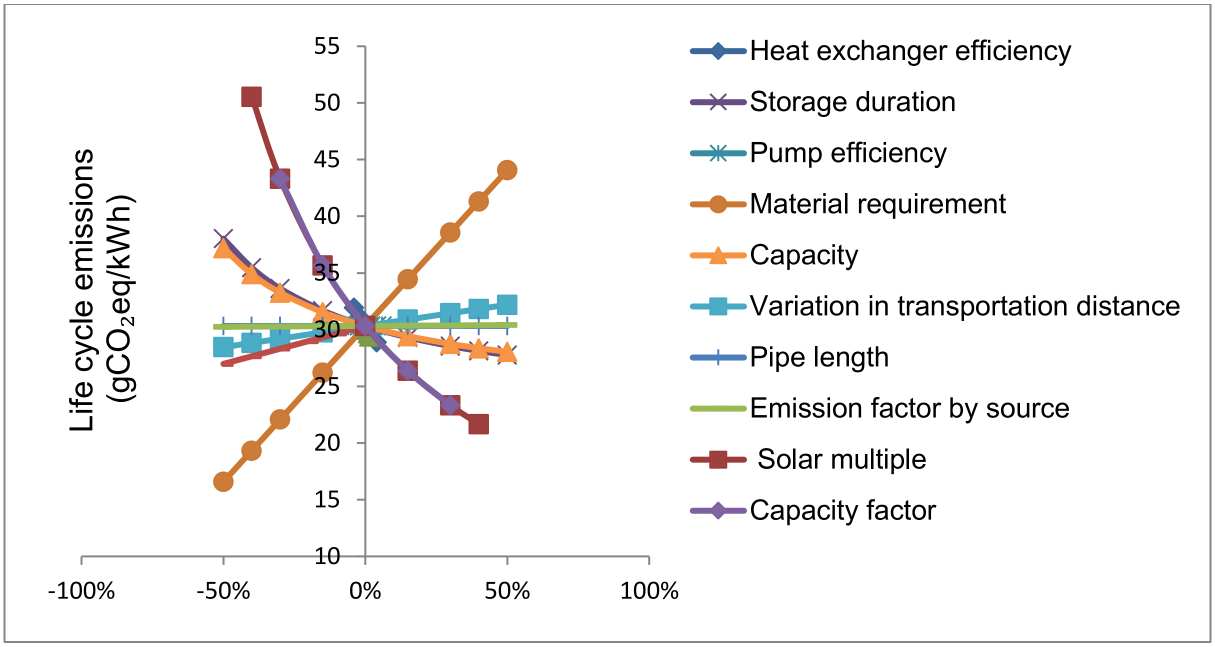

Figure 18: Life cycle emissions sensitivity plot for 2-tank indirect sensible heat storage (S1)

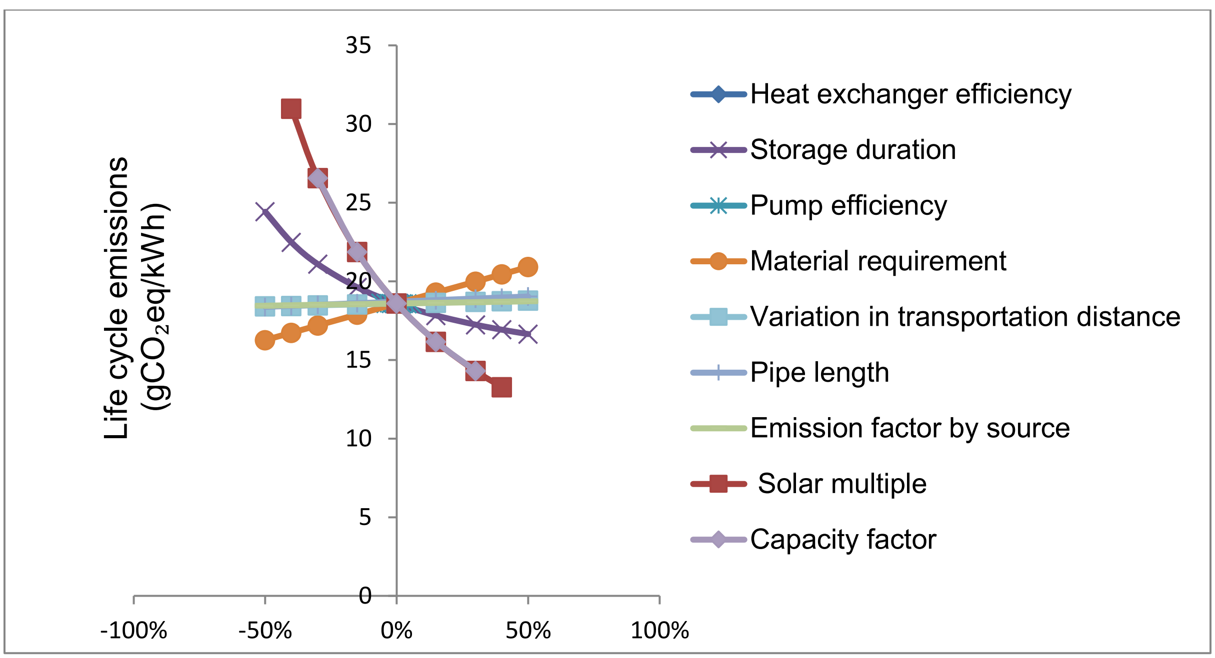

Figure 19: Life cycle emissions sensitivity plot for thermochemical storage (S5)

3.3.2 Net energy ratio

The net energy ratio for TES systems was evaluated by considering the following key parameters: heat exchanger efficiency, storage duration, solar multiple, capacity factor, electricity source emission factor, generator efficiency, pump efficiency, electricity emission factor for Canadian provinces, pipe length, material requirement, and plant capacity. Table 12 lists the base case values for each parameter considered in the calculation. The capacity for S1 was assumed to be 50 MW, in keeping with capacity from an existing plant [42], while 100 MW was considered for S2 – S5 since 133 MW is the largest turbine operating on a commercial scale in a CSP plant [40].

Table 12: Base parameter values

Base case values	S1[3]	S2 - S5	Refs.
Heat exchanger efficiency	95%	95%	[36]
Storage duration (hrs)	8.0	8.0	[43]
Generator efficiency	95%	95%	[44]
Pump efficiency	85%	85%	[30]
Solar multiple	1.75	1.75	[43]
Capacity factor (%)	40%	40%	[43]
Pipe length (m)	1700[4]	1400[5]	
Electricity emission factor for Canadian provinces (gCO_{2eq}/kWh)	820	820	
Capacity (MW)	50	100	[40, 42]
Electricity source emission factor (gCO_{2eq}/kWh)	41	41	

[3]S1: two-tank indirect sensible heat storage; S2: two-tank direct sensible heat storage; S3: one-tank direct sensible heat storage; S4: latent heat storage; S5: thermochemical storage
[4]The pipe length is estimated using the plant layout of the Andasol Solar Power Plant
[5]The pipe length is estimated using the plant layout of the Ivanpah Solar Power Facility

Figure 20 shows the NER results for all TES systems. S2 and S3 have higher NERs than the other systems. S2 and S3 lose less heat in the heat exchanger than S1. S1 requires additional heat exchangers to transfer heat from Dowtherm A©/Therminol VP© to the molten salt, which leads to heat loss. S2 and S3, on the other hand, use only one heat exchanger to generate superheated steam by exchanging heat between molten salt and water. S4 has the lowest NER of all the systems. This is mainly due to the high electricity requirement to produce the phase change material (lithium carbonate and potassium carbonate). The lower NER in S5 can be explained by the high energy demand to pump the ammonia at a high flow rate. S5 uses three heat exchangers, so there is heat loss, which affects the NER. The high energy demand to produce material such as stainless steel also contributes to S5’s NER.

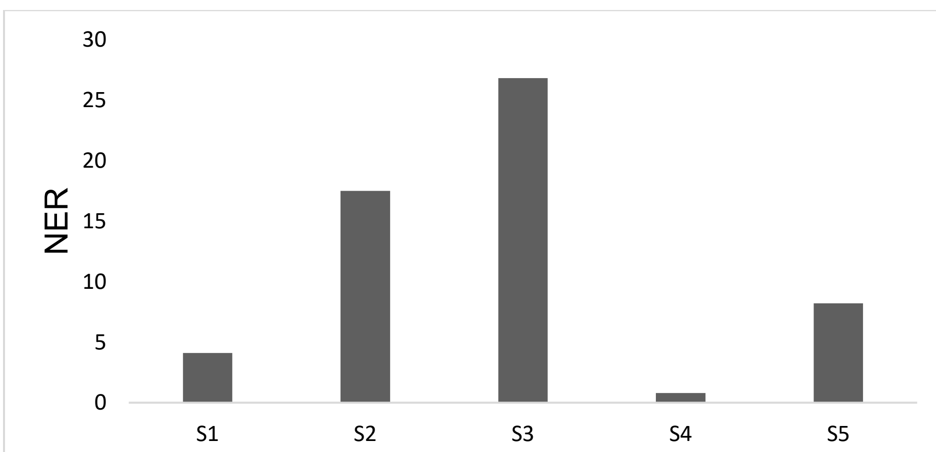

Figure 20: NER for thermal energy storage technologies

(S1: two-tank indirect sensible heat storage; S2: two-tank direct sensible heat storage; S3: one-tank direct sensible heat storage; S4: latent heat storage; S5: thermochemical storage)

A sensitivity analysis was performed to determine which parameters have the largest impact on overall NER results. It can be seen in Figure 21, heat exchanger efficiency, pump efficiency, and material requirement are highly sensitive parameters in S1. All other TES systems follow a similar trend as shown in Appendix B (Figures 26, 27, 29, and 31). The heat exchanger efficiency determines the amount of heat loss, which affects NER results. The pump efficiency is another parameter that has a high impact on NER values. Large quantities of heat transfer mediums such as molten salt, Dowtherm A©/Therminol VP©, and ammonia require high amounts of energy to be pumped from one heat exchanger to the next. The energy requirements to produce materials used in the construction of TES systems such as carbon steel, stainless steel, concrete, etc., are also key parameters influencing the NER value.

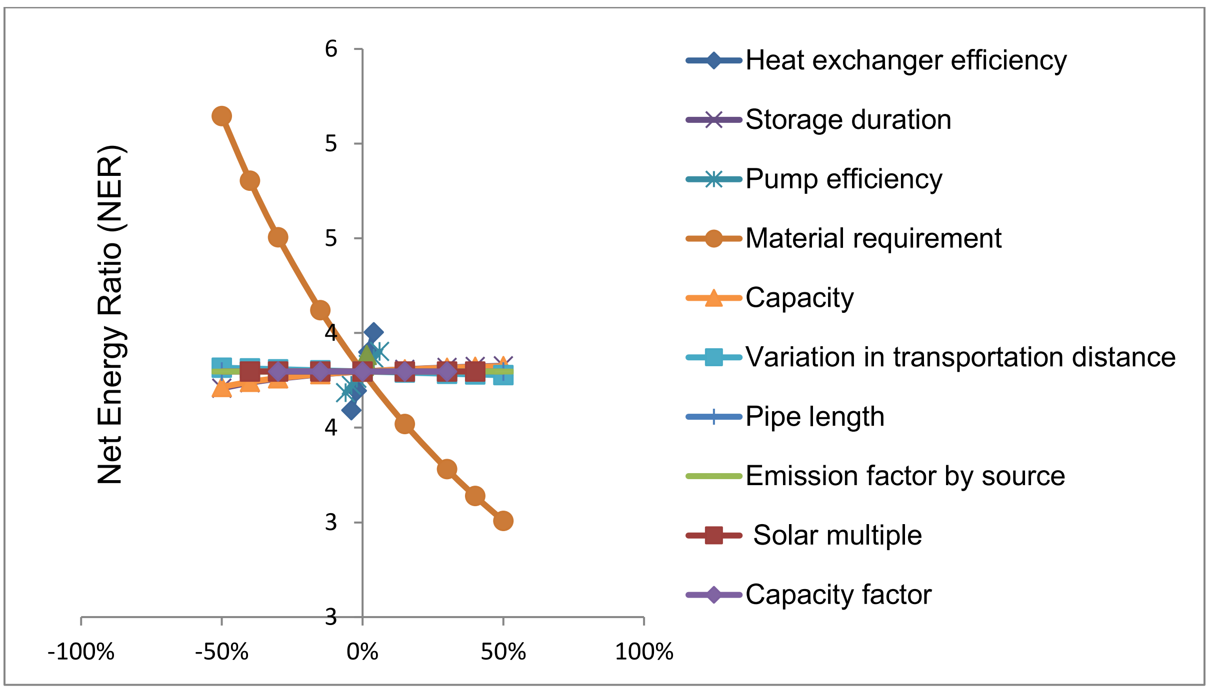

Figure 21: NER sensitivity plot for 2-tank indirect sensible heat storage (S1)

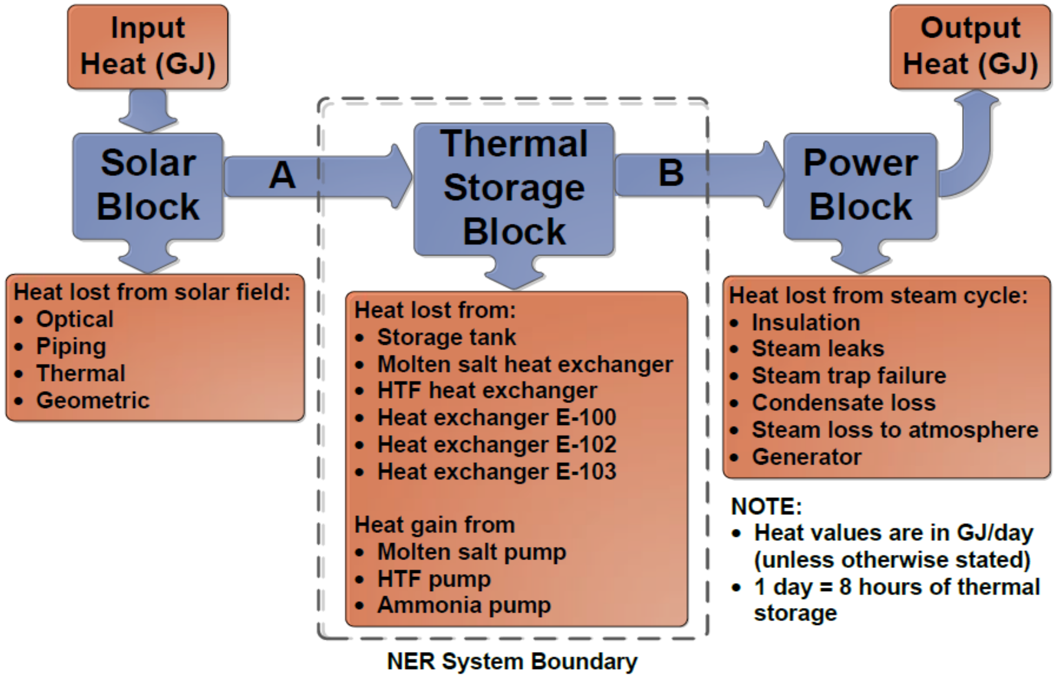

Figure 22: NER block diagram for the thermal energy storage systems

(S1: two-tank indirect sensible heat storage; S2: two-tank direct sensible heat storage; S3: one-tank direct sensible heat storage; S4: latent heat storage; S5: thermochemical storage)

Figure 22 and Table 13 show the heat loss and heat gain from individual equipment considered in the NER system boundary. The figure helps to better visualize the energy flow in the system. The heat values for “A” and “B” in Table 13 refer to the heat delivered to and from the thermal storage block, respectively, as shown in Figure 22.

Table 13: Heat values for the components in Figure 22

Thermal Storage Block	S1[6]	S2	S3	S4	S5
Input heat (GJ)	8555	18174	18074	18078	18587
A (GJ)	3080	5089	5061	5062	5204
B (GJ)	2172	4344	4344	4344	4344
Output heat (GJ)	1440	2880	2880	2880	2880
			Heat loss		

Storage tank (GJ)	102	58	19	7	N/A
Molten salt heat exchanger (GJ)	424	719	719	719	N/A
HTF heat exchanger (GJ)	446	N/A	N/A	N/A	N/A
Heat exchanger E-100 (GJ)	N/A	N/A	N/A	N/A	537
Heat exchanger E-102 (GJ)	N/A	N/A	N/A	N/A	748
Heat exchanger E-103 (GJ)	N/A	N/A	N/A	N/A	390
			Heat gain		
Molten salt pump (GJ)	31	32	21	8	N/A
HTF pump (GJ)	34	N/A	N/A	N/A	N/A
Pump 1 (GJ)	N/A	N/A	N/A	N/A	73
Pump 2 (GJ)	N/A	N/A	N/A	N/A	742
			Heat loss from solar block		
Optical (GJ)	1968	5634	5603	5604	5762
Piping (GJ)	855	1817	1807	1808	1859
Thermal (GJ)	684	1454	1446	1446	1487
Geometric (GJ)	1968	4180	4157	4158	4275
			Heat loss from power block		
Insulation (GJ)	139	278	278	278	278
Steam leaks (GJ)	163	326	326	326	326
Steam trap failure (GJ)	78	156	156	156	156
Condensate loss (GJ)	83	165	165	165	165
Steam loss to atmosphere (GJ)	161	321	321	321	321
Generator (GJ)	109	217	217	217	217

[6]S1: two-tank indirect sensible heat storage; S2: two-tank direct sensible heat storage; S3: one-tank direct sensible heat storage; S4: latent heat storage; S5: thermochemical storage

3.4 Uncertainty Analysis

There are different sources of uncertainty in life cycle assessment. Some are associated with the input and output data, some with the emissions factor, modeling parameter uncertainties, and assumptions, to name but a few. To capture the uncertainty from these sources, an uncertainty analysis was conducted using a Monte Carlo simulation. Figures 23 and 24 show a box plot representation of the uncertainty ranges for NER and GHG emissions, respectively. Triangle distributions of the following parameters were considered for the analysis: plant capacity, storage duration, heat exchanger efficiency, pump efficiency, and generator efficiency. All other parameters considered in the analysis are listed in Table 15 in Appendix B. Each parameter has three input values: minimum, most likely, and maximum values. The most likely value is the base value, while minimum and maximum values were taken from the literature.

Except for S2 and S3, whose values overlap, there is clear variation in the overall NER values, as shown in Figure 23. Though it is not clear whether S2 or S3 has the highest NER value, they both have a higher NER than the other three TES systems because they consume less energy than the other systems during the production phase. Figure 24 shows the GHG emissions' uncertainty results. The values overlap, which makes interpretation difficult. The overlap is largely a result of the GHG emissions from the production phase of manufacturing materials, which take the largest share of global GHG emissions in all five TES systems. The high emissions in the production phase are due to the use of electricity and/or fossil fuels to run equipment in a manufacturing facility. The mean values shown by the green dot in Figure 24 indicate that GHG emissions in S2 and S3 are lower than in the other systems; they are lower because less fossil fuel is consumed in S2 and S3 during the production phase.

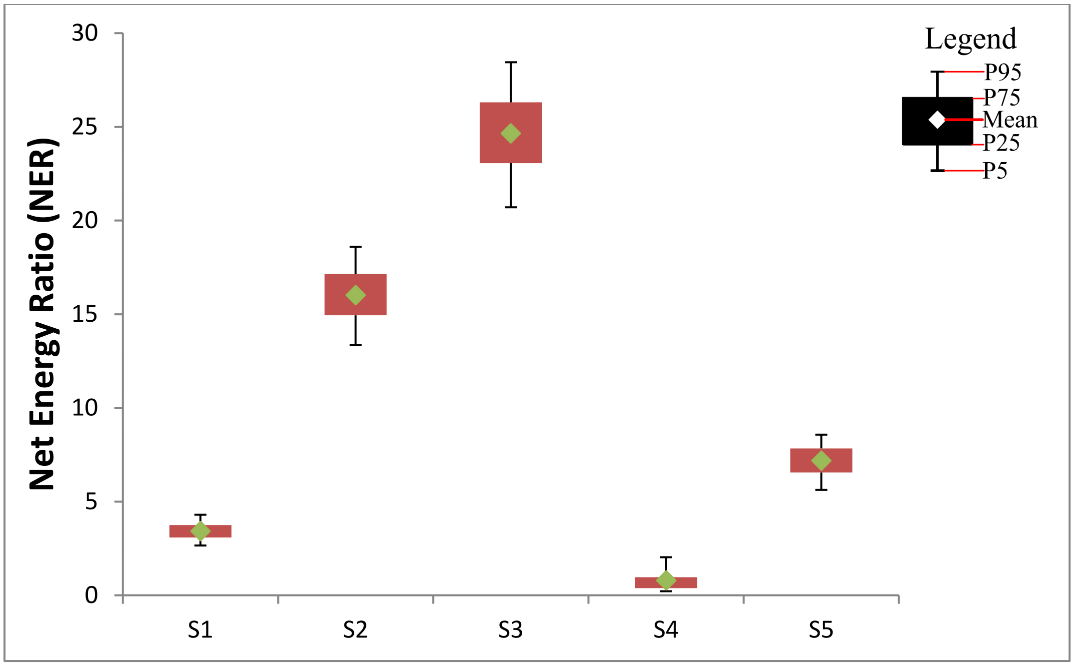

Figure 23: NER uncertainty box plot for thermal energy storage systems

(S1: two-tank indirect sensible heat storage; S2: two-tank direct sensible heat storage; S3: one-tank direct sensible heat storage; S4: latent heat storage; S5: thermochemical storage)

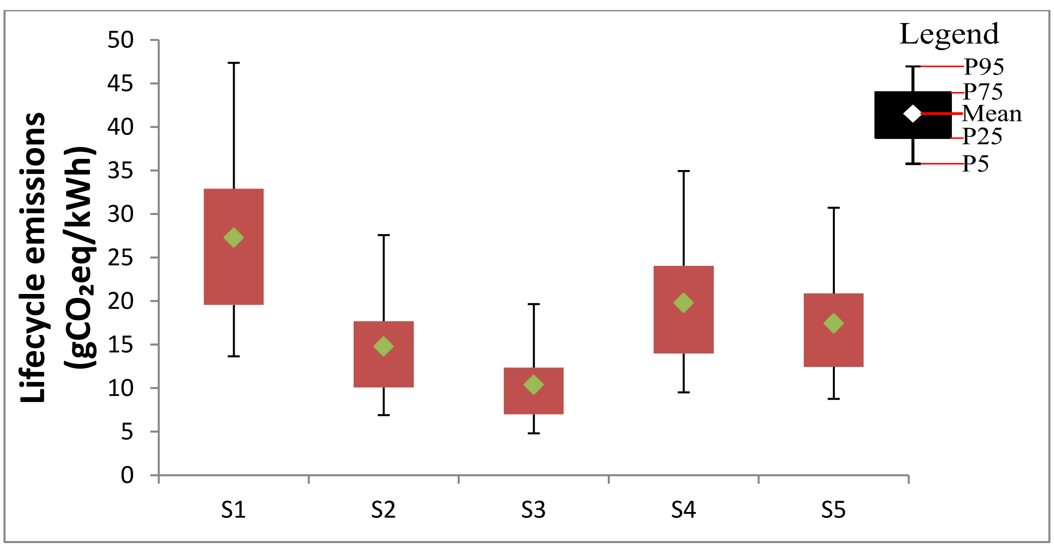

Figure 24: Life cycle GHG emissions uncertainty box plot for thermal energy storage systems

(S1: two-tank indirect sensible heat storage; S2: two-tank direct sensible heat storage; S3: one-tank direct sensible heat storage; S4: latent heat storage; S5: thermochemical storage)

3.5 Conclusion

The purpose of this study was to develop a data-intensive model to evaluate NER and life cycle GHG emissions. Both NER and GHG emissions were used to compare the solar-based TES technologies including sensible heat, latent heat, and thermochemical storage. To make a reasonable comparison between each technology, a common system boundary was established by considering the material and energy requirements along with associated GHG emissions from resource extraction, material production, transportation, operation, dismantling, and disposal. When we consider uncertainty, the mean GHG emission values for two-tank direct sensible heat storage and one-tank direct sensible heat storage are 15 gCO_{2eq}/kWh, and 11 gCO_{2eq}/kWh, respectively, which are lower than for the other systems. This is because the GHG emissions' contributions from the production of the heat transfer medium in 2-tank direct sensible heat storage and 1-tank direct sensible heat storage are approximately 47% and 36% of the life cycle emissions, respectively, which are below those of 2-tank indirect sensible heat storage (63%) and latent heat storage (70%). Thermochemical storage, however, uses ammonia as the heat transfer medium. Since ammonia production is energy intensive, the GHG emissions from manufacturing ammonia are approximately 67% of the life cycle emissions. Thus, it would be ideal to consider the scenario that requires the least amount of material during the production phase as it will reduce GHG emissions considerably and improve the NER. For these reasons, 2-tank direct sensible heat storage and 1-tank direct sensible heat storage can be favourable when implemented commercially.

References

[1] O. Edenhofer, R. Pichs-Madruga, Y. Sokona, E. Farahani, S. Kadner, K. Seyboth, et al., "Summary for policymakers climate change 2014, mitigation of climate change," IPCC 2014, Climate Change 2014: Contribution of Working Group III to the Fifth Assessment Report of the Intergovernmental Panel on Climate Change, 2014.

[2] C. Philibert, "Technology roadmap: solar thermal electricity—2014 edition," IEA, Paris, France, 2014.

[3] SolarReserve, Molten Salt Energy Storage. Available: http://www.solarreserve.com/en/technology/molten-salt-energy-storage; accessed February 3, 2018.

[4] D. Medveď, M. Kvakovský, and V. Sklenárová, "Latent heat storage systems," 2010. Available: http://home.zcu.cz/~tesarova/IP/Proceedings/Proc_2010/Files/001%20IP2010_Medved.pdf; accessed January 12, 2018.

[5] J. J. Burkhardt III, G. A. Heath, and C. S. Turchi, "Life cycle assessment of a parabolic trough concentrating solar power plant and the impacts of key design alternatives," Environmental science & technology, vol. 45, pp. 2457-2464, 2011.

[6] J. J. Burkhardt, G. Heath, and E. Cohen, "Life cycle greenhouse gas emissions of trough and tower concentrating solar power electricity generation," Journal of Industrial Ecology, vol. 16, 2012.

[7] N. A. Masruroh, B. Li, and J. Klemeš, "Life cycle analysis of a solar thermal system with thermochemical storage process," Renewable Energy, vol. 31, pp. 537-548, 2006.

[8] E. Oró, A. Gil, A. De Gracia, D. Boer, and L. F. Cabeza, "Comparative life cycle assessment of thermal energy storage systems for solar power plants," Renewable Energy, vol. 44, pp. 166-173, 2012.

[9] P. Denholm, Net energy balance and greenhouse gas emissions from renewable energy storage systems: Energy Center of Wisconsin, 2003. Available: http://fti.neep.wisc.edu/pdf/fdm1261.pdf; accessed February 10, 2018.

[10] R. Koppelaar, "Solar-PV energy payback and net energy: Meta-assessment of study quality, reproducibility, and results harmonization," Renewable and Sustainable Energy Reviews, vol. 72, pp. 1241-1255, 2017.

[11] C. Good, I. Andresen, and A. G. Hestnes, "Solar energy for net zero energy buildings–A comparison between solar thermal, PV and photovoltaic–thermal (PV/T) systems," Solar Energy, vol. 122, pp. 986-996, 2015.

[12] T. Larraín and R. Escobar, "Net energy analysis for concentrated solar power plants in northern Chile," Renewable Energy, vol. 41, pp. 123-133, 2012.

[13] ISO, "ISO 14040 International Standard - Environmental Management – Life Cycle Assessment – Principles and Framework," ed. Geneva, Switzerland International Organisation for Standardization, 2006.

[14] ISO, "ISO 14044 International Standard - Environmental Management – Life Cycle Assessment – Requirements and Guidelines," ed. Geneva, Switzerland International Organisation for Standardization, 2006.

[15] I. Bhat and R. Prakash, "LCA of renewable energy for electricity generation systems—a review," Renewable and Sustainable Energy Reviews, vol. 13, pp. 1067-1073, 2009.
[16] Argonne National Laboratory, GREET. Available: https://greet.es.anl.gov/; accessed February 20, 2018.
[17] PotashCorp. Available: http://www.potashcorp.com/contact/; accessed February 7, 2018.
[18] Dow Canada - Prentiss. Available: http://www.dow.com/canada/prentiss/index.htm; accessed January 12, 2018
[19] MGX Minerals Inc. Available: https://www.mgxminerals.com/assets.html; accessed January 19, 2018.
[20] GHGenius, The Addition of Freight Emissions to GHGenius, 2010. Available: https://ghgenius.ca/reports/GHGeniusFreightEmissions.pdf; accessed February 1, 2018
[21] S. Schlömer, T. Bruckner, L. Fulton, E. Hertwich, A. McKinnon, D. Perczyk, et al., "Annex III: Technology-specific cost and performance parameters," Climate change, pp. 1329-1356, 2014.
[22] Infratech Corporation. Available: http://infratech.cc/contact/; accessed February 20, 2018.
[23] S. Thaker, A. O. Oni, and A. Kumar, "Techno-economic evaluation of solar-based thermal energy storage systems," Energy Conversion and Management, vol. 153, pp. 423-434, 2017.
[24] R. I. Dunn, P. J. Hearps, and M. N. Wright, "Molten-salt power towers: newly commercial concentrating solar storage," Proceedings of the IEEE, vol. 100, pp. 504-515, 2012.
[25] R. Dunn, K. Lovegrove, and G. Burgess, "A review of ammonia-based thermochemical energy storage for concentrating solar power," Proceedings of the IEEE, vol. 100, pp. 391-400, 2012.
[26] A. Luzzi, K. Lovegrove, E. Filippi, H. Fricker, M. Schmitz-goeb, M. Chandapillai, et al., "Techno-economic analysis of a 10 MW e solar thermal power plant using ammonia-based thermochemical energy storage," Solar Energy, vol. 66, pp. 91-101, 1999.
[27] ASME Boiler and PV Code, "Section VIII Division 1," UG-126 Pressure Relief Valves to UG-129 Marking, ASME International, New York, 2010.
[28] Allowable Stress for Carbon Steel. Available: http://www.cis-inspector.com/asme-code-calculation-allowable-stresses.html; accessed January 31, 2018.
[29] S. M. J. Miller. Designing storage tanks. Available: http://coade.typepad.com/files/ptq-q4-2016-designing-storage-tanks.pdf; accessed January 15, 2018.
[30] E. McAllister, Pipeline rules of thumb handbook: a manual of quick, accurate solutions to everyday pipeline engineering problems: Gulf Professional Publishing, 2013.
[31] ASME B31.3, "Process Piping," American Society of Mechanical Engineering. Available: http://pishgam.co.ir/files/8527/DomainTemplates/pishgam.co.ir/timages/ASME-B31.3.pdf, 2002; accessed January 15, 2017.

[32] M. B. Whitaker, G. A. Heath, J. J. Burkhardt III, and C. S. Turchi, "Life cycle assessment of a power tower concentrating solar plant and the impacts of key design alternatives," Environmental Science & Technology, vol. 47, pp. 5896-5903, 2013.
[33] R. Moore, M. Vernon, C. K. Ho, N. P. Siegel, and G. J. Kolb, "Design considerations for concentrating solar power tower systems employing molten salt," SAND2010-6978, Sandia National Laboratories, Albuquerque, NM, 2010.
[34] E. Pihl, D. Kushnir, B. Sandén, and F. Johnsson, "Material constraints for concentrating solar thermal power," Energy, vol. 44, pp. 944-954, 2012.
[35] Volume Flow and Temperature Rise in Pump. Available: http://www.engineeringtoolbox.com/pumps-temperature-increase-d_313.html; accessed January 2, 2018
[36] Airec Heat Exchangers. Available: http://airec.se/heat-exchangers/; accessed January 14, 2018.
[37] SolarReserve, Molten Salt Energy Storage. Available: http://www.solarreserve.com/en/technology/molten-salt-energy-storage; accessed February 3, 2018.
[38] S. Kuravi, Y. Goswami, E. K. Stefanakos, M. Ram, C. Jotshi, S. Pendyala, et al., "Thermal energy storage for concentrating solar power plants," Technology & Innovation, vol. 14, pp. 81-91, 2012.
[39] A. Modi and C. D. Perez-Segarra, "Thermocline thermal storage systems for concentrated solar power plants: One-dimensional numerical model and comparative analysis," Solar energy, vol. 100, pp. 84-93, 2014.
[40] National Renewable Energy Laboratory, Ivanpah Solar Electric Generating System, Available: https://www.nrel.gov/csp/solarpaces/project_detail.cfm/projectID=62; accessed March 16, 2017.
[41] S. Izquierdo, C. Montanes, C. Dopazo, and N. Fueyo, "Analysis of CSP plants for the definition of energy policies: the influence on electricity cost of solar multiples, capacity factors and energy storage," Energy Policy, vol. 38, pp. 6215-6221, 2010.
[42] National Renewable Energy Laboratory, Andasol-1, Available: https://www.nrel.gov/csp/solarpaces/project_detail.cfm/projectID=3; accessed February 4, 2018.
[43] International Renewable Energy Agency, Concentrating Solar Power, 2012. Available: https://www.irena.org/DocumentDownloads/Publications/RE_Technologies_Cost_Analysis-CSP.pdf; accessed January 31, 2018.
[44] A. G. McDonald and H. Magande, Introduction to thermo-fluids systems design: John Wiley & Sons, 2012.

Chapter 4

4.1 Conclusions

This research evaluates the life cycle GHG emissions, LCOE, and NER of different TES technologies, namely sensible heat, latent heat, and thermochemical storage. Through a data-intensive, spreadsheet-based techno-economic and LCA model, the overall costs and environmental performances of different technologies were compared to identify the most economical TES technology and relevant life cycle stage that contributes significantly to global GHG emissions and NER. This comprehensive and holistic economic, environmental, and energy assessment can provide insights to decision makers in the energy sector.

The research makes reasonable deductions from the TES systems by developing system boundaries and examining the systems from both functional and technical perspectives. With uncertainty considered, the mean values for the GHG emissions in two-tank indirect sensible heat storage are higher compared to the other systems (i.e., two-tank direct sensible heat storage, one-tank direct sensible heat storage, latent heat storage, and thermochemical storage). This is because a two-tank indirect sensible heat storage system has a parabolic trough CSP plant configuration in which a heat transfer fluid such as Dowtherm A©/Therminol© is heated through solar radiation. The use of this heat transfer fluid requires more raw material and thus equipment costs increase for heat exchangers, pumps, piping, etc. Furthermore, the production of Dowtherm A©/Therminol© and the electricity consumed to operate additional pumps increase GHG emissions. The other systems (i.e., two-tank direct sensible heat storage, one-tank direct sensible heat storage, latent heat storage, and thermochemical storage), however, do not require Dowtherm A©/Therminol© as the heat transfer medium because they have a central tower CSP plant configuration.

One of the advantages a two-tank direct sensible heat storage system has over a two-tank indirect sensible heat storage system is lower investment cost; A two-tank direct sensible heat storage system does not need an additional heat exchanger or pumps for Dowtherm A©/Therminol©. The low investment costs are reflected in the LCOE. In addition to the costs, the mean value of the GHG emissions in a two-tank direct sensible heat storage system is lower because production emissions are lower. The production emissions in this study were computed by taking into consideration both the fossil fuel and electricity input requirements to produce raw materials (i.e., molten salt, stainless steel, carbon steel, concrete, Dowtherm A©/Therminol©, etc.).

The mean NER value is higher in a two-tank direct sensible heat storage system than in a two-tank indirect sensible heat storage system. This is because two-tank direct sensible heat storage uses less fossil fuel during raw material production than a two-tank indirect sensible heat storage system. In one-tank direct sensible heat storage, investment costs and GHG emissions are even lower than in two-tank direct sensible heat storage. This is because only one storage tank is used for both hot and cold molten salt. This can be useful, as discussed in Chapters 2 and 3; the molten salt requirement and tank volume for the one-tank direct sensible heat storage configuration would fall by approximately 66%. GHG emissions would fall, as less fossil fuels are required to manufacture the raw materials in a one-tank direct sensible heat storage system. Lower material consumption would also lower the investment costs. Ultimately, the lower amounts of fossil fuel required to produce the raw materials increase the NER for a one-tank direct sensible heat storage system.

The mean values for the LCOE and GHG emissions are higher in latent heat storage and thermochemical storage than in the other systems. This is because latent heat storage uses both phase change materials and molten salt as the heat transfer medium and thermochemical storage uses ammonia. Due to the large quantities of heat transfer mediums used in latent heat and thermochemical storage systems, both investment costs and GHG emissions increase. Thus, it can be deduced from this study that the mean values of the LCOE and GHG emissions are lower for a two-tank direct sensible heat storage and one-tank direct sensible heat storage systems. For these reasons, two-tank direct sensible heat storage and one-tank direct sensible heat storage systems can be more favourable scenarios to implement commercially.

4.2 Recommendations for future work

Further research can be performed in the following areas:

Improvement to the current model:

- Comprehensive thermochemical storage model: In the current study, ammonia was assumed to be the working fluid for thermochemical storage. Other compounds that can be used are methane, carbonates, and hydroxides, to name a few. A rigorous model should be developed to consider the costs and GHG emissions associated with using these compounds in thermochemical storage.
- Comprehensive sensible heat and latent heat storage model: The current model assumes the use of widely known heat transfer mediums such as molten salt,

Dowtherm A©/Therminol©, and phase change materials. However, there are a plethora of other chemical compounds that can be used for sensible heat and latent heat storage. The current model can be improved upon to further investigate the impact on the LCOE and GHG emissions by considering different compounds.

The inclusion of TES technologies used in district heating applications:

In this study, TES systems were modelled for their use in power generation. Another common application for thermal storage is district heating. Seasonal thermal storage technologies are often used for district heating. Some of the technologies used in seasonal thermal storage are underground tank thermal storage, pit thermal storage, borehole thermal storage, and aquifer thermal storage. A rigorous model should be developed to investigate the economic feasibility and environmental impact of seasonal thermal storage technologies.

Bibliography

A. De Gracia, L. Rincón, A. Castell, M. Jiménez, D. Boer, M. Medrano, et al., "Life Cycle Assessment of the inclusion of phase change materials (PCM) in experimental buildings," Energy and Buildings, vol. 42, pp. 1517-1523, 2010.

A. G. McDonald and H. Magande, Introduction to thermo-fluids systems design: John Wiley & Sons, 2012.

A. Luzzi, K. Lovegrove, E. Filippi, H. Fricker, M. Schmitz-goeb, M. Chandapillai, et al., "Techno-economic analysis of a 10 MW e solar thermal power plant using ammonia-based thermochemical energy storage," Solar Energy, vol. 66, pp. 91-101, 1999.

A. Modi and C. D. Pérez-Segarra, "Thermocline thermal storage systems for concentrated solar power plants: One-dimensional numerical model and comparative analysis," Solar Energy, vol. 100, pp. 84-93, 2014.

Airec Heat Exchangers. Available: http://airec.se/heat-exchangers/; accessed January 14, 2018.

Allowable Stress for Carbon Steel. Available: http://www.cis-inspector.com/asme-code-calculation-allowable-stresses.html; accessed January 31, 2018.

Annual capacity factor for a 100MW parabolic trough plant as a function of solar field size and size of thermal energy storage. 2014. Available: http://costing.irena.org/media/3585/75.png; accessed December 12, 2016.

Argonne National Laboratory, GREET Model. Available: https://greet.es.anl.gov/; accessed February 20, 2018.

ASME B31.3, "Process Piping," American Society of Mechanical Engineering. Available: http://pishgam.co.ir/files/8527/DomainTemplates/pishgam.co.ir/timages/ASME-B31.3.pdf, 2002; accessed January 15, 2017.

ASME Boiler and PV Code, "Section VIII Division 1," UG-126 Pressure Relief Valves to UG-129 Marking, ASME International, New York, 2010.

Aspen HYSYS, 2017. Available: http://www.aspentech.com/products/aspen-hysys/; accessed June 24, 2016

B. Corona, G. San Miguel, and E. Cerrajero, "Life cycle assessment of concentrated solar power (CSP) and the influence of hybridising with natural gas," The International Journal of Life Cycle Assessment, vol. 19, pp. 1264-1275, 2014.

B. Xu, P. Li, and C. Chan, "Application of phase change materials for thermal energy storage in concentrated solar thermal power plants: a review to recent developments," Applied Energy, vol. 160, pp. 286-307, 2015.

B. Xu, P. Li, C. Chan, and E. Tumilowicz, "General volume sizing strategy for thermal storage system using phase change material for concentrated solar thermal power plant," Applied Energy, vol. 140, pp. 256-268, 2015.

C. Good, I. Andresen, and A. G. Hestnes, "Solar energy for net zero energy buildings–A comparison between solar thermal, PV and photovoltaic–thermal (PV/T) systems," Solar Energy, vol. 122, pp. 986-996, 2015.

C. Parrado, A. Marzo, E. Fuentealba, and A. Fernández, "2050 LCOE improvement using new molten salts for thermal energy storage in CSP plants," Renewable and Sustainable Energy Reviews, vol. 57, pp. 505-514, 2016.

C. Philibert, "Technology roadmap: solar thermal electricity—2014 edition," IEA, Paris, France, 2014.

C. Smith, Y. Sunb, B. Webby, A. Beath, and F. Bruno, "Cost analysis of high temperature thermal energy storage for solar power plant," in Proceedings of the 52nd Annual Conference, Australian Solar Energy Society (Australian Solar Council) Melbourne, 2014.

C. Turchi, M. Mehos, C. K. Ho, and G. J. Kolb, "Current and future costs for parabolic trough and power tower systems in the US market," in Proceedings of the 16th SolarPACES Conference, Perpignan, France, 2010.

Current US Inflation Rates: 2006-2017. Available: http://www.usinflationcalculator.com/inflation/current-inflation-rates/; accessed March 7, 2016.

D. Medveď, M. Kvakovský, and V. Sklenárová, "Latent heat storage systems," 2010. Available: http://home.zcu.cz/~tesarova/IP/Proceedings/Proc_2010/Files/001%20IP2010_Medved.pdf; accessed November 3, 2017.

Dow Canada - Prentiss. Available: http://www.dow.com/canada/prentiss/index.htm; accessed January 12, 2018.

Dowtherm used in concentrated solar power. Available: https://www.dow.com/en-us/heat-transfer/applications/solar-power; accessed April 15, 2018.

E. McAllister, Pipeline rules of thumb handbook: a manual of quick, accurate solutions to everyday pipeline engineering problems: Gulf Professional Publishing, 2013.

E. Oró, A. Gil, A. De Gracia, D. Boer, and L. F. Cabeza, "Comparative life cycle assessment of thermal energy storage systems for solar power plants," Renewable Energy, vol. 44, pp. 166-173, 2012.

E. Pihl, D. Kushnir, B. Sandén, and F. Johnsson, "Material constraints for concentrating solar thermal power," Energy, vol. 44, pp. 944-954, 2012.

E. Wenger, M. Epstein, and A. Kribus, "Thermo-electro-chemical storage (TECS) of solar energy," Applied Energy, vol. 190, pp. 788-799, 2017.

Efficiency: More value to your facility Siemens Turbine Model SST-600. Available: https://www.siemens.com/content/dam/webassetpool/mam/tag-siemens-com/smdb/power-and-gas/steamturbines/steam-turbine-product-overview-01-2018.pdf; accessed January 25, 2018.

Energy Storage Facts & Figures. Available: http://energystorage.org/energy-storage/facts-figures; accessed December 12, 2017.

Environmental Protection Agency, Understanding Global Warming Potentials. Available: https://www.epa.gov/ghgemissions/understanding-global-warming-potentials; accessed January 20, 2018.

GHGenius. The Addition of Freight Emissions to GHGenius, 2010. Available: https://ghgenius.ca/reports/GHGeniusFreightEmissions.pdf; accessed February 1, 2018.

H. Grirate, N. Zari, A. Elmchaouri, S. Molina, and R. Couturier, "Life time analysis of thermal oil used as heat transfer fluid in CSP power plant," in AIP Conference Proceedings, 2016, p. 040005.

H. Lund, P. A. Østergaard, D. Connolly, I. Ridjan, B. V. Mathiesen, F. Hvelplund, et al., "Energy storage and smart energy systems," International Journal of Sustainable Energy Planning and Management, vol. 11, pp. 3-14, 2016.

H. Zhang, J. Baeyens, G. Cáceres, J. Degrève, and Y. Lv, "Thermal energy storage: Recent developments and practical aspects," Progress in Energy and Combustion Science, vol. 53, pp. 1-40, 2016.

I. Bhat and R. Prakash, "LCA of renewable energy for electricity generation systems—a review," Renewable and Sustainable Energy Reviews, vol. 13, pp. 1067-1073, 2009.
Infratech Corporation. Available: http://infratech.cc/contact/; accessed February 20, 2018

International Renewable Energy Agency, Concentrating Solar Power, 2012. Available: https://www.irena.org/DocumentDownloads/Publications/RE_Technologies_Cost_Analysis-CSP.pdf; accessed January 31, 2018.

International Renewable Energy Agency, Concentrating Solar Power. 2012. Available: http://www.irena.org/documentdownloads/publications/re_technologies_cost_analysis-csp.pdf; accessed November 3, 2016.

International Renewable Energy Agency, The LCOE of CSP plants as a function of the solar multiple and hours of thermal energy storage. 2014. Available: http://costing.irena.org/media/3550/fig-77.png; accessed December 12, 2016

International Renewable Energy Agency, Concentrating Solar Power Technology Brief. 2013, Available: http://www.irena.org/DocumentDownloads/Publications/IRENA-ETSAP%20Tech%20Brief%20E10%20Concentrating%20Solar%20Power.pdf; accessed December 3, 2016.

ISO, "ISO 14040 International Standard - Environmental Management – Life Cycle Assessment – Principles and Framework," ed. Geneva, Switzerland International Organisation for Standardization, 2006.

ISO, "ISO 14044 International Standard - Environmental Management – Life Cycle Assessment – Requirements and Guidelines," ed. Geneva, Switzerland International Organisation for Standardization, 2006.

J. H. Whitelaw, “Convective heat transfer,” Thermopedia: Guide to Thermodynamics, Heat & Mass Transfer and Fluids Engineering, p. 237, 1997.

J. J. Burkhardt III, G. A. Heath, and C. S. Turchi, "Life cycle assessment of a parabolic trough concentrating solar power plant and the impacts of key design alternatives," Environmental Science & Technology, vol. 45, pp. 2457-2464, 2011.

J. J. Burkhardt, G. Heath, and E. Cohen, "Life cycle greenhouse gas emissions of trough and tower concentrating solar power electricity generation," Journal of Industrial Ecology, vol. 16, 2012.

J. Sweet, E. Roth, and M. Moss, "Thermal conductivity of Inconel 718 and 304 stainless steel," International Journal of Thermophysics, vol. 8, pp. 593-606, 1987.

J. T. Hinkley, J. A. Hayward, B. Curtin, A. Wonhas, R. Boyd, C. Grima, et al., "An analysis of the costs and opportunities for concentrating solar power in Australia," Renewable Energy, vol. 57, pp. 653-661, 2013.

J.-C. Yeh and C.-H. Liao, "Impact of population and economic growth on carbon emissions in Taiwan using an analytic tool STIRPAT," Sustainable Environment Research, vol. 27, pp. 41-48, 2017.

L. EZA, A. Castell, and G. Pérez, "Life cycle assessment (LCA) of phase change materials (PCMs) used in buildings," Eco-efficient Construction and Building Materials: Life Cycle Assessment (LCA), Eco-Labelling and Case Studies, p. 287, 2014.

L. Heller and P. Gauché, "Modeling of the rock bed thermal energy storage system of a combined cycle solar thermal power plant in South Africa," Solar Energy, vol. 93, pp. 345-356, 2013.

L. Heller, B. Mesnil, and J. Hoffmann, "Initial investigation of liquid glass as a thermal medium in CSP plants," in 3rd Southern African Solar Energy Conference, South Africa, 2015.

M. B. Whitaker, G. A. Heath, J. J. Burkhardt III, and C. S. Turchi, "Life cycle assessment of a power tower concentrating solar plant and the impacts of key design alternatives," Environmental science & technology, vol. 47, pp. 5896-5903, 2013.

M. Hanel and R. Escobar, "Influence of solar energy resource assessment uncertainty in the levelized electricity cost of concentrated solar power plants in Chile," Renewable Energy, vol. 49, pp. 96-100, 2013.

M. I. Hussain, A. Ali, and G. H. Lee, "Performance and economic analyses of linear and spot Fresnel lens solar collectors used for greenhouse heating in South Korea," Energy, vol. 90, pp. 1522-1531, 2015.

M. J. Moran, H. N. Shapiro, D. D. Boettner, and M. B. Bailey, Fundamentals of engineering thermodynamics: John Wiley & Sons, 2010.

M. Liu, N. S. Tay, S. Bell, M. Belusko, R. Jacob, G. Will, et al., "Review on concentrating solar power plants and new developments in high temperature thermal energy storage technologies," Renewable and Sustainable Energy Reviews, vol. 53, pp. 1411-1432, 2016.

M. Mehos, C. Turchi, J. Jorgensen, P. Denholm, C. Ho, and K. Armijo, "Advancing concentrating solar power technology, performance, and dispatchability," ed: Golden, CO: National Renewable Energy Laboratory. NREL/TP-5500-65688, 2016.

M. Mehos, J. Jorgenson, P. Denholm, and C. Turchi, "An assessment of the net value of CSP systems integrated with thermal energy storage," Energy Procedia, vol. 69, pp. 2060-2071, 2015.

M. Montes, A. Abánades, and J. Martínez-Val, "Performance of a direct steam generation solar thermal power plant for electricity production as a function of the solar multiple," Solar Energy, vol. 83, pp. 679-689, 2009.

M. Nitsche and R. O. Gbadamosi, "Chapter 1 - Heat Exchanger Design," in Heat Exchanger Design Guide, ed Boston: Butterworth-Heinemann, pp. 1-19, 2016.

M. Nitsche and R. O. Gbadamosi, "Chapter 2 - Calculations of the Temperature Differences LMTD and CMTD," in Heat Exchanger Design Guide, ed Boston: Butterworth-Heinemann, pp. 21-35, 2016.

M. Seitz, M. Johnson, and S. Hübner, "Economic impact of latent heat thermal energy storage systems within direct steam generating solar thermal power plants with parabolic troughs," Energy Conversion and Management, vol. 143, pp. 286-294, 2017.

M. van der Hoeven and D. Houssin, "Energy technology perspectives 2015: mobilising innovation to accelerate climate action," International Energy Agency, 2015.

MGX Minerals Inc. Available: https://www.mgxminerals.com/assets.html; accessed January 19, 2018.

N. A. Masruroh, B. Li, and J. Klemeš, "Life cycle analysis of a solar thermal system with thermochemical storage process," Renewable Energy, vol. 31, pp. 537-548, 2006.

National Energy Board, Market Snapshot: Batteries Dominate Early Stage Testing for Energy Storage in Canada. Available: https://www.neb-one.gc.ca/nrg/ntgrtd/mrkt/snpsht/2016/07-03bttrsdmnttstng-eng.html; accessed January 15, 2018.

National Renewable Energy Laboratory, Andasol-1. Available: https://www.nrel.gov/csp/solarpaces/project_detail.cfm/projectID=3; accessed February 4, 2018

National Renewable Energy Laboratory, Gemasolar Thermosolar Plant, 2011. Available: https://www.nrel.gov/csp/solarpaces/project_detail.cfm/projectID=40; accessed April 5, 2018.

National Renewable Energy Laboratory, Ivanpah Solar Electric Generating System. Available: https://www.nrel.gov/csp/solarpaces/project_detail.cfm/projectID=62; accessed March 16, 2017.

National Renewable Energy Laboratory, Ivanpah Solar Electric Generating System. Available: https://www.nrel.gov/csp/solarpaces/project_detail.cfm/projectID=62; accessed September 30, 2016.

National Renewable Energy Laboratory, System Advisor Model (SAM) Case Study: Andasol-1. Available: https://sam.nrel.gov/sites/default/files/content/case_studies/sam_case_csp_physical_trough_andasol-1_2013-1-15.pdf; accessed March 19, 2017

O. Edenhofer, R. Pichs-Madruga, Y. Sokona, E. Farahani, S. Kadner, K. Seyboth, et al., "Summary for policymakers climate change 2014, mitigation of climate change," IPCC 2014, Climate Change 2014: Contribution of Working Group III to the Fifth Assessment Report of the Intergovernmental Panel on Climate Change, 2014.

Operations and maintenance costs for parabolic trough and solar tower CSP plants. 2014. Available: http://costing.irena.org/media/3553/fig-73.png; accessed December 10, 2016.

Organization for Economic Co-operation and Development, Average annual wages. Available: https://stats.oecd.org/Index.aspx?DataSetCode=AV_AN_WAGE; accessed February 16, 2016.

P. Beiter and T. Tian, "2015 renewable energy data book," National Renewable Energy Laboratory, 2016.

P. Denholm, Net energy balance and greenhouse gas emissions from renewable energy storage systems: Energy Center of Wisconsin, 2003. Available: http://fti.neep.wisc.edu/pdf/fdm1261.pdf; accessed February 10, 2018.

PotashCorp. Available: http://www.potashcorp.com/contact/; accessed February 7, 2018

R. Amirante, E. Cassone, E. Distaso, and P. Tamburrano, "Overview on recent developments in energy storage: Mechanical, electrochemical and hydrogen technologies," Energy Conversion and Management, vol. 132, pp. 372-387, 2017.

R. Chacartegui, L. Vigna, J. Becerra, and V. Verda, "Analysis of two heat storage integrations for an Organic Rankine Cycle Parabolic trough solar power plant," Energy Conversion and Management, vol. 125, pp. 353-367, 2016.

R. Dunn, K. Lovegrove, and G. Burgess, "A review of ammonia-based thermochemical energy storage for concentrating solar power," Proceedings of the IEEE, vol. 100, pp. 391-400, 2012.

R. Gabbrielli and R. Singh, "Economic and scenario analyses of new gas turbine combined cycles with no emissions of carbon dioxide," in ASME Turbo Expo 2004: Power for Land, Sea, and Air, 2004, pp. 665-673.

R. I. Dunn, P. J. Hearps, and M. N. Wright, "Molten-salt power towers: newly commercial concentrating solar storage," Proceedings of the IEEE, vol. 100, pp. 504-515, 2012.

R. Koppelaar, "Solar-PV energy payback and net energy: Meta-assessment of study quality, reproducibility, and results harmonization," Renewable and Sustainable Energy Reviews, vol. 72, pp. 1241-1255, 2017.

R. Moore, M. Vernon, C. K. Ho, N. P. Siegel, and G. J. Kolb, "Design considerations for concentrating solar power tower systems employing molten salt," SAND2010-6978, Sandia National Laboratories, Albuquerque, NM, 2010.

R. Sioshansi and P. Denholm, "The value of concentrating solar power and thermal energy storage," IEEE Transactions on Sustainable Energy, vol. 1, pp. 173-183, 2010.

S. Boudaoud, A. Khellaf, K. Mohammedi, and O. Behar, "Thermal performance prediction and sensitivity analysis for future deployment of molten salt cavity receiver solar power plants in Algeria," Energy Conversion and Management, vol. 89, pp. 655-664, 2015.

S. Colclough and T. McGrath, "Net energy analysis of a solar combi system with Seasonal Thermal Energy Store," Applied Energy, vol. 147, pp. 611-616, 2015.

S. Hübner, M. Eck, C. Stiller, and M. Seitz, "Techno-economic heat transfer optimization of large scale latent heat energy storage systems in solar thermal power plants," Applied Thermal Engineering, vol. 98, pp. 483-491, 2016.

S. Izquierdo, C. Montañés, C. Dopazo, and N. Fueyo, "Analysis of CSP plants for the definition of energy policies: the influence on electricity cost of solar multiples, capacity factors and energy storage," Energy Policy, vol. 38, pp. 6215-6221, 2010.

S. Kuravi, Y. Goswami, E. K. Stefanakos, M. Ram, C. Jotshi, S. Pendyala, et al., "Thermal energy storage for concentrating solar power plants," Technology & Innovation, vol. 14, pp. 81-91, 2012.

S. M. Flueckiger, B. D. Iverson, and S. V. Garimella, "Simulation of a Concentrating Solar Power Plant with Molten-Salt Thermocline Storage for Optimized Annual Performance," in ASME 2013 7th International Conference on Energy Sustainability collocated with the ASME 2013 Heat Transfer Summer Conference and the ASME 2013 11th International Conference on Fuel Cell Science, Engineering and Technology, 2013.

S. M. J. Miller. Designing storage tanks. Available: http://coade.typepad.com/files/ptq-q4-2016-designing-storage-tanks.pdf; accessed January 15, 2018.

S. Schlömer, T. Bruckner, L. Fulton, E. Hertwich, A. McKinnon, D. Perczyk, et al., "Annex III: Technology-specific cost and performance parameters," Climate change, pp. 1329-1356, 2014.

S. Thaker, A. O. Oni, and A. Kumar, "Techno-economic evaluation of solar-based thermal energy storage systems," Energy Conversion and Management, vol. 153, pp. 423-434, 2017.

SolarReserve, Molten Salt Energy Storage. Available: http://www.solarreserve.com/en/technology/molten-salt-energy-storage; accessed February 3, 2018

T. Larraín and R. Escobar, "Net energy analysis for concentrated solar power plants in northern Chile," Renewable Energy, vol. 41, pp. 123-133, 2012.

Thermal Energy Storage Market by Technology, Storage Material, Application, End-User, and Region - Global Forecast to 2022. 2016. Available: http://www.crossroadstoday.com/story/34975289/thermal-energy-storage-market-by-technology-storage-material-application-end-user-and-region-global-forecast-to-2022; accessed January 12, 2016.

U.S. Department of Energy, Solar energy technologies office FY2016 budget at-a-glance. 2015, Available: https://energy.gov/sites/prod/files/2015/03/f20/fy16_seto_at-a-glance.pdf; accessed January 20, 2016.

Volume Flow and Temperature Rise in Pump. Available: http://www.engineeringtoolbox.com/pumps-temperature-increase-d_313.html; accessed January 2, 2018.

World Energy Council, World Energy Perspective Cost of Energy Technologies, 2013. Available: https://www.worldenergy.org/wp-content/uploads/2013/09/WEC_J1143_CostofTECHNOLOGIES_021013_WEB_Final.pdf; accessed April 12, 2017.

Appendix A: Derivation of LCOE

N	Capital cost ($)	Variable O&M Cost ($)	Fixed O&M Cost ($)	Sell price ($)	Sum
0	C				
1		C(0.02)	C(0.02)	(x)(energy)	$\frac{(\mathrm{x})(\mathrm{energy}) - (\mathrm{C})(0.02) - (\mathrm{C})(0.02)}{(1+\mathrm{D})}$
2		C(0.02)(1 + g)	C(0.02)	(x)(energy)	$\frac{(\mathrm{x})(\mathrm{energy}) - (\mathrm{C})(0.02)(1+\mathrm{g}) - (\mathrm{C})(0.02)}{(1+\mathrm{D})^2}$
3		C(0.02)($(1+g)^2$)	C(0.02)	(x)(energy)	$\frac{(\mathrm{x})(\mathrm{energy}) - (\mathrm{C})(0.02)(1+\mathrm{g})^2 - (\mathrm{C})(0.02)}{(1+\mathrm{D})^3}$
.		.	.	.	.
.		.	.	.	.
.		.	.	.	.
30		C(0.02)($(1+g)^{29}$)	C(0.02)	(x)(energy)	$\frac{(\mathrm{x})(\mathrm{energy}) - (\mathrm{C})(0.02)(1+\mathrm{g})^{29} - (\mathrm{C})(0.02)}{(1+\mathrm{D})^{30}}$

$$\mathrm{NPV} = 0 = -\mathrm{C} + \frac{(\mathrm{x})(\mathrm{energy}) - (\mathrm{C})(0.02) - (\mathrm{C})(0.02)}{(1+\mathrm{D})} + \frac{(\mathrm{x})(\mathrm{energy}) - (\mathrm{C})(0.02)(1+\mathrm{g}) - (\mathrm{C})(0.02)}{(1+\mathrm{D})^2} + \cdots + \frac{(\mathrm{x})(\mathrm{energy}) - (\mathrm{C})(0.02)(1+\mathrm{g})^{29} - (\mathrm{C})(0.02)}{(1+\mathrm{D})^{30}}$$

$$\mathrm{NPV} = 0 = -\mathrm{C} + (\mathrm{x})(\mathrm{energy})\left[\frac{1}{1+\mathrm{D}} + \frac{1}{(1+\mathrm{D})^2} + \cdots + \frac{1}{(1+\mathrm{D})^{30}}\right] - (\mathrm{C})(0.02)\left[\frac{1}{1+\mathrm{D}} + \frac{1+\mathrm{g}}{(1+\mathrm{D})^2} + \cdots + \frac{(1+\mathrm{g})^{29}}{(1+\mathrm{D})^{30}}\right] - (\mathrm{C})(0.02)\left[\frac{1}{1+\mathrm{D}} + \frac{1}{(1+\mathrm{D})^2} + \cdots + \frac{1}{(1+\mathrm{D})^{30}}\right]$$

$$\mathrm{NPV} = 0 = -\mathrm{C} + (\mathrm{x})(\mathrm{energy})[\mu] - (\mathrm{C})(0.02)[\beta] - (\mathrm{C})(0.02)[\gamma]$$

where:

$$\mu = \frac{1}{1+\mathrm{D}} + \frac{1}{(1+\mathrm{D})^2} + \cdots + \frac{1}{(1+\mathrm{D})^{30}}$$

$$\beta = \frac{1}{1+\mathrm{D}} + \frac{1+\mathrm{g}}{(1+\mathrm{D})^2} + \cdots + \frac{(1+\mathrm{g})^{29}}{(1+\mathrm{D})^{30}}$$

$$\gamma = \frac{1}{1+\mathrm{D}} + \frac{1}{(1+\mathrm{D})^2} + \cdots + \frac{1}{(1+\mathrm{D})^{30}}$$

Sum of a geometric series can be computed as follows:

$$a + ar^2 + ar^3 + ar^4 + \cdots + ar^n = \frac{a(1-r^n)}{1-r} \; ; r \neq 1$$

$$\mu = \left(\frac{1}{1+D}\right)\left(\frac{\left(1-\left(\frac{1}{1+D}\right)^N\right)}{1-\left(\frac{1}{1+D}\right)}\right) \tag{15}$$

$$\beta = \left(\frac{1}{1+D}\right)\left(\frac{\left(1-\left(\frac{1+g}{1+D}\right)^N\right)}{1-\left(\frac{1+g}{1+D}\right)}\right) \tag{16}$$

$$\gamma = \left(\frac{1}{1+D}\right)\left(\frac{\left(1-\left(\frac{1}{1+D}\right)^N\right)}{1-\left(\frac{1}{1+D}\right)}\right) \tag{17}$$

$$NPV = 0 = -C + (x)(energy)[\mu] - (C)(0.02)[\beta] - (C)(0.02)[\gamma] \tag{18}$$

Sub Equations 15, 16, and 17 into Equation 18:

$$0 = -C + (x)(energy)\left(\left(\frac{1}{1+D}\right)\left(\frac{\left(1-\left(\frac{1}{1+D}\right)^N\right)}{1-\left(\frac{1}{1+D}\right)}\right)\right) - (C)(0.02)\left(\left(\frac{1}{1+D}\right)\left(\frac{\left(1-\left(\frac{1+g}{1+D}\right)^N\right)}{1-\left(\frac{1+g}{1+D}\right)}\right)\right) - (C)(0.02)\left(\left(\frac{1}{1+D}\right)\left(\frac{\left(1-\left(\frac{1}{1+D}\right)^N\right)}{1-\left(\frac{1}{1+D}\right)}\right)\right)$$

Multiply both sides by 1+D

$$0 = -C(1+D) + (x)(energy)\left(\frac{\left(1-\left(\frac{1}{1+D}\right)^N\right)}{1-\left(\frac{1}{1+D}\right)}\right) - (C)(0.02)\left(\frac{\left(1-\left(\frac{1+g}{1+D}\right)^N\right)}{1-\left(\frac{1+g}{1+D}\right)}\right) - (C)(0.02)\left(\frac{\left(1-\left(\frac{1}{1+D}\right)^N\right)}{1-\left(\frac{1}{1+D}\right)}\right)$$

Therefore

$$x = LCOE = \frac{\left(C(1+D)\right) + \left((C)(0.02)\left(\frac{\left(1-\left(\frac{1+g}{1+D}\right)^N\right)}{1-\left(\frac{1+g}{1+D}\right)}\right)\right) + \left((C)(0.02)\left(\frac{\left(1-\left(\frac{1}{1+D}\right)^N\right)}{1-\left(\frac{1}{1+D}\right)}\right)\right)}{(Energy)\left(\frac{\left(1-\left(\frac{1}{1+D}\right)^N\right)}{1-\left(\frac{1}{1+D}\right)}\right)}$$

Appendix B: Supporting Information

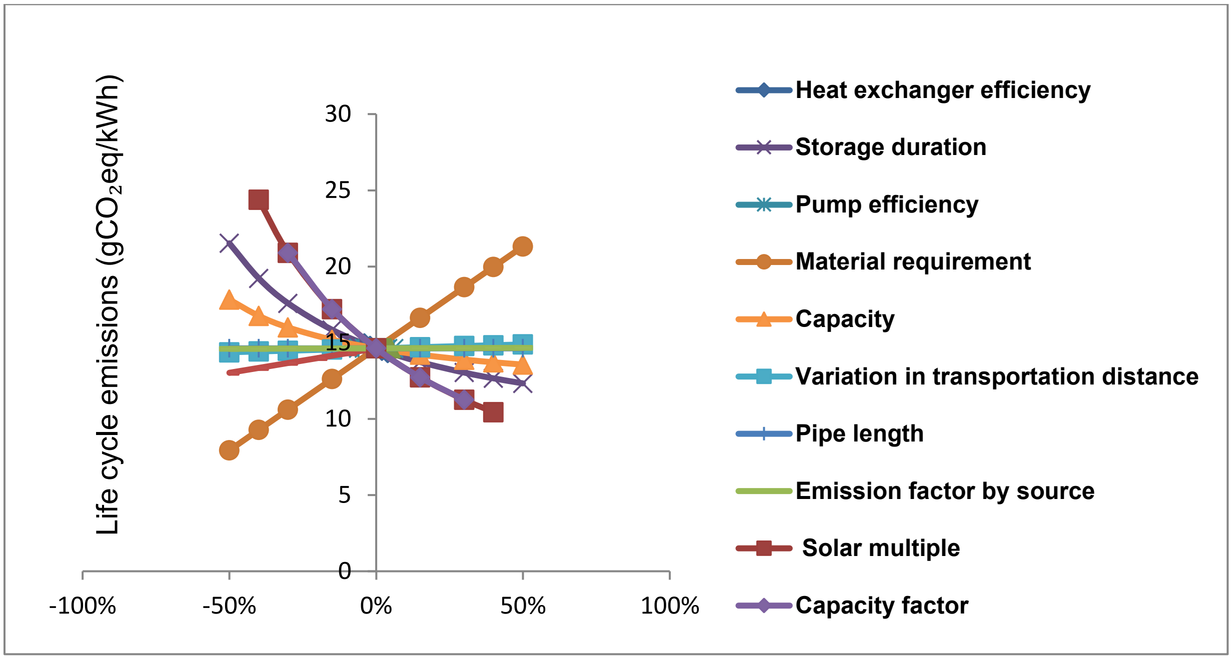

Figure 25: GHG emissions for 2-tank direct sensible heat storage (S2)

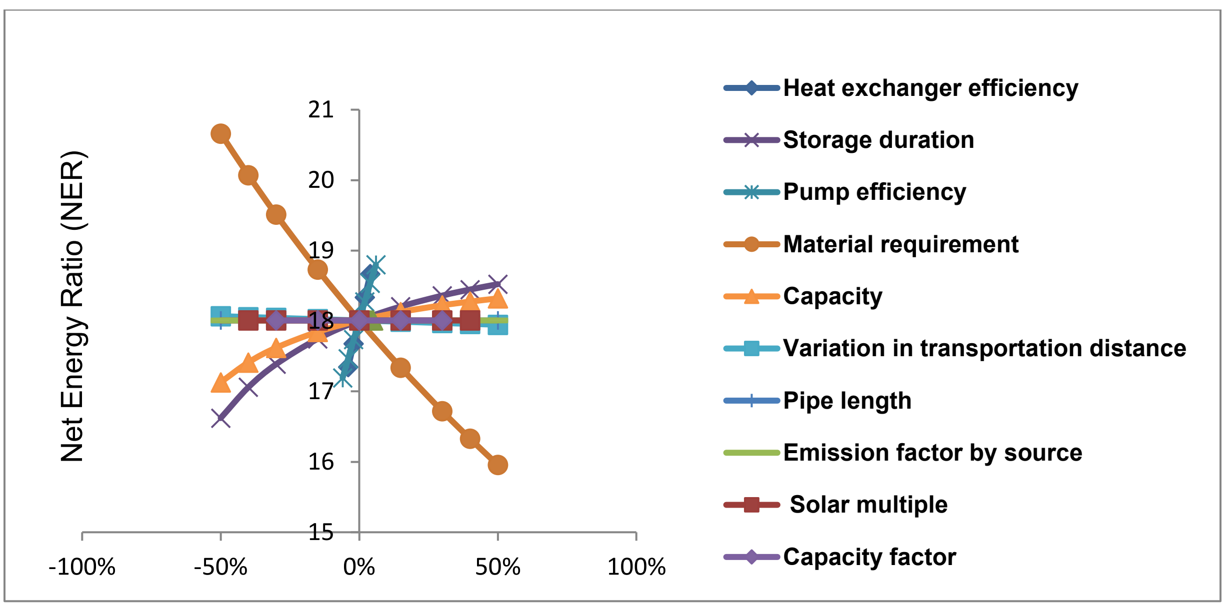

Figure 26: NER for 2-tank direct sensible heat storage (S2)

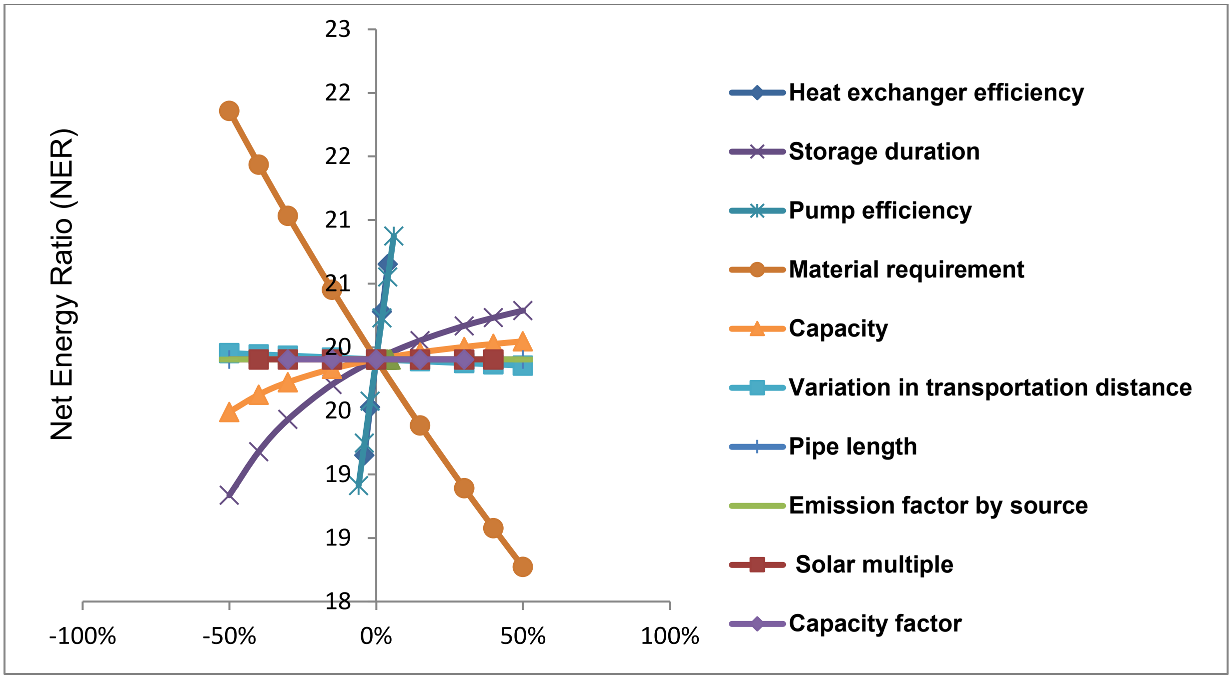

Figure 27: NER for 1-tank direct sensible heat storage (S3)

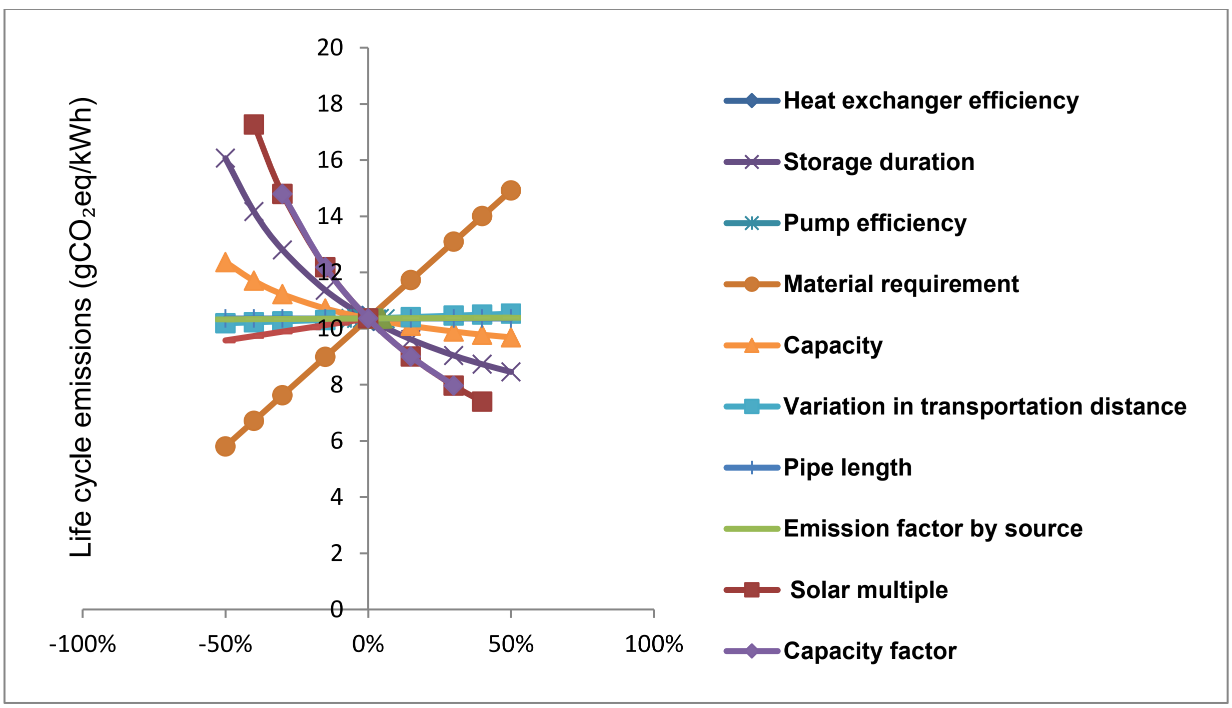

Figure 28: GHG emissions for 1-tank direct sensible heat storage (S3)

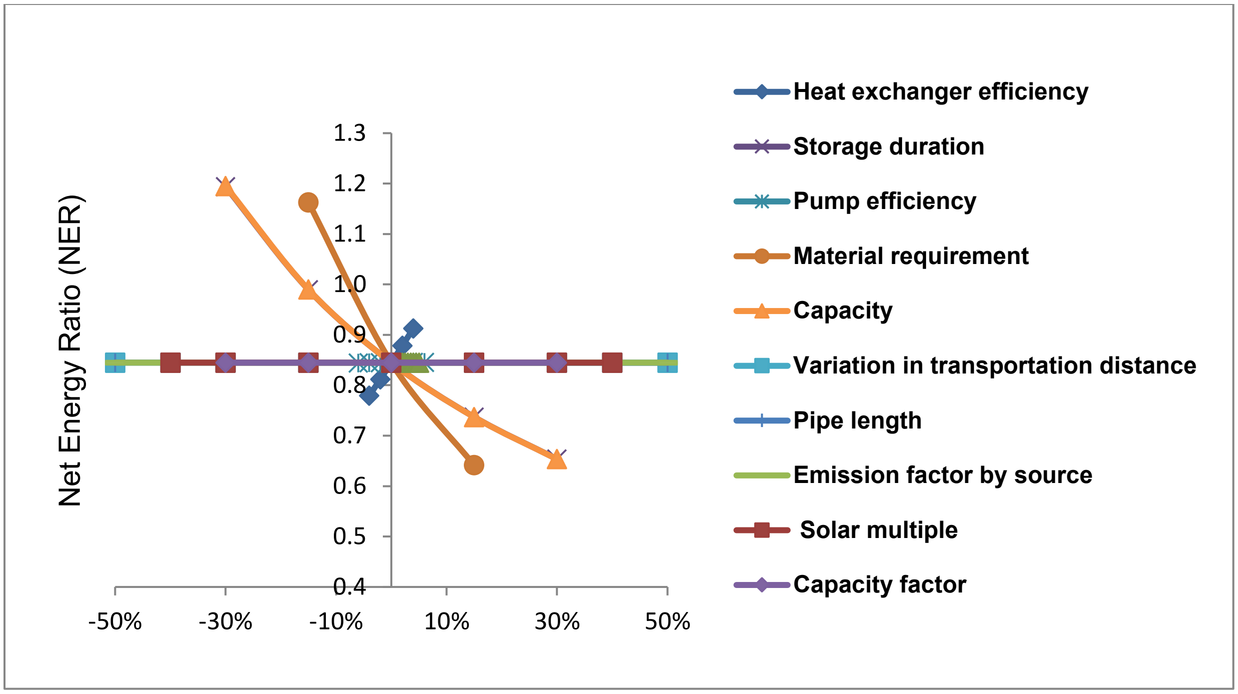

Figure 29: NER for latent heat storage (S4)

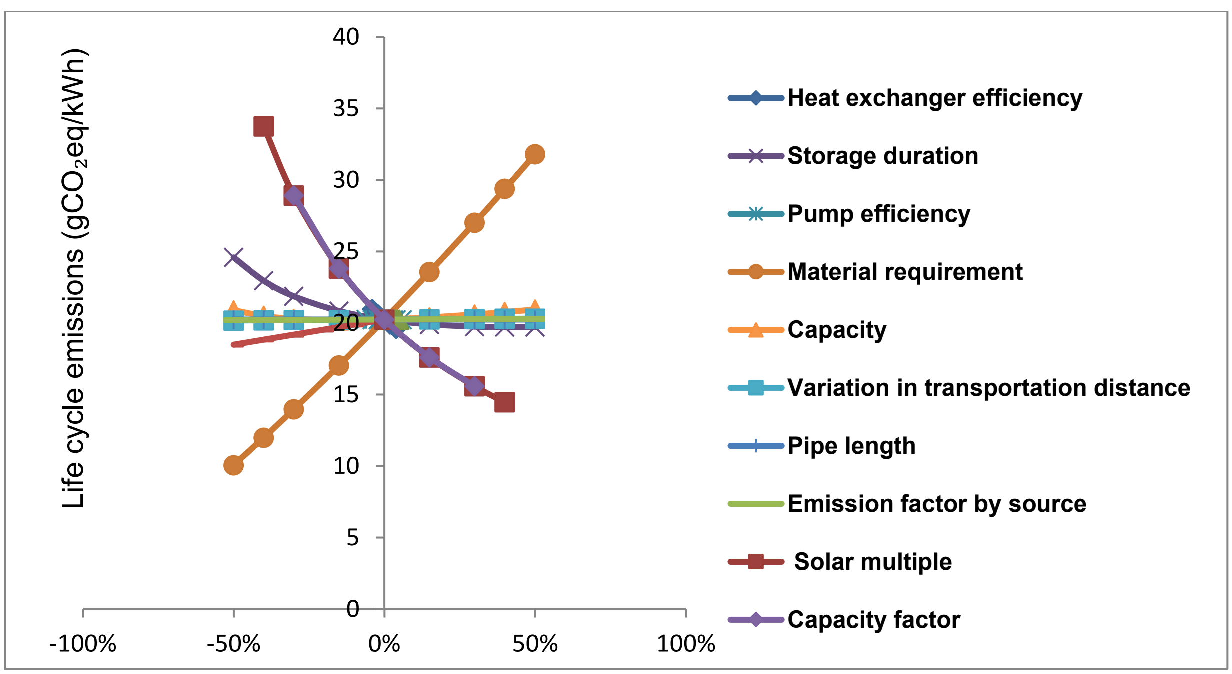

Figure 30: GHG emissions for latent heat storage (S4)

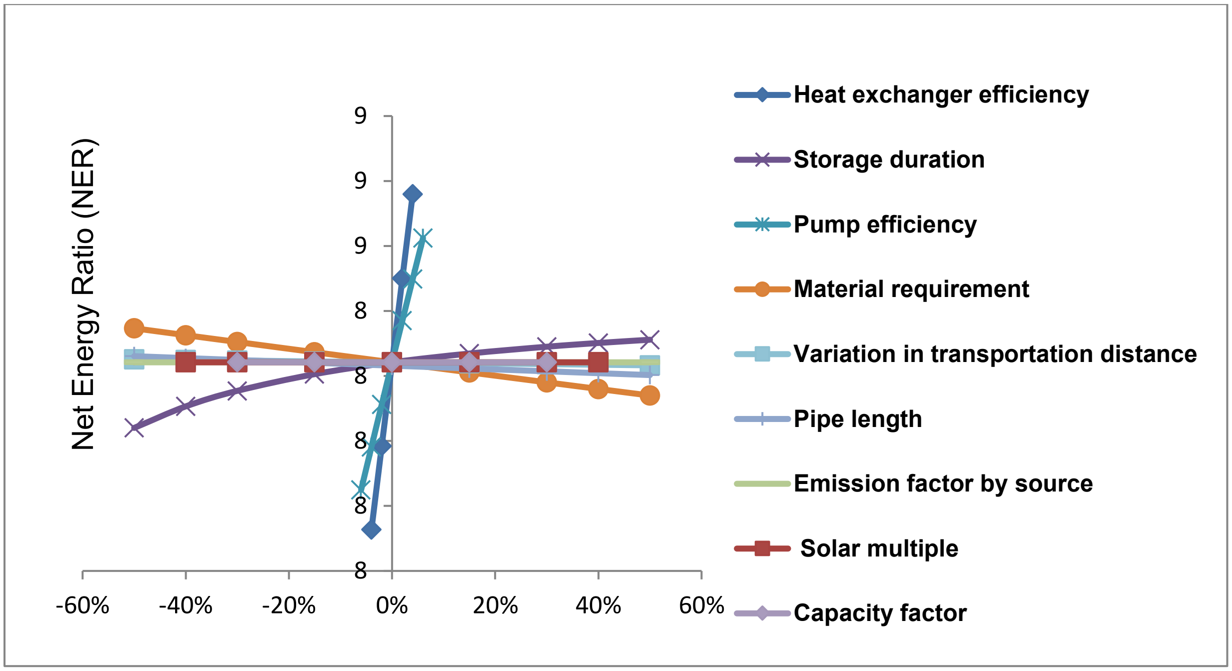

Figure 31: NER for thermochemical storage (S5)

Table 14: Sampling error, standard deviation, and number of samples

	Sampling error	**Standard deviation**	**# of samples**
GHG Emissions (gCO_2eq/kWh)	0.03	7.45	200000
Net Energy Ratio (NER)	0.01	5.74	200000

Table 15: Monte Carlo input distributions

Costs	**Monte Carlo input distributions**
Heat exchanger efficiency	VoseTriangle (0.70,0.95,0.95)
Storage duration (hrs)	VoseTriangle (1.05,8,15)
Generator efficiency	VoseTriangle (0.88,0.95,0.99)
Pump efficiency	VoseTriangle (0.80,0.85,0.90)
Material requirement	VoseTriangle (0.5,1, 1.5)

Pipe length for S1	VoseTriangle (850,1700,2550)
Pipe length for S2 – S5	VoseTriangle (850,1400,2550)
Electricity emission factor for Canadian provinces (gCO_{2eq}/kWh)	VoseTriangle (410,820,820)
Solar multiple	VoseTriangle (1,1.75,3.5)
Variation in transportation distance	VoseTriangle (0.5,1, 1.5)
Capacity (MW)	VoseTriangle (50,100,250)
Electricity source emission factor (gCO_{2eq}/kWh)	VoseTriangle (21,41, 61)